2020

Early hippocampal dysfunction in a mouse model of dementia with Lewy bodies: Mechanisms of cellular dysfunction caused by alpha-synuclein accumulation

Cowan, Katrina

http://hdl.handle.net/10026.1/16752

http://dx.doi.org/10.24382/714
University of Plymouth

UNIVERSITY OF
PLYMOUTH

Early hippocampal dysfunction in a mouse model of dementia with Lewy bodies: Mechanisms of cellular dysfunction caused by alpha-synuclein accumulation

By

Katrina Ruth Cowan

A thesis submitted to the University of Plymouth in partial fulfilment for the degree of

DOCTOR OF PHILOSOPHY

Peninsula School of Medicine

December 2020

Acknowledgements

The last four years have provided me with some of the most frustrating yet exciting and fascinating times of my life. There has been so much that I have gained from my experiences at Plymouth University, and I am incredibly grateful for the people who made it not only an educational and rewarding period but also an enjoyable process, which hopefully I can take with me into the future.

I would like to thank first and foremost my supervisors who have each provided me with so much support and advice throughout the entire four years I have been at Plymouth University. I would most like to thank Dr. Oleg Anichtchik and Dr. Shouqing Luo, who have both been my Director of Studies whilst I have been at Plymouth University. They have both taken so much of their time and effort to train me in many different techniques and provided me with the tools necessary to become a scientist and it is because of them that I have managed to come so far. I would also like to thank Dr. Robert Fern, who as my third supervisor has provided some invaluable technical advice and suggestions for my work.

Aside from my supervisors there have been a number of people who have provided support in the lab during my time as a PhD student for which I am hugely grateful. I would most like to thank two in particular, both of whom have been members of the same lab group and have truly taken time out of their day to help and support me, for which I am exceptionally grateful. Dr Tracey Evans, who I met on my very first day, has been nothing but supportive and generous, and I am inspired by her intelligence and dedication. I would like to especially thank Dr. Wai Ling Kok for her friendship and guidance throughout the PhD, and it was a great pleasure to work with her. I wish them both every success in their future career as brilliant scientists.

Away from the lab, I have met many new people who have made living and working in Plymouth easier and more enjoyable. I would especially like to thank my several housemates. In particular, I would like to thank Agnes Tulwin, Ashleigh Sladen and Maria Husband, who I have lived with in various houses throughout the three and half years I have been living in Plymouth. I think I would not have enjoyed it quite as much if they had not been there; their companionship and friendship made it so much easier and I thank them all so much for the good times we had, the numerous cups of tea, relaxing evenings and weekends and the meals we have cooked together. Living with them has let me meet many interesting and inspiring people so I thank them for providing me with a such a fun and relaxing environment to come home to every day.

Next, I like to thank the three most important people, who have given me so much support right from the very start. My parents, Colin and Jessica Cowan, and my brother Andrew. There is no doubt that I would not have been able to do this without any of them. They have provided some much needed encouragement and unwavering emotional support throughout my entire scientific education, and I cannot thank them enough for everything.

Lastly, I would like to thank Plymouth University itself, for granting the scholarship. Without the funding by Plymouth University I would not have been here at all, so I am thankful to the University for the opportunity to study here in Plymouth. It has been difficult at times, but I am so glad that I did it. Thank you to everyone who made it possible.

Author's declaration

At no time during the registration for the degree of Doctor of Philosophy has the author been registered for any other University award without prior agreement of the Doctoral College Quality Sub-Committee.

Work submitted for this research degree at the Plymouth University has not formed part of any other degree either at Plymouth University or at another establishment. This study was financed with the aid of a studentship from Plymouth University

Publications (or public presentation of creative research outputs):

Cowan, K., O. Anichtchik, and S. Luo, *Mitochondrial integrity in neurodegeneration*. CNS Neurosci Ther, 2019. **25**(7): p. 825-836. DOI: 10.1111/cns.13105

Presentation and Conferences Attended:

Alzheimer's Research UK Conference, Manchester: Attended (2016)
Alzheimer's Research UK Conference, London: Poster (2018)
VOYAGE Ageing Research Conference: The development of dementia: Oral (2016)
Annual presentation for the Plymouth University seminar series: Oral (2015-2018)
Annual presentation at ARE event with Plymouth University: Poster (2015-2016), Oral (2016)

Word count of main body of thesis: 32,974 (excluding references)

Signed: Katrina Ruth Cowan

Date: 08/12/2020

Abstract

Katrina Cowan

Early hippocampal dysfunction in a mouse model of dementia with Lewy bodies: mechanisms of cellular dysfunction caused by alpha-synuclein accumulation.

Dementia with Lewy bodies (DLB) is a devastating neurodegenerative disease, accounting for 5% of all dementia cases, for which there is no cure. Whilst there are currently many different animal models currently available for researchers studying PD, there are comparatively fewer DLB-specific mouse models. The limited amount of effective DLB mouse models presents a significant issue in the pursuit for DLB treatment.

In my project, I aim to determine the accuracy of a novel DLB-specific mouse model, focusing on changes in mitochondrial function. Additionally, I explore the role of the wild-type and a DLB-related mutation of the protein beta-synuclein on mitochondrial function. The novel mouse model, known as CamS120, expresses a truncated form of the human alpha-synuclein promoter, expressed under the CamKIIa promoter, which drives the expression of the transgene to the forebrain region, including the hippocampus. The CamS120 mouse model was examined for behavioural changes, and then further examined for changes in mitochondrial number, dynamics, mitochondrial membrane potential and reactive oxygen species (ROS) production. The CamS120 mouse model was complemented with an alpha-synuclein overexpressing cell line (aFL), which was used to examine further changes in mitochondrial function, including changes in mitochondrial membrane potential, ROS production and mitophagy. The CamS120 mouse model was also examined for changes in beta-synuclein protein levels and distribution. In addition, wild-type beta-

synuclein and DLB-related mutated beta-synuclein (V70M) overexpressing cells were also examined for changes in mitochondrial function.

From my experiments I discovered that the CamS120 mice did not show any accompanying changes in mitochondrial function. The aFL cells on the other hand showed impairment in mitochondrial dynamics, disruption in mitochondrial membrane potential and an increase in ROS production. Examining beta-synuclein protein levels in CamS120 mice found that beta-synuclein protein levels were decreased in 12 months CamS120 mice. Wild-type and V70M mutated beta-synuclein overexpressing cells seemed to have a weak effect on mitochondrial dynamics, but only mutant beta-synuclein showed a disruption of the mitochondrial membrane potential and increased generation of ROS.

I concluded that while CamS120 mice showed symptoms of recognition memory impairment, changes in mitochondrial function could not be conclusively associated with this memory impairment. However, results did show a potentially interesting difference between wildtype and mutated beta-synuclein, where mutations in beta-synuclein appeared to exert a toxic effect onto the relatively innocuous wildtype protein, which if confirmed, could be a future point of scientific interest.

Abbreviations

4-HNE	4-hyroxy-2-nonenal
AD	Alzheimer's disease
ANT	Adenine nucleotide translocator
APOE	Apolipoprotein E
ATP	Adenosine triphosphate
Aβ	Amyloid-beta
CHIP	C-terminus of U-box domain of co-chaperone Hsp70-interacting protein
CNS	Central nervous system
CR	Calretinin-expressing hilar cells
CsA	Cyclosporin A
CypD	Cyclophilin D
DAT	Dopamine transporter
DLB	Dementia with Lewy bodies
EC	Entorhinal cortex
ETC	Electron transport chain
FADH2	Flavin adenine dinucleotide
fMRI	Functional magnetic resonance imaging
FTD	Frontotemporal dementia
H2O2	Hydrogen peroxide
HD	Huntington's disease
HICAP	Hilar commissural associational path
IMM	Inner mitochondrial membrane
Mn-SOD	Manganese-superoxide dismutase
MOPP	Molecular layer perforant path associated
mPTP	Mitochondrial permeability pore
MSA	Multiple systems atrophy
MTS	Mitochondrial targeting sequence
NAC	Non-amyloid-β component
NADH	Nicotinamide adenine dinucleotide

NO	Nitric oxide
NOR	Novel object recognition
NOS	Nitric oxide
O2-	Superoxide anions
O2●-	Superoxide
OH-	Hydroxyl ion
OH●	Hydroxyl radical
OMM	Outer mitochondrial membrane
ONOO-	Peroxynitrile
PARL	Presenilin Associated Rhomboid Like protease
PD	Parkinson's disease
PDD	Parkinson's disease with dementia
Pink1	PTEN-induced putative kinase 1
PLK2	Polo-like kinase 2
PNP-14	Phosphoneuropeptide-14
PSP	Progressive supranuclear palsy
Q	Ubiquinone
RBD	REM sleep behaviour disorder
ROS	Reactive oxygen species
SN	Substantia nigra
SNpc	Substantia nigra pars compacta
SPECT	Single-photon emission computerised tomography
TCA	Tricyclic carboxyl acid
TH	Tyrosine hydroxylase
VDAC	Voltage dependent anion channel

Table of Contents

List of Figures

List of Tables

Chapter One: Introduction

1.1. Dementia with Lewy Bodies

1.1.1. The prevalence and aetiology of dementia with Lewy bodies

1.1.1.1. Prevalence of dementia with Lewy bodies

Dementia with Lewy bodies (DLB), a devastating neurodegenerative disease, is widely regarded as the second most common form of neurodegenerative dementia after Alzheimer's disease (AD) [1]. It accounts for around 40-60% of all dementia cases and is most prevalent in elderly patients [2-4]. Overall, DLB accounts for roughly 5% of all neurodegenerative dementia types, while other forms of neurodegenerative disease with cognitive impairment include vascular dementia, frontal-temporal dementia (FTD), progression supranuclear palsy (PSP) and Huntington disease (HD) [5-9].

1.1.1.2. Symptoms in DLB patients

DLB patients have reported a wide range of symptoms, including visual hallucinations, impairment in attention, overall cognitive fluctuations, visual-spatial memory impairments and Parkinson-like symptoms [10, 11]. Other symptoms sometimes reported by DLB patients include disturbances in REM sleep behaviour (RBD) and increased narcoleptic sensitivity. Less common symptoms sometimes seen include autonomic dysfunction (including urinary incontinence), depression and systematised delusions [12, 13].

While patients of AD also display alterations in attention, concentration and executive function, these cognitive functions however were seen to be more significantly affected in DLB patients [14]. In addition, both motor dysfunction and visual hallucinations are thought to be more severely affected in DLB compared to AD, whereas in AD memory impairments are a more prominent feature [15, 16]. These differences between clinical

symptoms can be used to differentiate DLB from AD or other neurodegenerative dementias.

DLB has similar symptoms with Parkinson's disease (PD) as well, where many DLB patients show symptoms such as bradykinesia, postural instability and tremor [17]. The reverse can sometimes also be true, where certain PD patients shows signs of dementia. This particular subgroup of PD is separate from pure PD, and patients showing cognitive impairment are diagnosed with PD with dementia (PDD) [18]. The strong similarities between DLB and PDD can often make it more difficult to properly differentiate the two diseases and so has been a great source of debate amongst clinicians [19-21]. The defining feature to separate the two diseases is the time of onset, with regard to the Parkinsonism symptoms. With PDD, the parkinsonism symptoms, which are the more prominent symptoms, present at least one year earlier than the cognitive deficits, unlike DLB where the cognitive deficits occur earlier and are more prominent [22].

1.1.1.3. Risk Factors for DLB

As with other neurodegenerative diseases such as AD,PD or HD, the majority of studies have shown that the major risk factor for DLB is old age [23]. Aside from old age, environmental factors may also cause DLB neuropathology. Whilst there are not many studies which have examined the risk factors for DLB, there have been extensive research into risk factors for both AD and PD; for example studies which looked at environmental factors for PD in European countries found that exposure to pesticides, hypnotics, anti-depressant drugs and tobacco were found to be strong risk factors for PD [24-26]. Meta-analysis into environmental risk factors in Parkinson's disease shows that the strongest risk factors for PD include anxiety, beta-blockers drugs and smoking[27]. In addition, connections between the absence of smoking

history and PD have also been made, with some studies showing an inverse relationship between smoking and PD symptoms [27, 28] Studies into the risk factors for AD have found similar risk factors, including an increased risk of AD when smoking or with alcohol consumption [29]. A complete list of the risk factors for DLB has not yet been discovered, however one study which showed an association between anxiety, depression and DLB [26]. In addition to environmental risk factors, there have been certain genes identified as a risk factor for DLB pathology. One important allele identified in DLB patients is APOE (apolipoprotein E) ε4. The APOE gene is commonly found in humans in three different forms (APOE2, APOE3 and APOE4). Elevated levels of APOE ε4 has been previously seen in cases of AD, but a similar increased level of the gene was also seen in studies of DLB [26, 30]. Whilst studies differ on the effects of the APOE isoforms, the general consensus is that, as with AD, the increased presence of the APOE gene increases the risk of DLB.

1.1.2. Lewy body pathology in DLB

DLB is classified as a form of synucleinopathy, which a group of disease which includes PD and Multiple System Atrophy (MSA) [31]; these diseases are all classified as such due to the presence of abnormal alpha-synuclein protein within neuronal cell bodies and neurites, forming aggregates known as Lewy bodies and Lewy neurites. The progression of Lewy body neuropathology which occurs specifically in DLB has not been extensively examined, however research into Lewy body pathology in PD has previously been examined by Braak and colleagues, who proposed the development of a grading system to classify stages of Lewy body pathology [32]. Braak proposed six stages of PD-related pathology, which indicated that Lewy body pathology appeared to spread upwards through the brainstem, including the medulla oblongata, through to the mid- and forebrain regions such as the hippocampus and

hypothalamus, and then further through onto the neocortex (Figure 1). Whilst these stages were proposed using data from PD patients, this progression may also be relevant in DLB neuropathology where Lewy body formation might potentially follow a similar progression.

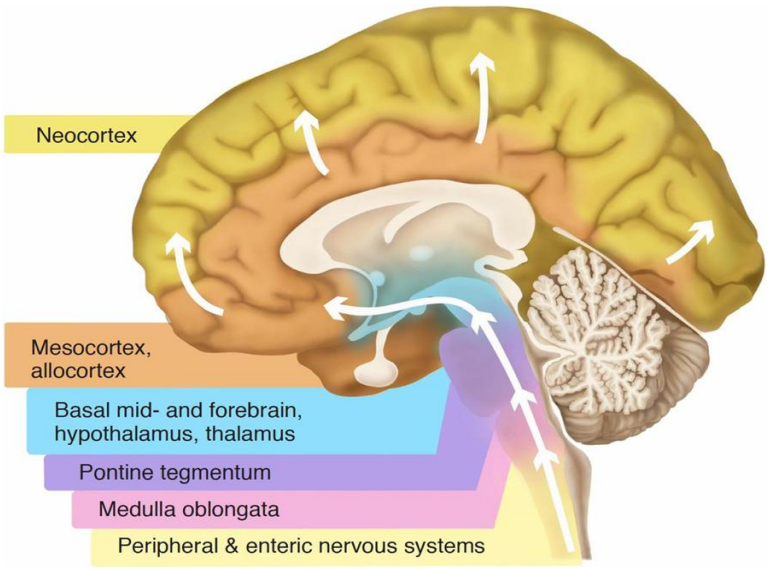

Figure 1. **General overview of the spread of Lewy body pathology in PD, as suggested by Braak**. Braak [32] proposes the progression of Lewy body pathology up towards the brain via the brain stem (1), affecting the medulla oblongata and pontine tegmentum, which can spread further into the basal mid- and forebrain, affecting the hypothalamus (2). In later Braak stages, neuropathology may affect the meso cortex -neocortex (3).This illustration was taken form Visanji et al. [33], which is available under the common creative licence, no changes were made to the original.

1.1.2.1. Brain regions affected by Lewy body pathology

Using post-mortem brain samples from diagnosed DLB patients, mild Lewy bodies and neurites pathology was found within the neocortex in DLB patients [34, 35]. The alpha-synuclein containing granular component of Lewy bodies detected in the superior frontal cortex of DLB patients was found in pyramidal neurons within cortical layers V-VI [36]. The presence of Lewy neurites in the superior frontal cortex however was not detected. Functional studies, using functional magnetic resonance imaging (fMRI), has shown that reduced activity in the white matter tracts within frontal cortex, as well

as in the corpus callosum, suggesting that abnormalities in the connecting white matter tracts contributes to neurodegeneration seen in DLB [37, 38].

DLB patients have additionally shown a noticeable disruption in the visual cortex and vision-associated brain regions, such as in the occipito-parietal regions, accounting for visual-related symptoms in DLB [39]. Using SPECT (single-photon emission computerized tomography) imaging and fMRI scans show that activity is significantly reduced in occipito-parietal brain regions [40], which may potentially be responsible for the changes in vision or visual hallucination which has been reported by patients with DLB.

Alpha-synuclein immunoreactivity was also found in the substantia nigra (SN) of DLB brain tissue. Studies on DLB patients have shown the strong alpha-synuclein immunoreactivity, confirming the presence of ubiquitinated, intracytoplasmic Lewy bodies and Lewy neurites within neuronal perikarya of nigral cells in the SN [41, 42]. Nigrostriatal cell loss and dopaminergic transporter degradation have also been seen in DLB patients [43]. The SN is known to be closely involved in motor function. In PD, where patients shows motor symptoms such as bradykinesia and tremors, the SN is the most affected brain region. The neuronal loss in the SN seen in DLB patients is therefore thought to be closely related to the Parkinsonism symptoms reported.

Lewy bodies have also been found in DLB post-mortem tissue within the paralimbic regions of the brain. The entorhinal cortex and insula cortices have both been shown to be affected in DLB [41], with mild Lewy body and Lewy neurite pathology in layers V-VI, as well as the presences of Lewy bodies in layer III [36]. These structures have important roles in sensory processing, memory and cognitive function, and Lewy body

neuropathy within these regions has been shown to contribute to the abnormalities in mood and memory seen in DLB patients [44, 45].

Alpha-synuclein immunoreactivity can also be seen in the cingulate gyrus, with ubiquitinated Lewy bodies and Lewy neurites detected in the cingulate gyrus of DLB post-mortem tissues [42]. The cingulate gyrus from part of the limbic system and is involved in mood, sensory and behavioural processing [46]. This is consistent with symptoms seen in DLB, where patient reports impaired autonomic function, as well mood and cognitive function. The cingulate gyrus is also affected in AD, which seemed to have a greater extent of impairment than in DLB patients. It was therefore proposed as a potential marker to distinguish between AD and DLB during diagnosis [47].

The presence of Lewy neurites within the hippocampus region has also been identified in DLB brain tissue [48]. The hippocampus is the main focus in the examination of the mouse models using in my research project and so I shall discuss the structure and function of the hippocampus as well as the extent of Lewy body pathology that can be seen within the hippocampus in DLB in more depth in the following subsection.

1.1.2.1.1. Hippocampus structure, function and involvement in DLB.

The hippocampus is a structure located in the medial temporal lobe of the brain (Figure 2). The term hippocampus typically refers collectively to two main regions: the dentate gyrus and the hippocampus proper, the latter of which is further compartmentalised into four additional sub-regions, CA3, CA2 and CA1.

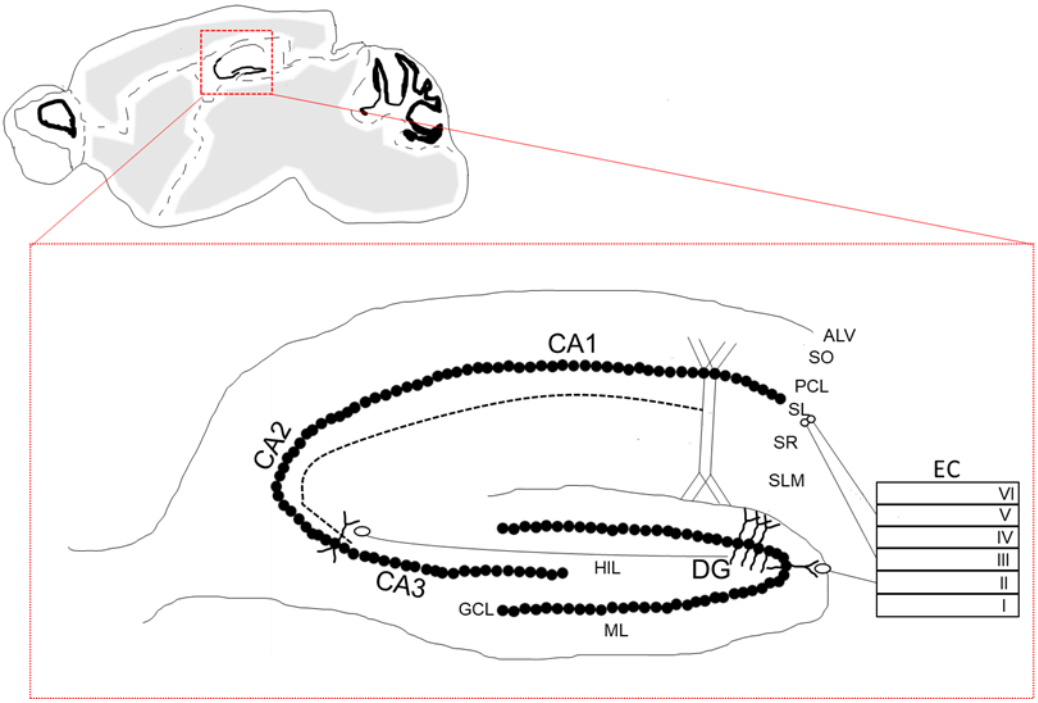

Figure 2. An outline of the mouse hippocampus structure. The hippocampal area, highlighted by the red box, is shown as an enlarged image. Connections between the hippocampal regions (including dentate gyrus, CA3, CA2 and CA1) and the entorhinal cortex (EC, layer 1-VI) are shown.

The hippocampus receives multiple inputs from the surrounding regions. A particularly important input comes from the entorhinal cortex (EC). The EC, which consists of six layers (I-VI), is the major input into the hippocampus formation and neuronal afferents from the layer II of the EC project to the dentate gyrus and the CA subregions, via a pathway known as the perforant pathway (Figure 3) [49]. This pathway is unidirectional, which means that the dentate gyrus receives input from the EC, but the dentate gyrus does not project neurons back to the EC [50]. In addition to this connectivity to the dentate gyrus and CA3 region, EC also sends afferent projections to the CA1 and subiculum regions, originating from layer III of the EC.

The dentate gyrus contains three different cell types: granule cells, hilar mossy cells (both of which are glutamatergic, excitatory neurons) and interneurons [51]. The

dentate gyrus is separated into three layers, with the majority of mature granule cell bodies located in granule cell layer. These mature granule cells contain a network of dendrites which reach into the molecular layer of the dentate gyrus. EC afferents are projected towards these dendrites within the molecular layer. Granule cells have long axonal processes which extend down into both polymorphic layer of the dentate gyrus, sometimes referred to as the hilus, as well as the CA3 [52]. Axons originating from granule cells are referred to as mossy fibres, due to the presence of large boutons on the axons, referring to these axons as mossy fibres; these mossy fibres then project to the CA3 subregion as the major output of the dentate gyrus. While the cell bodies of mature granule cells are typically be found in the granular cell layer, other forms of granule cells can be found in the surrounding cell layers, such as semilunar granular cell in the inner molecular layer, ectopic granule cells in the hilus region and adult - born granule cells found in the subgranular layer [53].

Hilar mossy cells are a different cell type, named as such due to the appearance of thorny excrescences on the soma and are found in the hilus where they act as modulatory neurons [53]. These mossy cells project back into the molecular layer of dentate gyrus. The dentate gyrus contains multiple GABAergic inhibitory interneurons, such as MOPP (molecular layer perforant path associated) cells, axo-axonic cells, basket cells, HICAP (hilar-commissural associational path) and calretinin-expressing hilar cells (CR)1 cells many of which are found within the molecular layer of the dentate gyrus, which are thought to have a regulatory effect on granule cell activity and are important for memory function [54]. Many of these interneurons are found within the hilus of the dentate gyrus, although basket cells and axo-axonic cells originate in the granular cell layer, and MOPP cells originate in the outer molecular layer [53].

Unlike the dentate gyrus, all three CA regions contain only one excitatory cell type: the glutamatergic pyramidal cells . The soma of these neurons are tightly packed to a form the pyramidal cell layer [55, 56]. In the CA3 region, apical dendrites are projected away from the soma and through the stratum radiatum, stratum lucidum and the stratum lacunosum molecular layer. The pyramidal cells receive three means of input within these layers not only from the dentate gyrus, but also from the entorhinal cortex and from lateral axon collaterals of other pyramidal cells within the CA3 region [52]. Pyramidal neurons also contain basal dendrites within the stratum oriens layers protruding from the soma [57]. Axons from CA3 pyramidal neurons pass through the stratum oriens, where they form the Schaffer collateral (Figure 3), a direct pathway from the CA3 to the CA1 subregion [58]. The afferent axons from pyramidal neurons in the CA1 region then project out of the hippocampus proper, through the stratum oriens and alveus layers away from the hippocampus into the subiculum, the major output for the hippocampus proper [59]. The subiculum, which also consists of pyramidal cells, send out projections to the surrounding limbic structure, with some cells projecting back to the entorhinal cortex as well [60].

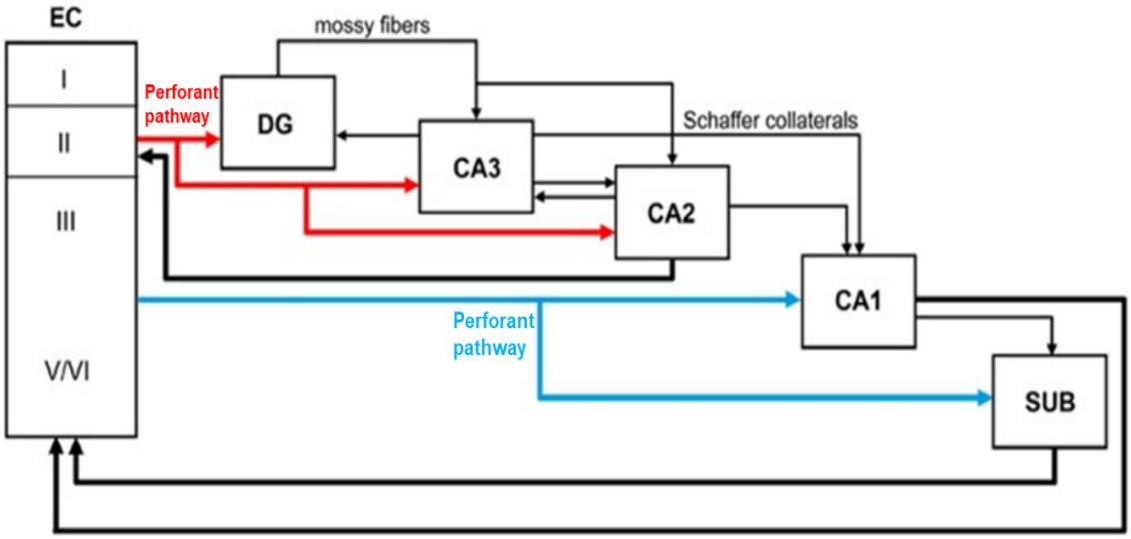

Figure 3. The connections between the subregions in the hippocampal formation. This image is taken and adapted from the original created by Llorens-Martín et al., 2014 ([61]) which is available under the creative commons licence. The connections between the entorhinal cortex (EC) and the DG and CA3 (red) and CA1 and subiculum (blue) via the perforant pathway is shown.

The hippocampus is an especially important region for long-term and spatial memory [62], which can be seen in patients with dysfunctional hippocampi who show severe memory impairment. Lesions to the CA1 subregion resulted in severe memory impairment, suggesting that CA1 subregion is particularly important for long-term memory [63]. Although the hippocampus has been shown to not as strongly affected in DLB as it is in AD, analysis in left, right and total hippocampal volume shows a significant decrease in patients suspected with DLB compared to control groups [45]. This was also seen when examining DLB patients using brain imaging, which found that atrophy of the hippocampus was seen in DLB [64]. Using post-mortem tissue from DLB patients has also shown that the hippocampus is affected to a certain extent by Lewy body pathology. Whilst studies have shown that there is low Lewy body presence, Lewy neurites can be seen most prominently within the CA2/3 regions [41, 48]. Alpha-synuclein immunoreactivity has also been detected within the EC in DLB

patients, which were determined to represent classic Lewy bodies [41, 48, 65]. These finding show that Lewy body pathology occurs within the hippocampal region, which when accompanied by atrophy in total hippocampal volume, may be responsible for the memory and cognitive deficits seen in DLB patients. Neuropathology within the EC may contribute to the clinical symptoms seen in DLB patients as well, due to the region's key role in spatial memory and sensory information processing [66].

1.1.3. Treatment of DLB

As with many other neurodegenerative diseases. The search for a treatment which is able to target the neuropathology and cure DLB disease has so far proved largely unsuccessful. DLB patients are treated for their symptoms, but due to contra-indication and side-effects of the drugs, the availability of treatment can be limited. DLB patients have severe sensitivity to antipsychotic drugs (such as haloperidol) including severe, sometimes irreversible parkinsonism and impaired consciousness, which should therefore be avoided. Guidelines have listed different treatments to treat the various symptoms seen in DLB [17]. Cholinesterase inhibitors for example, such as donepezil, have been administered to patients showing memory and attentional problems, and SSRI drugs [67] are used to treat symptoms such as depression. Whilst these might treat the symptom, finding a treatment for DLB would be beneficial for actually targeting the neurophysiological processes that cause DLB, and therefore detailed research into the disease is important.

1.2. Role of alpha-synuclein in DLB

1.2.1 Aggregation of alpha-synuclein and Lewy body formation

The protein alpha-synuclein, which is a major component of Lewy bodies, has been identified as a member of the synuclein family. In addition to alpha-synuclein, the

synuclein family also includes beta-synuclein and gamma-synuclein. The alpha-synuclein gene (SNCA) has been localised to chromosome 4q31, while the beta-synuclein gene (SNCB) to chromosome 5q35 [68] and gamma-synuclein (SNCG) to chromosome 10q23.2- q23.3 [69]. The synuclein family share a high homology with each other, with an approximately 61% homology between alpha-synuclein and beta-synuclein [70], and the synuclein proteins each contain between 127 and 140 amino acids [70]. The synuclein family proteins are intrinsically unstructured and contain between five to seven imperfect 11 amino acid repeats with the consensus sequence KTKEGV [71]. Each member of the synuclein family consists of a lipid-binding N-terminus and an acidic C-terminus. The alpha-synuclein protein also contains a particular segment within the N-terminus, identified as the non-amyloidogenic component (NAC) of amyloid protein, which is prone to aggregate [72, 73]. The NAC region consists of 35 amino acids and forms a central hydrophobic region of the alpha-synuclein protein, and is a fragment that has also been found in amyloid plaques typically associated with AD

Both alpha-synuclein and beta-synuclein are predominantly found in the CNS. Whilst gamma-synuclein can be found within the brain, gamma-synuclein is predominantly in the peripheral nervous system. Additionally, the SNCG gene overexpression (otherwise known as the BCSG1) was identified as a possible marker of breast cancer [74], suggesting a wider role of the protein outside the brain.

Research has shown that alpha-synuclein has an important role in many different functions, including the regulation of the vesicular pool in presynaptic nerve terminals [75]. These particular functions are closely related to its localisation, as alpha-

synuclein is normally found predominately within the presynaptic membranes in most neurons in the CNS [76]. Alpha-synuclein has been shown to be involved in other neuronal functions, including for example lipid binding [77]. Alpha-synuclein is an intrinsically unstructured protein and so can be found freely within the presynaptic terminal, but also may also be lipid-bound [78]. Alpha-synuclein protein is able to bind to lipid membranes through its N-terminus section. This amino-terminal section, which contains multiple lysine residues, binds to negatively charged proteins.

Beta-synuclein protein is also found within the presynaptic nerve terminals, similarly to alpha-synuclein [79]. Coupled with the high homology to alpha-synuclein, this has led researchers to suggest that beta-synuclein plays a similar cellular role as alpha-synuclein. As part of my project focuses on beta-synuclein, this particular protein will be discussed in more depth later.

The current understanding of Lewy bodies formation and neuropathological process has mostly been inferred from information collected from PD studies, with there being relatively little information on DLB pathology itself. Whilst it is unknown whether the process is exactly the same in both DLB and PD, the presence of Lewy bodies in both diseases, as well as several alpha-synuclein aggregates intermediates, might suggest that Lewy body formation may develop in a similar fashion to PD. Efforts to examine Lewy body pathology progression in DLB specifically has suggested that within the cerebrum pathology is initially seen in the amygdala, and then seen later in the limbic cortex and then the neocortex, however the progression of pathology within other subcortical regions have not been examined [36].

PD research has shown that there are three major ways which can increase the probability for the aggregation process; multiplication (either duplication of triplication)

of the SNCA gene, a mutation of the SNCA gene or post-translational modification of the protein. During the aggregation process alpha-synuclein's secondary structure is altered to produce aggregation prone proteins (Figure).

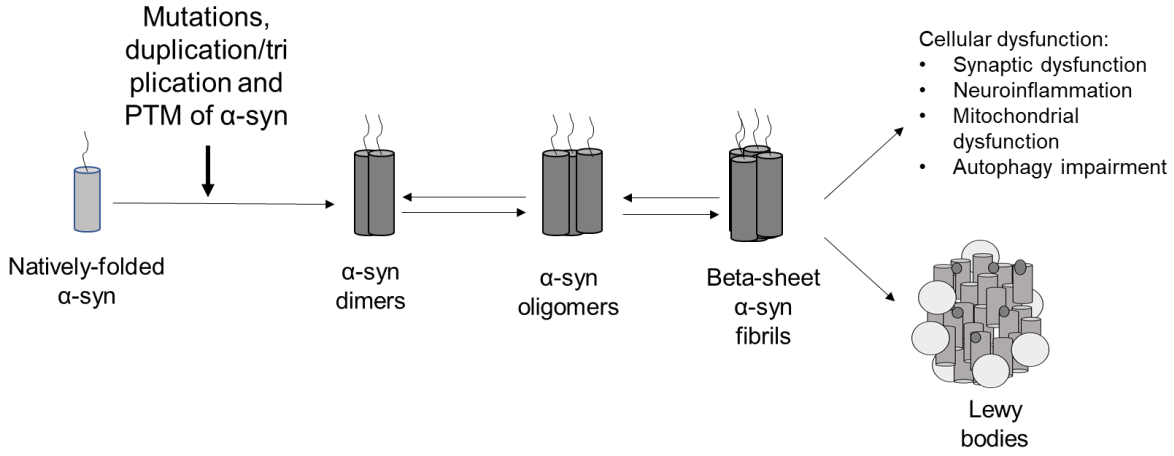

Figure 4. Progression of alpha-synuclein fibrillisation, Lewy bodies formation and cellular dysfunction. When alpha-synuclein receives post-translational modifications (PTMs) or become mutated, its secondary structure is altered into an alpha-helical formation. These altered alpha-synuclein proteins can form dimers and densely packed fibrils, which can cause cellular dysfunction. Alpha-synuclein also forms a large part of the Lewy body aggregate. Lewy bodies also contain other proteins including ubiquitin (darker, small circles) and tau protein (lighter, large circles).

Aggregation of these proteins cause the generation of beta-sheet rich insoluble oligomers and fibrils, which bind with other oligomers form a large component of Lewy bodies and Lewy neurites [80]. Lewy bodies are typically between 5-25µm in diameter, with an eosinophilic core and an outer zone containing alpha-synuclein filaments, roughly 5-10nm in diameter surrounding the core [42, 81]. Whilst alpha-synuclein is a key component, Lewy bodies are comprised of other proteins as well, including ubiquitin [82], Parkin [83] and in some cases tau [84].

The identification of the toxic form of alpha-synuclein has been in dispute, however common consensus, as reviewed in [85] has suggested that the Lewy bodies found in

PD or DLB patients are not primarily responsible for cellular dysfunction, and that in fact it is the insoluble oligomeric aggregates which precedes Lewy body formation, that are responsible for the toxic effect on the cells.

1.2.1.1. Post-translation modification of alpha-synuclein

After translation, alpha-synuclein undergoes post-translation modification which involves the addition of several different molecules such as phosphate or ubiquitin, or the removal of a fragment of the protein through truncation.

Phosphorylation of alpha-synuclein in particular has been widely researched after the identification of phosphorylated alpha-synuclein at serine-129 (pS129) in cingulate and temporal cortex of DLB patients [86]. Studies have shown that phosphorylation at the site S129 can alter alpha-synuclein interaction with other proteins and is able to directly affect alpha-synuclein turnover. A significant accumulation of pS129 alpha-synuclein has been found in DLB brain tissue, highlighting a possible connection between increased pS129 and DLB pathology, although whether this significant increase in pS129 within Lewy bodies indicates a direct association between alpha-synuclein and neuropathology seen in DLB is not fully understood [87]. A similar relationship between alpha-synuclein phosphorylated at S129 and alpha-synuclein fibrillisation was seen in mice models as well [88]. It was discovered that phosphorylation of alpha-synuclein is caused predominantly by the enzyme Polo-like kinase 2 (PLK2) and an increase in PLK2 has been seen in DLB patients [89], thus highlighting further the increased phosphorylation of alpha-synuclein in DLB pathology.

Alpha-synuclein protein is also susceptible to nitration. When mitochondrial release the reactive oxygen species (ROS) peroxynitrile (ONOO-) into dopaminergic cells, this highly reactive nitrate reacts with alpha-synuclein protein, causing alpha-synuclein to fibrillise and form aggregates. Oligomeric alpha-synuclein isolated from DLB patients have identified the presence of nitrated alpha-synuclein, which may be associated with mitochondrial damage [90]. This has been supported by a cell model expressing nitrated alpha-synuclein, which was shown to cause cytotoxicity [91].

Ubiquitination of alpha-synuclein is another common modification of alpha-synuclein protein which is able to affect alpha-synuclein function. It has been shown that alpha-synuclein inclusion found in DLB patients contain ubiquitinated alpha-synuclein, which was not seen in control groups [92]. There have been several regulatory proteins implicated in the degradation of alpha-synuclein aggregates, which includes the major E3 ligases Nedd4 and CHIP (C-terminus of U-box domain of co-chaperone Hsp70-interacting protein). Whilst Nedd4 initiates the alpha-synuclein ubiquitination through lysine-63 [93, 94], CHIP mediates alpha-synuclein ubiquitination through its U-box domain to bind to alpha-synuclein protein [95]. Whilst these two E3 ligase have been shown to recognise and bind to specific sequence within the alpha-synuclein gene, promoting the addition of polyubiquitin chain and its degradation through the lysosomal pathway, a different E3 ligase, SIAH-1 (seven in absentia homolog) [96], has been shown to ubiquitinate alpha-synuclein but does not target it for degradation. Instead SIAH-1, which is thought to ubiquitinate alpha-synuclein at four possible lysine residues (K21, K23, K32 and K42) was shown to promote alpha-synuclein aggregation and increased cell toxicity by increasing alpha-synuclein insolubility [96]. Although the exact mechanism by which this occurs is not known, this does suggest that the various regulatory proteins have different effects on alpha-synuclein degradation.

C-terminally truncating alpha-synuclein has been shown to alter alpha-synuclein structure, leading to increased fibrillation of alpha-synuclein and accelerated

aggregation of the protein. There are a few candidates for proteins which proteolyse alpha-synuclein to form this truncated protein, such as neurosin, Matrix metalloprotease 3 and calpain I [97-100] When cleavage occur within the N-terminus, near the NAC region, this may have a more beneficial role and reduce aggregation, however if cleavage occurs within the C-terminus, roughly after 97 amino acids, this may increase aggregation [101]. Lewy bodies isolated from DLB patients have determine the presence of truncated alpha-synuclein protein, further highlighting its role in DLB pathology [48, 101].

1.2.1.2. Alpha-synuclein genetic mutations in DLB

In addition to the post-translational modification of alpha-synuclein, mutations in the alpha-synuclein protein has also been shown to be involved in DLB pathology. Not surprisingly, the majority of these mutations occur within the alpha-synuclein gene. Typically these mutations of alpha-synuclein occur near the NAC region of the protein, which has been shown to be an important region for the binding to other alpha-synuclein proteins and may initiate the aggregating process [102, 103]. Whilst the alpha-synuclein mutation A53T has been identified in PD patients who have reported dementia as a symptom, whether it is also seen in DLB patients is still not completely clear. The alpha-synuclein mutant E46K is another possible DLB specific mutation. The E46K mutated SNCA gene in a probable case of DLB was detected in a family from the Basques Country. The family in question showed Lewy bodies and Lewy neurites present in the substantial nigra, locus coeruleus and the hippocampus, and shows symptoms of visual hallucination and impairment in attention, which are signs of DLB pathology [104].

1.2.2. Cellular dysfunction in DLB

Whilst the process of neurodegeneration can be complex, there are several key processes which are consistently compromised. Whether these are caused by aggregating proteins directly is still largely uncertain. Disruption in synaptic function, decreased autophagy processes and mitochondrial dysfunction are three such cellular processes affected in multiple neurodegenerative diseases [105-108]. The exact biological pathological underlying the DLB in particular is not so generally well-known, and as such the literature behind DLB is not very extensive. However, the available literature examining tissue taken from DLB patients have highlighted specific cellular dysfunctions in DLB.

Synaptic function is a fundamental process which underpins neuronal transmission. Neurons communicate by sending neurotransmitters from a presynaptic nerve terminal, across the synaptic cleft, which then binds to receptors, continuing the action potential propagating down the post-synaptic neuron. This process has been found to be severely affected in DLB cases, which can be accompanied by a reduction in the dendritic spines, resulting in fewer connections between neurons, and an impairment in the neurotransmitter pool [109].

Autophagy is the process of segregating and degradation of damaged protein, organelles and debris. When autophagy is initiated, a double-membrane structure, a phagosome, is recruited to the area, where it encircles the target. The autophagosome fuses to form a continuous double membrane around the debris. Once completed, lysosomes are then recruited, where they bind to the autophagosome. Lysosomes contain a plethora of enzymes, such as several cathepsin proteins. These enzymes are released into the autophagosome, which degrade the substrates within. Certain papers examining the autophagosome-lysosomal pathways in synuclein-related

pathology has provided some evidence of reduced lysosomal function, includes reduced lysosomal enzyme production and reduced clearance of autophagosomes [110, 111]. As cell death occurs, lysosomes are recruited to enhance degrade debris within the cells. In addition to lysosomal disruption, autophagosome function is often affected in DLB as well, through the impairment of autophagosome clearance, which overloads the autophagy system and prevents proper cell debris and protein degradation [112].

As mentioned earlier, mitochondrial dysfunction is another example of cellular dysfunction which occurs during neurodegenerative diseases. Mitochondria have a diverse range of functions within the cell, including ATP production, calcium signalling and ROS production [113-115]. Mitochondria and alpha-synuclein in particular has been shown to be closely linked [116], which is further supported by the relationship between mitochondrial function and DLB, where for example DLB patients were shown to have significantly reduced mitochondrial complexes I-IV compared to control groups [116, 117]. Such changes in mitochondrial function will be discussed in the following section.

1.3. Mitochondrial function in Synucleinopathies

1.3.1. Mitochondrial structure and function

The generation of energy as ATP is a necessity for all cellular function and is achieved mostly via organelles called mitochondria, which are found abundantly within neurons throughout the nervous system. Mitochondria have a diverse number of functions in addition to energy production, such as its important role in calcium storage and neuronal survival [118, 119]. Mitochondria are unique organelles as they contain their own DNA, which is distinct from the chromosomal genome [120]. This mitochondrial DNA encodes for certain proteins, which are directly related to mitochondrial function and structure, however the majority of proteins required for mitochondrial function are imported through complex processes [120].

Mitochondria themselves are often varied in shape, but they contain in the centre a fluid matrix. This matrix is encased by the inner mitochondrial membrane (IMM), which is itself encased by a second membrane, known as the outer mitochondrial membrane (OMM) [121]. Both membranes contain many different proteins and channels which allow the passage of certain proteins through the double membranes into the matrix. Due to the fact that the majority of mitochondrial structural proteins are transcribed in the cell nucleus and not from mtDNA, the mitochondrial structural proteins need to be translocated through the mitochondrial membranes, the process of which has been reviewed before [122]. One of the key machineries in the transport of proteins into the mitochondria is the Tom and Tim complex proteins (Figure 5). The Tom proteins are situated on the outer mitochondrial membrane, with the Tim proteins on the inner mitochondrial membrane. The complexes are comprised of multiple subunits, with Tom40 and Tim23 forming the central pore proteins of the Tom and Tim complexes respectively [123]. The surrounding subunits play a role in guiding the traversing

proteins towards and through the complexes and across the mitochondrial membrane in towards the mitochondrial matrix.

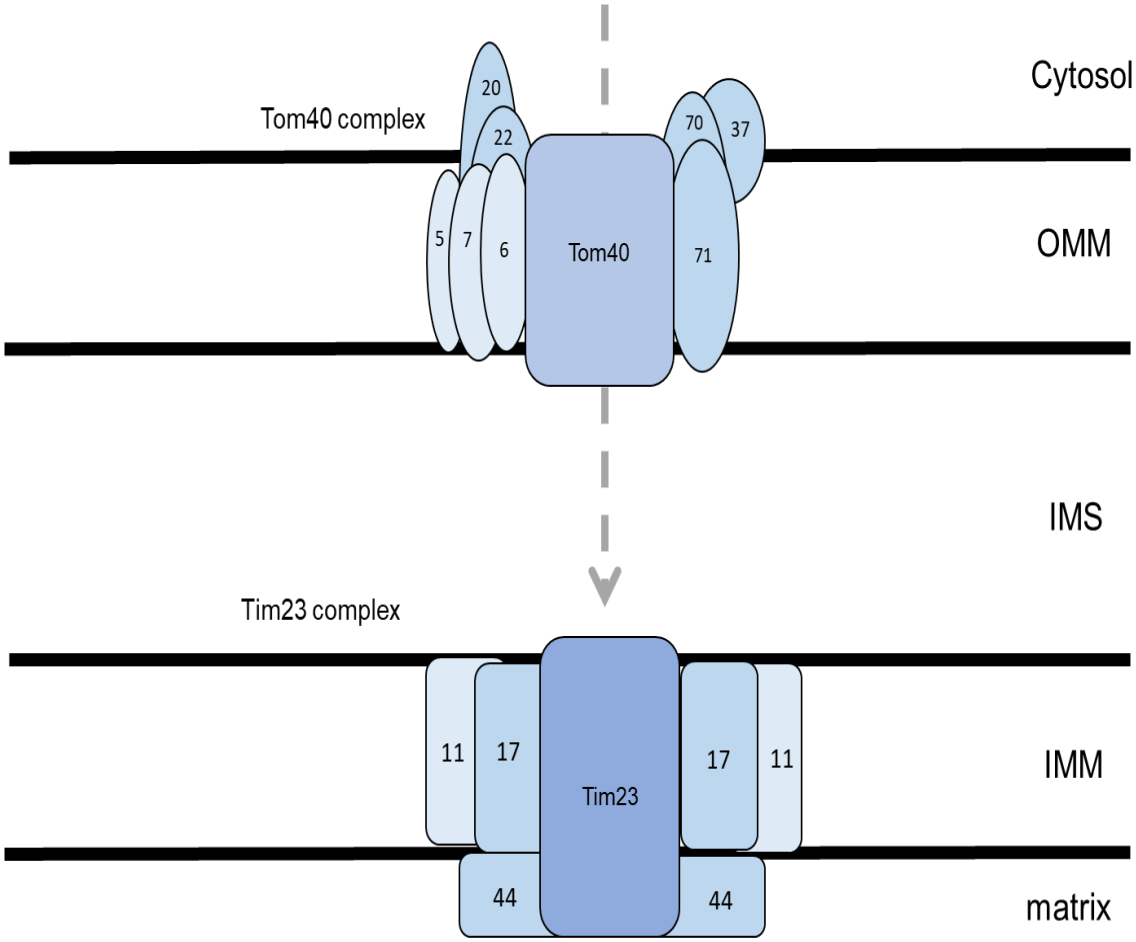

Figure 5. Tim and Tom machinery structure. Tom40 and Tim23 form the major pore within the OMM and IMM respectively. The Tom and Tim complex contains several different subunits (numbered) which help to direct the import of protein from the cytosol into the IMS and matrix respectively.

In addition to these transport proteins, there are multiple proteins required for the biochemical processes which occur within the mitochondria during respiration. The predominant location for the production of ATP takes place within the IMM. The electron transfer transport chain (ETC) is the major site of respiration and is comprised of multiple complexes (complexes I- IV) [124]. Electrons on complex IV, transferred

via a series of redox reactions along the ETC, are used to convert ADP to ATP, which is utilised by the cell as a form of energy.

Both NADH (nicotinamide adenine dinucleotide) and $FADH_2$ (flavin adenine dinucleotide) are cofactors released from the tricarboxylic acid cycle (TCA) and have a prominent role in metabolism [125]. During the TCA cycle, three NADH molecules are produced from NAD+, as a result of the dehydrogenation of isocitrate, alpha-ketoglutarate and malate as seen in the review by [125]. $FADH_2$ on the other hand is produced from FAD, as a result from the oxidation of succinate into fumarate, catalysed by succinate dehydrogenase, an enzyme found on the inner mitochondrial membrane and which also participates in the electron transport chain as well as the TCA [126]. NADH and $FADH_2$ become oxidised by complex I and complex II of the ETC, which subsequently releases protons into the mitochondrial matrix [127]. These protons are used to fuel the proton motive force across the mitochondria and is ultimately linked with the membrane potential across IMM. Protons are pumped out into the inter membrane space, via complex I – IV, which then drives the flow of protons back into the mitochondrial matrix through the enzyme F_1F_0 -ATPase, which comprises of two major subunits, the F_1 and F_0 subunits [128]. F_1F_0-ATPase catalyses the phosphorylation of an ADP molecule that binds to the F_1-stalk to form ATP [129]. Whilst ATP is produced during the Kreb's cycle, in the matrix, as well as during glycolysis, which is an oxygen–independent process, the majority of ATP produced (34 ATP) is from the ETC. Dysregulation in F_1F_{0-} ATPase has been previously shown to be involved in neurodegenerative diseases such as AD, which leads to a decrease in oxidative phosphorylation [130].

The mitochondrial membrane potential is generated by the net flow of proton pumped from the ETC within the IMM into the IMS down a proton gradient, leading to an overall

negative charge across the mitochondrial membrane [131]. It is a crucial aspect of mitochondrial function, as not only does it drive the generation of ATP through oxidative phosphorylation by the F_1F0-ATPase complex, it is also necessary for the import of charged proteins into or out of the mitochondria, with cations preferentially moving into negatively-charged mitochondria, and anions moving outwards. This import process is important as the majority of mitochondrial structural proteins are translated in the cell nucleus. Many of these nuclear-encoded mitochondrial proteins often contain a mitochondrial targeting sequence (MTS) within its N-terminus, which guides them towards the correct mitochondrial compartment [132]. The mitochondrial membrane potential and ATP in mitochondria function are therefore important in mitochondrial stability and function and so are maintained at a stable level.

The mitochondrial membrane potential also has a direct effect on the permeability of the mitochondrial membrane, which is controlled mostly by the mitochondrial permeability transition pore (mPTP). The mPTP is a transport protein complex found throughout both the OMM and IMM that will in the case of Ca^{2+} ions overload open, which therefore rapidly increases the permeability of the membrane, and allows the influx of large proteins with a size of up to 1.5kDa [133, 134]. This process was first explored in 1979 by the scientists Haworth and Hunter [135]**.** Aside from Ca^{2+} overload, the opening of the mPTP pore can also be affected by certain metal ions (such as Mg^{2+}), metabolic environment, pH or ROS levels [136]. When the mPTP opens and ions diffuse across the membrane, this causes rapid depolarisation in the mitochondrial membrane potential, leading to further mitochondrial function impairment, including ATP depletion through mitochondrial uncoupling and inhibition of oxidative phosphorylation, and ultimately mitochondrial swelling [137]. The mPTP has been found to contain two major complexes; these include the proteins VDAC

(voltage dependent anion channel) and ANT (adenine nucleotide translocator). VDAC, which is dependent on the mitochondrial membrane potential to open, is found embedded within the OMM, and forms a large part of the pore leading into the IMS from the cytoplasm. When the mitochondrial membrane potential is altered this has a direct effect on the probability of mPTP opening. ANT contains a dimer forming a pore through the IMM. ANT in particular was determined to be an essential component of the mPTP, which is responsible for the transfer for ADP into the matrix, which has been converted from ATP [138]. As well as these two major proteins, there are other smaller regulatory protein which are also part of the mPTP complex. For example, the cyclophilin D protein has been found to bind to the ANT protein; in particular found within the matrix section of the ANT protein. The function or importance of the mPTP has been explored since the emergence of various drugs and compounds which have been found to alter mPTP activity, including the drug cyclosporin A. Cyclosporin A (CsA) has been used clinically, typically used to suppress the immune response during organ transplantation. Further research into its method of action, discovered that it is able to prevent the mPTP from opening. In particular, the drug is thought to act by binding to the protein cyclophilin D (CypD). The CypD/CsA complex has been proven to inhibit the production of the enzyme calcineurin which is able to stimulate an inflammatory response [139].

1.3.2. Mitochondrial alterations in synucleinopathies

Mitochondrial dysfunction is one the core features in PD and DLB pathology (an overview is seen in Figure 6 below). Post-mortem brain tissues taken from PD and DLB patients have shown alteration in mitochondrial function. For example frontal cortex tissues taken from DLB patients have reduced mRNA and protein expression of mitochondrial ETC subunits and is associated with a reduced activity in four

mitochondrial complexes (complex I - IV) [117]. The examination of post-mortem brain tissues from PD patients have also shown an impairment in energy production, as seen as a reduction in ATP synthase within the SN [140]. Inhibition of complex I was found to be severely reduced in PD patients [141, 142].

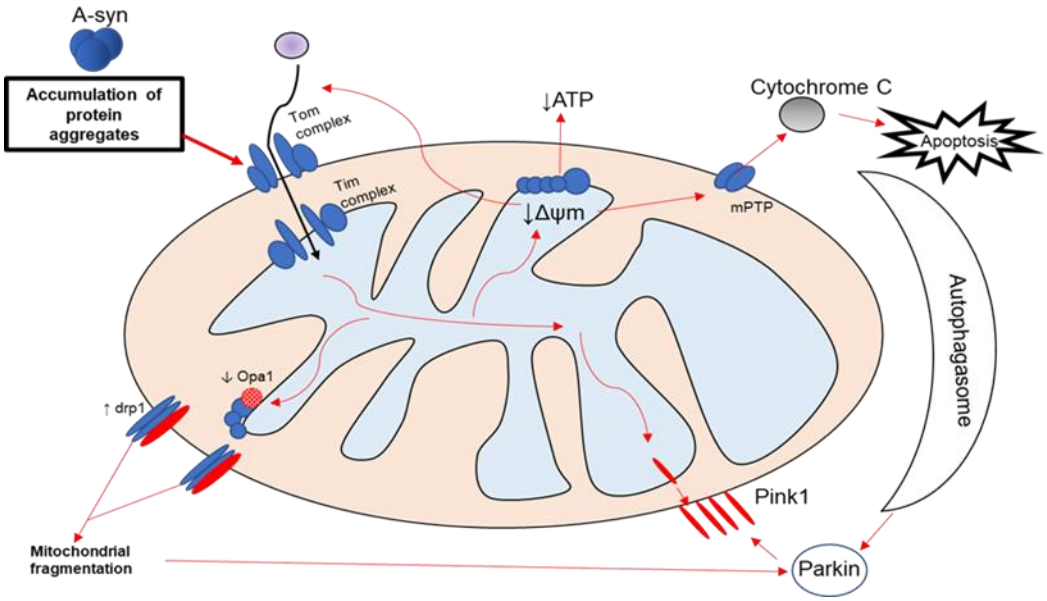

Figure 6. Overview of mitochondrial disruption in response to alpha-synuclein aggregates. Alpha-synuclein aggregates have been found to cause mitochondrial dysfunction. In particular, alpha-synuclein aggregates can prevent mitochondrial import into the mitochondria, cause disruption in Drp1 and Opa1 expression, cause disruption in mitochondrial membrane potential, increase OMM-bound Pink1 protein and increase mitophagy and apoptosis. mPTP = mitochondrial permeability transition pore. ΔΨm = mitochondrial membrane potential.

Due to its major role within synucleinopathies, the effect of alpha-synuclein on mitochondrial function has often been explored in models of PD. Alpha-synuclein protein, which has been discovered to be able to bind to mitochondria directly [116], is able to aggregate and cause mitochondrial disruption. As was seen with the examination of post-mortem brain tissue from PD patients, certain mouse models of PD have showed impairments in mitochondrial respiration. Mice overexpressing the A53T mutant form of alpha-synuclein presented abnormal activity of complex IV of the ETC within the spinal cord [143]. In addition, mice injected with the neurotoxin MPTP,

which is commonly to generate PD mouse models, caused impairment in motor function as well as reduced ATP levels and increased cell death [144]. Alpha-synuclein oligomers within cells are also to disrupt mitochondrial membrane permeability by inducing the MPT pore to open, causing the mitochondria to swell, produce enhanced levels of ROS, which was accompanied by increased cell death [145]. Certain cell models which overexpress aggregated alpha-synuclein have also showed strong mitochondrial impairment, showing inhibition of complex I of the ETC in the mitochondria [146].

Studies on changes in mitochondrial function have also identified abnormalities in mitochondrial quality control. Mitochondrial within cell lines containing high levels of alpha-synuclein appear fragmented, which is thought to be a result of increased mitochondrial fission, indicating a disruption in mitochondrial dynamics, and was able to be reversed when mitochondrial fusion was promoted [147].

Whilst sporadic causes of neurodegenerative diseases are more common, 10% of most neurodegenerative disease are familial in form. In patients with PD, the more common genetic mutations occur within proteins involved in the mitophagy process: the Pink1 and Parkin mitophagy genes. Mutations in the serine/threonine kinase Pink1 for example have been shown to cause early-onset recessive hereditary PD. Multiple Pink1 mutations have been identified, including Q129X, G440E, Q456X and many others, which have been shown to occur throughout the entire Pink1 protein [148]. Some of the Pink1 mutations, the Q129X and mutation G440E in particular, was found to occur in a homozygous state and were shown to be the most pathogenic mutations. Using mouse models expressing mutations in Pink1, a deficiency in complex I of the ETC was seen, showing that it can cause a disruption in the normal function of the mitochondria by affecting ATP generation [149].

Aside from Pink1, mutation in the protein Parkin, an E3 ubiquitin ligase coded by the gene PARK2, has been discovered in PD patients. Mutations in Parkin has in particular been associated with autosomal recessive PD in adults over 45 years of age, presenting as an early-onset form of the disease [150]. Research also found that Parkin was localised to Lewy bodies in both PD and DLB patients, supporting the importance of Parkin in synucleinopathies. Parkin, which can be found in the cytoplasm, facilitates the covalent addition of ubiquitin onto OMM surface proteins and so works together with Pink1 to target damaged mitochondria for uptake into the autophagosomes [151]. It has been shown that Parkin deficiency can promote mitochondrial dysfunction and an increased susceptibility to oxidative stress [152]. A common form of Parkin mutation was found as single-nucleotide substitution within exon 7, where a cysteine in position 924 (C924T) is converted to a threonine amino acid, identified in the SN from a PD patient [83]. Several other mutants of Parkin have been identified, including R42P, R275W, A240R, and T415N [153]. These mutations listed all occur within the ubiquitin-like domains in the N-terminus of Parkin (RING-1 and -2 domains) which are zinc-associated and provides stability to the protein structure. The Parkin mutations were shown to have reduced ubiquitination, affecting mitophagy activity [153]. Using another Parkin mutant, Q311X, researchers have developed a Parkin-related mouse model, where the mutant Parkin protein is expressed under a dopamine transporter promoter [154]. These mice showed increased alpha-synuclein accumulation, oxidative damage, dopaminergic neuronal loss, as well as exhibiting motor impairment.

1.3.3. Mitochondrial quality control

Due to their complexity as an organelle and their important role in production energy for the cells, they are at high risk of dysfunction, which can be devastating when it

occurs. Mitochondria have therefore developed certain regulatory systems by which they can ensure mitochondrial population quality is upheld. These processes involved both mitochondrial dynamics and mitophagy processes.

Mitochondria are able to directly affect the general mitochondrial population by interacting directly with other mitochondria. The total number of mitochondria within the cells is not constant, with the numbers either slightly increasing or decreasing constantly. Mitochondria are able to undergo either mitochondrial fusion or fission, which causes mitochondria to either fuse together or divide into two mitochondria, respectively. During mitochondrial fusion, the receptor proteins Mitofusin 1 and Mitofusin 2 embedded on the OMM fuse with the same protein on the OMM of a second mitochondria. During mitochondrial fusion, the receptor proteins Mitofusin 1 and Mitofusin 2 localised on the OMM fuse with the same protein on the OMM of a second mitochondria. Once they bind together, the OMM is broken down, exposing the IMM of both mitochondria. Opa1 proteins on the inner membranes of both mitochondria, then bind together in a similar manner, which then allows the IMM to lyse. The IMM and OMM binds again with the second mitochondria, which then forms a continuous membrane across the combined matrices, forming a new elongated mitochondrion [155]. During mitochondrial fission, a single mitochondrion is split into two smaller individual mitochondria. Here, it is thought that the mitochondrion undergoing the mitochondrial fission is encircled by a multimeric ring of the mitochondrial fission protein Drp1. The Drp1 ring encircles the mitochondrion, causing the mitochondrial membranes to lyse, and then split to form two completely new mitochondria. Whilst Drp1 is regarded as the major protein in mitochondrial fission, additional mitochondrial fission proteins Fis1 and Mff can also be found on the OMM and are involved in the mitochondrial fission process [156].

These two processes are finely balanced, and under normal conditions, they work together to ensure the mitochondrial population is functional. This system works to help prevent the unhealthy mitochondria from also fusing with healthy mitochondria, [157].

The process by which mitochondria is removed from the cells is also very important and so mitochondria need to have close connection with autophagy proteins. Autophagy is the process by which damaged organelles are engulfed by autophagosomes, broken down by enzymes secreted by lysosomes which fuse with the autophagosomes [158]. Mitochondria have a specific link with the autophagy process, leading to the process known as mitophagy [159]. Here, mitochondria single themselves out for the mitophagy process, where autophagosomes are recruited to the mitochondria and are then lysed by enzymes within the lysosomes. Damaged mitochondria are able to attract autophagosomes through the expression of the proteins Pink1 (PTEN-induced putative kinase 1) and Parkin [160]. Pink1 is a mitochondrial serine/threonine kinase, normally localised in the IMM. Pink1 is a nuclear-encoded protein, and therefore translocates to the mitochondria from the nucleus. Pink1 proteins contain an MTS which is responsible for the transport into the mitochondrial matrix, via the Tom and Tim complexes. Upon reaching the mitochondrial matrix, Pink1 is cleaved by the mitochondrial enzyme Presenilin Associated Rhomboid Like protease (PARL) at position Ala-63 and Phe-104; reducing the originally 63kDa protein to a roughly 53kDa protein [161]. This causes the protein to be further sorted into the IMM. When mitochondria undergo damage, Pink1 protein migrates to the OMM, causing Pink1 protein to accumulates on the OMM and are then auto-phosphorylated. The activated Pink1 proteins then phosphorylate the OMM protein ubiquitin at serine 65. Additionally Pink1 proteins also phosphorylate the

ubiquitin-like domain on Parkin, activating Parkin and stimulating the degradation of the mitochondria [162]. Additionally, when mitochondrial damage occurs, the import of the Pink1 protein through Tom20 is blocked, which prevents uptake of Pink1 into the mitochondria through the OMM, further increasing the accumulation of Pink1 on the OMM.

Aside from ATP generation, one of the roles of the mitochondria involves the release of ROS and the initiation of pathways involved in cell death, where notably the apoptotic protein cytochrome C is released. Once the mitochondria undergo severe damage, the OMM is lysed, allowing the release of proteins situated in the mitochondrial IMS out into the cytoplasm [163]. Cytochrome C normally has an important role within the ETC [164], where it acts to transfer electrons from complex III and complex IV. Cytochrome C itself has been proposed to stimulate ROS production. ROS molecules include hydrogen peroxide (H_2O_2), superoxide anions (O_2^-), hydroxyl radical (OH●), and the free radical nitric oxide (NO) [165]. These molecules are normally released as by-products and are produced by the mitochondria as a result of mitochondrial metabolism. ROS molecules are therefore generated from the ETC, which is the site of oxidative phosphorylation in mitochondria. The generation of ROS under normal metabolic conditions is thought to play a role in various cellular signalling pathways including the cell cycle [166]. For example H_2O_2 is constantly released into the cytoplasm and is thought to be involved in signal transduction, oxidative stress response and cell apoptosis [167]. However, when mitochondria are damaged, the generation of cytosolic oxidants are increased to a significant amount, which go on to cause further harm to the cell by damaging DNA, RNA and proteins in the cell. H_2O_2 may be generated through several different ways; for example H_2O_2 can be generated through the enzyme mono-amino oxidase, which is found on the OMM

and converts O_2 to H_2O_2 [168]. Studies have also showed that the H_2O_2 originates from the free radical superoxide ($O_2^{\bullet -}$) generated from mitochondrial respiration [169].

A major mitochondrial sub-compartment for ROS production was shown to be complex III of the ETC, where O_2 is converted to superoxide, $O_2^{\bullet -}$ [165]. The $O_2^{\bullet -}$ molecules are generated from the part of complex III known as ubiquinone (Q), through the reduction of O_2 molecules. The Q complexes are found on two sites on the IMM; with one facing the matrix (Q_1) and the other facing the IMS (Q_0). At both sites, the Q complex catalyses the conversion from O_2 to $O_2^{\bullet -}$, which is then released into the matrix (Q_1) and the IMS (Q_0). The $O_2^{\bullet -}$ molecules are then further converted to H_2O_2 by the enzyme Mn-superoxide dismutase (Mn-SOD), a form of SOD which has been found in the mitochondrial matrix and the IMM [170, 171], the chemical process of which is discussed in detail in the review [172].

When hydroxyl radicals are excessively produced, they can have a lethal effect on the cell, causing intense damage to even lipids and carbohydrates. Hydroxyl radicals are produced by the interaction between H_2O_2 and $O_2^{\bullet -}$ [173]. Research into this interaction have suggested that hydroxyl radicals are produced through the Fenton reaction. This reaction involves the reduction of iron ions (Fe^{2+}), which acts as ligands for both H_2O_2 and $O_2^{\bullet -}$. Under the Fenton reaction, Fe^{2+} reacts with H_2O_2 to form the $OH^{\bullet}$ radical, Fe^{3+} ion, and hydroxyl ion (OH-) [174]. The Fe^{3+} ion then reacts with $O_2^{\bullet -}$ to form O_2 and another Fe^{2+} ion. These iron ligands are known to be abundant within the mitochondria, and so this reaction readily occurs during oxidative stress conditions, leading to significantly increased $OH^{\bullet}$ and severe cell damage.

The free radical NO has also been identified as an important ROS molecule. This free radical is produced by the enzyme nitric oxide synthase (NOS), which converts L-

arginine and O_2 to NO [175]. There have been reports of NOS expression in all mammalian cells, including the endothelial and neuronal NOS isoforms. Certain papers have debated the presence of NOS found in mitochondria specifically, with some studies showing that NOS can be found specifically in the IMM; this is discussed in the review [176]. This NO is also then thought to have an effect on the mitochondria itself. NO is known as a vasodilator, which affect blood flow and oxygen release, which can indirectly affect blood supply to mitochondria, which disrupts respiration. In addition, NO can directly and reversibly bind to cytochrome C oxidase in the ETC and by doing so compete with O_2 which usually binds to cytochrome C [177].

1.3.4. Final comments

As mitochondrial dysfunction is one of the defining features of any neurodegenerative diseases, including PD and DLB, there is an increasing need to further our knowledge about the precise mechanisms that underlie the mitochondrial dysfunction seen in these diseases. Further information about how mitochondrial dysfunction which occurs within DLB patients specifically might provide possible targets for treating DLB.

1.4. Beta-synuclein

1.4.1. Beta-synuclein structure and function

The protein beta-synuclein, then known as the protein phosphoneuropeptide-14 (PNP-14), was first isolated from the bovine brain and was shown to have a molecular mass of 16kDa and consisted of 134 amino acids [178]. PNP-14, isolated from the human brain, was then found to show to be highly homologous to the 140 amino acid peptide discovered in the *Torpedo Californica*, known as alpha-synuclein [70]. It was then discovered that human beta-synuclein was ~61% homologous to alpha-synuclein, showing that the structure of beta-synuclein is very similar to that of alpha-synuclein. Furthermore, the molecular weight of beta-synuclein, at 16kDa, has also been discovered to be comparable to that of alpha-synuclein (14kDa) [179]. As with alpha-synuclein, beta-synuclein is an intrinsically unstructured protein, and contains six imperfect 11 amino acid repeats with the consensus sequence KTKEGV. Beta-synuclein contains a positively charged N-terminus and a hydrophobic C-terminus [178, 180]. Research into the structure of beta-synuclein has however shown that the major difference between alpha-synuclein and beta-synuclein is the presence of the NAC region within the N-terminus. This region, found in the central hydrophobic region in alpha-synuclein, has been shown to be important for causing the aggregation of synuclein [72]. This NAC region is however not present in beta-synuclein and so this has been correlated to its limited fibrillogenic properties. Additionally, unlike alpha-synuclein, post-mortem analysis has determined there is a lack of the beta-synuclein protein within aggregates seen in DLB/PD patients [181, 182]. Currently, little is known about the protein beta-synuclein in comparison to alpha-synuclein. However, studies have shown that beta-synuclein is expressed, like alpha-synuclein, throughout the CNS, and that expression of the beta-synuclein is, as with alpha-synuclein,

predominantly found in the presynaptic nerve terminals. Previous studies have shown that beta-synuclein can be found in several regions throughout the rat brain, such as the olfactory bulb, thalamus, pons, cerebellum, SN and hippocampus, showing a similar, although not entirely identical distribution pattern to alpha-synuclein [183, 184]. The precise function of beta-synuclein is largely unknown, however due to its proximity to alpha-synuclein, it is theorised that it may have similar functions to alpha-synuclein and so may have a role in synaptic transmission and vesicular pooling. In support of this, analysis into synaptic vesicle content has shown that both alpha-synuclein and beta-synuclein can be present within synaptic vesicles [185]. Some studies have also shown a possible role of beta-synuclein as a molecular chaperone, which can prevent aggregation of various proteins [186].

1.4.2. Interaction with toxic proteins

There have now been a few studies aiming to understand the interaction between beta-synuclein and its homolog alpha-synuclein [187-189]. The two proteins are thought to be localised in presynaptic terminals, throughout the CNS. The close proximity to each other suggests that interaction between the two proteins is at least possible. Research has found that when beta-synuclein is added to aggregation-prone alpha-synuclein the rate of alpha-synuclein aggregation was reduced and alpha-synuclein-related cellular dysfunction was alleviated [187-189]. Several different studies which have examined the effect of the addition of the beta-synuclein *in vitro* to alpha-synuclein expressing cells have previously been done. One research study used HEK293 cells transfected with wildtype human alpha-synuclein, which was then subsequently transfected with beta-synuclein [190]. They showed, using co-immunoprecipitation, that beta-synuclein and alpha-synuclein bind to each other, and that while alpha-synuclein accumulation was only seen in the cells expressing human

alpha-synuclein alone, cells transfected with beta-synuclein showed significantly reduced alpha-synuclein accumulation. In the same study, doubly transgenic mice which expressed both alpha- and beta-synuclein were developed. Behavioural analysis into these doubly transgenic mice showed an improvement in the motor dysfunction normally seen in alpha-synuclein only transgenic mice. In addition, these mice did not show the accumulation of alpha-synuclein seen in the alpha-synuclein only transgenic mice. These results were also subsequently seen by another research group [191].

The exact method by which beta-synuclein interacts with alpha-synuclein is not completely understood. However, one study has shown that the N-terminus region of beta-synuclein protein is particularly important [192]. The study tested different truncated versions of beta-synuclein to determine which section of the beta-synuclein protein is responsible for the interaction with alpha-synuclein. The study tested the co-immunoprecipitation between alpha-synuclein and five different beta-synuclein peptide fragments from within the N-terminus; 1-15aa (amino acids 1-15), 16-27aa, 28-38aa, 39-50aa and 51-61aa. They found that the 1-15aa peptide fragment was the only one to bind to alpha-synuclein, suggesting it is the first fifteen amino acids that are the most important for its binding to alpha-synuclein. The results from these studies show that alpha-synuclein and beta-synuclein do interact with each other and that beta-synuclein can bind to alpha-synuclein directly, however they did not determine at what stage of alpha-synuclein filbrillisation this interaction actually occurs in disease; whether the interaction occurs only at the monomeric phase, or later on in the process when alpha-synuclein forms dimers and then oligomers. Other studies however have shown that the interaction between alpha-synuclein aggregation and beta-synuclein most often occurs in the earliest stages of aggregation; however certain

papers have seen that alpha-synuclein and beta-synuclein monomeric exhibit weak interactions, but when alpha-synuclein dimers are formed beta-synuclein monomers show a higher affinity to the alpha-synuclein dimer than an additional alpha-synuclein does [182]. Beta-synuclein was also shown to bind strongly to alpha-synuclein oligomers as well. This interaction is thought to be behind the anti-aggregating property of the beta-synuclein protein, whereby beta-synuclein binds to the NAC site of the alpha-synuclein, which is responsible for autocatalytic processes leading to aggregation, in effect competing against alpha-synuclein for binding to the NAC site and then once bound preventing other alpha-synuclein monomers for reaching the autocatalytic site on the surface of alpha-synuclein fibrils. In addition, when beta-synuclein was overexpressed in an A53T mutant alpha-synuclein mouse model, beta-synuclein was able to reduce alpha-synuclein accumulation. These results show that beta-synuclein has the ability to inhibit the accumulation of both wildtype and the mutant A53T form of alpha-synuclein, and therefore is able to play a regulatory role within the cell [193].

The mechanisms behind the binding of beta-synuclein to alpha-synuclein at the molecular level is mostly unknown. However, nuclear magnetic resonance experiments have examined how the two proteins bind to each other [194]. A transient heterodimer formation, formed of an alpha-synuclein and a beta-synuclein protein, was seen to inhibit alpha-synuclein aggregation. A dimer is comprised of two proteins, which can be oriented in two different ways: either head to head or tail to head. The beta-synuclein protein binds to alpha-synuclein in a head to tail configuration, however alpha-synuclein has been shown to form homodimers, with either a head to head or head to tail, but this results in a weaker and a more transient interaction in comparison to the interaction with beta-synuclein [194]. The study showed that the alpha-/beta-

synuclein heterodimer complex, when arranged in the head-to-tail orientation, hinders the formation of alpha-synuclein fibrils. The study also determined a certain region within the N-terminus of alpha-synuclein, involved in the interaction between the alpha-synuclein protein and either alpha-synuclein or beta-synuclein. This particular site is able to bind to the negatively charged C-terminus of the second alpha-synuclein or beta-synuclein protein, creating the head-to-tail formation. The C-terminus of beta-synuclein showed subtle differences in residues compared to alpha-synuclein, which results in an increased interaction site with the N-terminus region of alpha-synuclein [194], suggesting beta-synuclein has a stronger affinity for alpha-synuclein than a second alpha-synuclein protein.

This interaction was seen to be frequently localised to lipid-bilayer surfaces and, similar to that seen with alpha-synuclein, beta-synuclein is known to bind readily to lipid membranes. When alpha-synuclein binds to lipid membrane, alpha-synuclein alters the conformation of the N-terminus, forming an alpha-helical secondary structure [77]. Beta-synuclein may also facilitate binding of alpha-synuclein to fatty-acids on the membrane instead, which promotes the structural conversion of alpha-synuclein proteins to an alpha-helical structure, rather than a beta-sheet structure that is highly hydrophobic and leads to an increase in probability of protein aggregation [190]. Beta-synuclein, while it does bind to lipid membranes as well, does not readily change conformation, except under certain environmental conditions, for example when there are changes in pH [195], in the presence of certain metal ions such as Zn^{2+} or Cu^{2+} [196], or most notably, when the temperature is raised to above $60^{o}C$, this can cause beta-synuclein fibrillisation, with the formation of proto-fibrils [182].

This interaction between similar proteins from the same family has become of great interest to researchers, and was found with other proteins as well, including the

amyloid-beta protein (Aβ), where the isoform Aβ42 is prone to become aggregated, whereas Aβ40, was found to be more resilient to aggregation, and when expressed with Aβ42 was able to reduce the extent of aggregation [197]. Research into alpha-synuclein role in diseases such as PD has also brought up evidence for the interaction between alpha-synuclein and the AD-related cytoskeletal protein tau, as tau protein has also been identified in Lewy bodies taken from PD patients [84], showing strong evidence for the mutual interaction between alpha-synuclein and tau protein. Due to the homology between alpha-synuclein and beta-synuclein, it is possible that beta-synuclein might be able to influence the tau proteins as well, and there is some evidence that tau protein is able to bind to beta-synuclein protein [198]. The effect of beta-synuclein on other toxic proteins is however largely an unexplored area of research and so little is known about it.

1.4.3. Mutations in beta-synuclein

As mentioned before, the beta-synuclein protein was not found to contain the NAC region which is present in alpha-synuclein protein. This region is thought to be important for alpha-synuclein aggregation, and its absence in beta-synuclein protein suggests that beta-synuclein does not readily aggregate under normal physiological conditions. However, beta-synuclein has been shown to aggregate when the beta-synuclein gene become mutated, although whether or not these beta-synuclein aggregates are as damaging to the cells as alpha-synuclein aggregates is unknown. Two forms of mutations in the beta-synuclein gene, P123H and V70M (Figure 7), have recently been identified in DLB patients. The V70M beta-synuclein mutation has been found in sporadic DLB patients, whereas P123H is associated with familial cases of DLB [199].

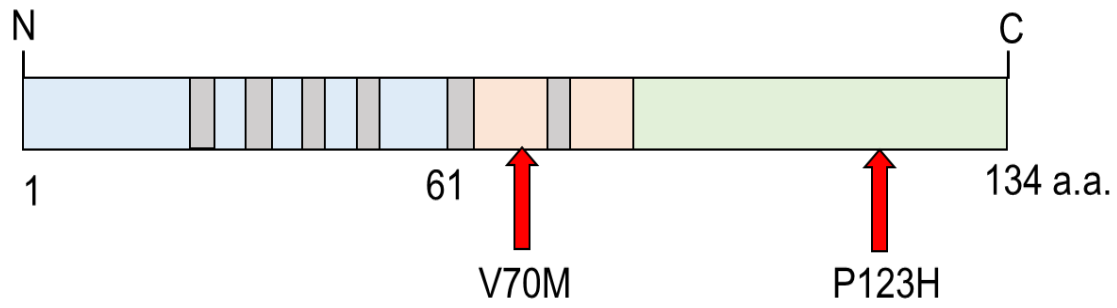

Figure 7. Mutations within beta-synuclein. Beta-synuclein is a 134 amino acid (a.a.) length protein. There are two major beta-synuclein mutations (indicated by the red arrows) – V70M and P123H. Six imperfect KTKEGV repeats are found within the N-terminus of the beta-synuclein (sections shaded in grey).

1.4.4. Cellular dysfunction

Research into beta-synuclein has looked at the effect of both wildtype and mutant beta-synuclein on cell function, including changes in synaptic function [200], proteasomal activity [187], autophagy and mitochondria function. Of these functions, this next section will focus on the effect of beta-synuclein on autophagy and mitochondria in particular, due to their relevance in my project. A summary of the pathological changes caused by wild-type and mutated beta-synuclein can be seen in the following table:

Reference	Beta-synuclein form	Model type	Neuropathy
Taschenberger et al., 2013	Wildtype	Rat-nigrostriatal neurons	Mitochondrial fragmentation; ion handling and respiration was not altered.
Evans et al., 2019	Wildtype/V70M	HeLa cells	Increased LC3II levels; attenuation of autophagy flux
Wei et al., 2007	V70M/123H	B103 neuroblastoma beta-synuclein overexpressing cells	Enhanced lysosomal pathology (cathepsin B, LAMP2 and GM2)
Fujita et al., 2010	P123H	P123H beta-synuclein transgenic mice	Beta-synuclein immunoreactive axonal swelling; gliosis
Sekigawa et al., 2012	P123H	P123H beta-synuclein transgenic mice	Mild oxidative stress; normal mitochondria

Table 1. Summary of studies investigating beta-synuclein related cellular dysfunction.

1.4.4.1. Beta-synuclein and autophagy

Alpha-synuclein has previously been proven to significantly impair autophagy response [201], and so research has turned its attention to beta-synuclein. In a recent study conducted by Evans et al., 2019, the relationship between beta-synuclein in DLB patients and autophagosomes was explored [202]. The study examined changes in autophagy markers in the frontal cortex and occipital cortex of post-mortem tissue taken from DLB patients. Using the marker LC3-II and p62, an increase in immunostaining within beta-synuclein containing cells was seen, showing an increase in autophagic activity. Both BE(2)-M17 neuroblastoma cells and Hela cells overexpressing either wildtype beta-synuclein or V70M mutant beta-synuclein showed a consistent increase in LC3-II protein levels. Alterations in autophagy flux can be assessed using the autophagosome-lysosomal fusion inhibitor, chloroquine. The

paper found a more pronounced increase in LC3-II protein levels when chloroquine was added to the beta-synuclein and V70M beta-synuclein mutant cells. In this study, chloroquine alters the autophagy flux which can be measured by calculating the difference in protein levels between beta-synuclein overexpressing cells with and then without chloroquine. The study by Evans et al., also determined that both beta-synuclein wildtype and the mutant V70M were able to significantly reduce the autophagy flux in comparison to the control cells, however little difference could be seen between the wildtype and V70M mutants.

Lysosomes have the ability to bind to autophagosomes, and release enzymes to digest the substrates within. When the autophagy demand is high, this will lead to an increase in lysosomal protein. One research group found that whilst cells overexpressing wildtype beta-synuclein did not show an increase in the lysosomal enzyme cathepsin B, the beta-synuclein mutants P123H and V70M both showed a strong increase in cathepsin B activity, and in this experiment both the beta-synuclein mutants showed an even greater increase in cathepsin B than alpha-synuclein overexpressing cells. To support these results, the effect of overexpressing beta-synuclein V70M and P123H on the lysosomal marker Lamp2 levels was examined. A marked increase in Lamp2 within P123H overexpressing cells was found, while interestingly no change was seen in the proteasome, suggesting that the beta-synuclein mutation selectively affects lysosomes [203].

1.4.4.2. Beta-synuclein and mitochondrial function

The full extent of the effect of the overexpression of beta-synuclein on other cellular functions, such as mitochondrial function, is yet not completely understood. There have been only a few studies which look at the effect of either wildtype or mutant (specifically the mutant P123H) on mitochondria. Aggregated wildtype beta-synuclein

was shown to contribute to neurodegeneration and cause mitochondrial fragmentation [204]. In this study however, they were not able to find changes in calcium ion regulation, mitochondrial membrane potential, mitochondrial mobility or oxygen consumption rate. Studies have also examined the effect of the P123H mutation on axonal structure and mitochondrial function in mice [205, 206].. Using electron microscopy the presence of axonal swelling derived from GABAergic projection neurons, could be detected in the brain of P123H expressing mice [207]. A particular form of axonal swelling known as globules, which are small spheroid structures containing small vesicles and multi-layered membranes, were identified in the mice. Examining brain section of the P123H beta-synuclein mice beta-synuclein containing globules were found in the striatum and globus pallidus especially [207]. While staining for 4-HNE(4-hyroxy-2-nonenal) , which is a product of lipid peroxidation and therefore sometimes used as a marker of oxidative stress, they discovered that P123H transgenic mice displayed mild increased levels of oxidative stress. Further analysis however showed no evidence of mitochondria within the axonal swellings of P123H transgenic mice, and so the paper was unable to determine the mechanism underlying the mild oxidative stress seen in the P123H transgenic mice [205].

1.4.5. Final remarks

Beta-synuclein still remains a poorly studied member of the synuclein family, and further research in beta-synuclein field is urgently needed. Similarly to alpha-synuclein, wildtype beta-synuclein may have several important cellular functions, but this changes when beta-synuclein protein undergoes conformational changes due to mutations in the SNCB gene [208], and so beta-synuclein may have an importance in DLB pathology itself. The dual nature of beta-synuclein, where it is capable of being both neuroprotective and neurotoxic at the same time is reminiscent of other isoforms,

such as Aβ in AD for example. This distinction between the protective and the toxic nature of beta-synuclein might therefore be an interesting line of research to follow. The exact nature of how mutated beta-synuclein can cause DLB-like symptoms also might provide alternative ideas for treating DLB.

1.5. Rodent models of synucleinopathies

There are two different types of rodent models typically used to model aspects of neurodegeneration: toxin-based mouse models and transgenic mouse models. These mice models were generated to reproduce the biochemical and behavioural changes seen in human patients of synucleinopathy diseases, which include PD, DLB and MSA [209]. Toxin-based models are often used as a model of PD. The toxins MPTP and 6-OHDA for example are well-known neurotoxins [210, 211], which when administered to normal mice has been shown to cause dopaminergic cell loss. The use of toxin-based models is limited in DLB research, as no available toxins would reproduce reliable specific hippocampal-limbic neurodegeneration. On contrary, numerous transgenic models of synucleinopathies, which focus on the overexpression of proteins of the synuclein family, mostly alpha-synuclein, were generated. In human synucleinopathies, alpha-synuclein may be found to be overexpressed or mutated [104, 212]; and rodent models which express these particular forms of alpha-synuclein have been produced.

Transgene expression in rodent models of neurodegenerative diseases are able to be region specific, through the use of cell-type specific promoters [213, 214]. The choice of promoter is therefore important factor to consider. Expression of the transgene under the control of the prion promoter (PrP) for example occurs in glial cells as well as neuronal cells [215]. A common promoter used in AD research for example is the CamKIIα promoter, which drives the expression of the transgene in the forebrain, affecting regions such as the hippocampus, olfactory bulb, ventral orbital cortex, caudoputamen, thalamus and SN, which are regions that are affected in AD and other dementia diseases [216]. In PD research however, the tyrosine hydroxylase (TH)

promoter is a well-used promoter. The TH promoter drives the expression of TH enzyme, which is involved in the generation of neurotransmitters within catecholaminergic neurons, including dopaminergic neurons [214]. This means that the promoter may be suitable for the localised expression of the transgene in regions of the brain that are relevant to PD, including the SN.

In my project I investigate a novel mouse model of DLB, and so in this section I shall be discussing the current availability of mouse models used to model synucleinopathy diseases. Due to the high prevalence of PD patients, in comparison to the other synucleinopathy diseases, the vast majority of animal models are PD specific, and there are almost no rodent models that have shown to be DLB-specific. I shall therefore be focusing mainly on the available alpha-synuclein PD-related transgenic mouse models and shall present the effects of the transgene on phenotype and neuronal function shown in these studies.

1.5.1 Alpha-synuclein related mouse models

1.5.1.1. Full-length alpha-synuclein overexpression

Genetic analysis has found increased copy number of the SNCA gene and both duplicates and triplicates of the gene have been discovered in autosomal dominant PD [217], which were found to correlated with PD symptoms in a copy number-dependant manner. Several mice models that overexpress wildtype alpha-synuclein have been widely generated and used in synucleinopathy-related research.

Mice expressing the human version of alpha-synuclein protein under the promoter Thy1, which is expressed in all neuronal tissue, displayed an increased overall expression of human alpha-synuclein throughout the entire brain, which has been found in many studies to be sufficient to cause PD-like pathology [218]. An

overexpression in wildtype alpha-synuclein within the SN of mice is sufficient enough to show motor-impairment in mice, which includes increased tremor, alterations in grip strength, stride length and decrease in acceleration [219].

Transgenic mice overexpressing human wildtype alpha-synuclein under the pan neuronal promoter, the PDGF (platelet derived growth factor) promoter, have been shown to contain increased levels of alpha-synuclein. The presence of ubiquitinated human alpha-synuclein containing inclusions, found as intranuclear deposits and cytoplasmic inclusions, were detected in the neocortex, CA3 region of the hippocampus and the SN. However, unlike in PD patients, alpha-synuclein fibrils were not detected within the inclusions [220]. Analysis of wildtype alpha-synuclein overexpression driven by the PDGF promoter showed a loss of dopaminergic nerve terminals in the basal ganglia. Additionally, transgenic mice showed signs of motor skill impairment and memory retention, using behavioural tests such as the rotarod and the Morris water maze [220, 221].

In PD, patients shows signs of severe movement impairment accompanied by increased Lewy body pathology in the SN, with increased dopaminergic neuron and dopamine transporter (DAT) loss [222]. Whilst cognitive deficits are more prominently seen in DLB, memory impairment has also been shown to be affected in some PD patients as well [223]. Many of the mouse models overexpressing human wildtype alpha-synuclein have shown signs of severe neurodegenerative impairment, including the presence of Lewy body-like inclusions as well as motor and cognitive impairment, showing a strong degree of neuropathology similar to that seen in PD and DLB pathology, indicating that these models may possibly be useful for understanding the neuropathology underpinning PD and DLB pathology.

1.5.1.2 Post-translation modification in mouse models of PD

As discussed in the previous introduction section, after alpha-synuclein is produced from the nucleus, the protein undergoes post-translation modification, which can include phosphorylation, nitration, ubiquitination and truncation. When this process is aberrant in human PD and DLB patients, this can cause excessive alpha-synuclein accumulation in the brain. The process of truncation in particular has been examined and used in mouse models of PD. Truncated mice, resulting in a 120 amino acid length protein, driven the TH promoter have shown alpha-synuclein accumulation in the olfactory bulb, SN and striatum, although not within cortical regions [224, 225]. Localisation of the alpha-synuclein protein was found within the somatodendritic compartment of dopaminergic neurons in the SN. Cytoplasmic insoluble inclusions which were discovered to containing truncated forms of the synuclein protein could be seen in dopaminergic neurons within the SN. These mice also showed behavioural alterations, typical of PD pathology, such as alteration in motor coordination impairment and gait abnormalities [225]. Interestingly, 1-120 truncated alpha-synuclein formed oligomers in this model, and pre-treatment with the oligomer-modulator small molecule anle138b rescued dopamine release deficit and cell death [225]. A mouse model which expresses truncated alpha-synuclein in the key regions affected by DLB, could provide additional information regarding cellular dysfunction, and serve as a unique model of specifically DLB pathology. The evidence for the neurotoxic effect of truncated alpha-synuclein in models of PD forms an important basis for my own project, where I use a mouse model expressing 1-120 amino acid truncated form of alpha-synuclein as a novel model of DLB. In order to target the expression of human alpha-synuclein protein into brain regions specific to DLB, the truncated alpha-synuclein transgene expression was driven by the forebrain-specific

CamKIIα promoter. This promoter restricted the expression of the alpha-synuclein to the forebrain region, which includes the cortex, olfactory bulb and the hippocampus, the latter of which is the main focus of my project.

In addition to 1-120 truncated alpha-synuclein, a similarly truncated 1-130 amino acid alpha-synuclein protein, under the TH promoter as well, has been examined in one known study, with similar results [226]. The study showed the presence of alpha-synuclein accumulation within the soma and axons of dopaminergic neurons within the SN. Whilst there were no alterations in motor coordination, there was a general impairment in locomotion seen in these truncated mouse model.

These studies examining truncated alpha-synuclein have highlighted the toxicity of truncated alpha-synuclein and that when these truncated alpha-synuclein are expressed in the SN, they can replicate the behavioural and biochemical impairments typically seen in PD patients, making it a viable alternative to transgenic mice models.

1.5.1.3. Mutated alpha-synuclein in Parkinson's disease mouse models

Several missense mutations in the SNCA gene (including A53T [212], A30P [227], H50Q [228] and E46K [104]) have been identified in PD patients (Figure 8).

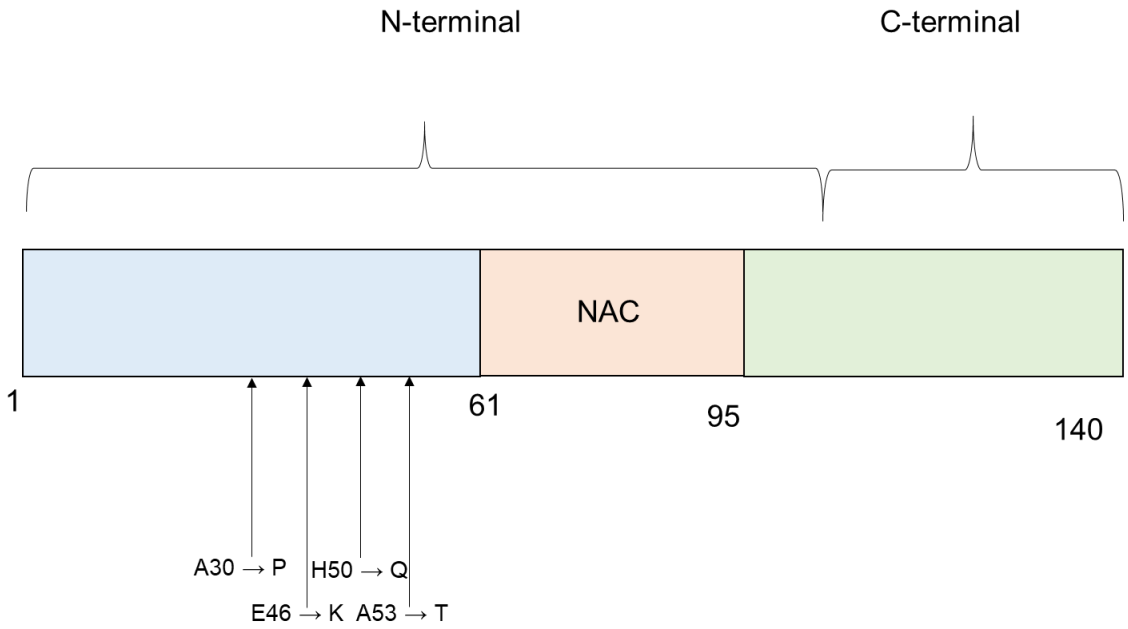

Figure 8. The major alpha-synuclein mutations seen in certain PD patients. The four major alpha-synuclein mutations tend to occur within the N-terminus of the alpha-synuclein gene. The four mutations are: A30P, E46K, A53T and H50Q.

These mutations, which tend to cluster near the N-terminus of the alpha-synuclein protein and within the NAC region, can cause alpha-synuclein protein to misfold and aggregate to form toxic oligomers. These mutations have then since been used to generate multiple different mouse models of PD pathology.

1.5.1.3.1. A53T mutated alpha-synuclein models

The A53T mutation is often used to model PD in mice, and there have been multiple mouse models generated which overexpress A53T mutated alpha-synuclein.

A transgenic A53T mutant PD mouse model, driven by the Thy1 promoter, has been created and analysed for biochemical and motor impairment [229, 230]. Transgenic mice have shown increased levels of transgene mRNA expression compared to control mice, as well as a corresponding increase in alpha-synuclein protein levels in half-brain lysates. Immunostaining showed the presence of alpha-synuclein in neurons throughout the entire nervous system, in particular brainstem and motor

neurons. The studies however did not find any significant alpha-synuclein expression within the SN, which is usually found in PD patients. However, alpha-synuclein was shown to cause axonal damage in motor neurons, and the transgenic mice, using the rotarod test which tests the fine movement and coordination of mice, showed signs of severe motor impairment.

The effect of A53T mutated alpha-synuclein on neuronal function has been further analysed through different mouse models, many of which express the A53T alpha-synuclein transgene under the prion promoter [231-233]. As with Thy1 promoter driven A53T transgenic mice, each of the studies using transgenic A53T mice showed that alpha-synuclein overexpression under the prion promoter led to significantly higher whole-brain alpha-synuclein protein levels in comparison to control mice, showing between a 4-fold to 15-fold increase in alpha-synuclein. In addition, they all found increased levels of ubiquitinated alpha-synuclein protein within the cerebellum, midbrain and the spinal cord in particular was most vulnerable to alpha-synuclein transgene overexpression. One study however did show that there were increased mRNA levels in the SNpc (substantia nigra pars compacta), however this was not accompanied by an increase in alpha-synuclein aggregation [233]. Further analysis into alpha-synuclein distribution identified the presence of alpha-synuclein protein within the axons, perikarya and dendrites [231]. Axonal processes in particular were shown to contain alpha-synuclein fibrils, and ultrastructural analysis of axons in the spinal cord showed deteriorating myelin in damaged axonal processes [232]. In addition to these neuronal impairments, transgenic mice also showed clear signs of severe motor impairment in the later stages of disease progression, such as in the rotarod test, grip strength and abnormal gait patterns [231], bradykinesia, postural instability [233] and paralysis of the limbs [232].

The use of the prion and Thy1 promoter has resulted in widespread PD related symptoms in A53T transgenic mice, there has one report using transgenic A53T mice using a TH promoter [234], however despite an increased accumulation of alpha-synuclein within the SN, there was no Lewy body formation in these mice, and the authors concluded that the alpha-synuclein accumulation is not always sufficient for Lewy formation.

1.5.1.3.2. A30P mutated alpha-synuclein mouse models

A30P is also a well-documented alpha-synuclein mutation found in certain PD patients [227]. As with A53T, there have been several different A30P mutated mouse model variations used in PD research.

When A30P mutant alpha-synuclein is driven by the Thy1 promoter in transgenic mice, alpha-synuclein mRNA expression was detected in the cerebellum, striatum, SN, brainstem, spinal cord, hippocampus and neocortex [235-238]. Whole brain analysis found a two-fold increase in alpha-synuclein protein, and distribution of alpha-synuclein protein was detected in the same brain regions, in particular the brain stem and spinal cord, where insoluble and phosphorylated alpha-synuclein fibrils were detected in one study [238]. Alpha-synuclein protein was found within the neuropil [236], affecting the neurites and synapses, although no synaptic dysfunction could be detected [235]. Whilst two of these papers report signs of significant locomotor dysfunction in A30P mutant mice [233, 237], typically middle to late onset, two paper also reported an age-dependent alteration in cognitive function, with impairment in spatial memory tested in the Morris water maze, and impairment in fear conditioning [237, 238].

Overexpressing A30P mutant alpha-synuclein under the prion promoter instead results in similar alterations in alpha-synuclein expression. Studies have seen between 5-20 fold increase in alpha-synuclein protein levels, in particular within the soma of neurons within the CNS [239]. Although alpha-synuclein immunoreactivity could be detected in the SN, alpha-synuclein protein was not ubiquitinated and insoluble inclusions were not detected. Despite the lack of neuronal dysfunction [233], studies did see a change in motor function in an age-dependent manner, with older mice showing motor impairment such as dystonia, tremor and gait impairment [239].

Expressing A30P mutant under the TH promoter was shown to concentrate alpha-synuclein protein into the noradrenergic neurons in the brainstem and dopaminergic neurons in the SNpc, however, as was seen in A53T mice, no insoluble alpha-synuclein inclusions were detected [234].

Animal models which express an A30P mutant alpha-synuclein transgene have been largely unsuccessful in showing the presence of insoluble alpha-synuclein inclusion in the SN, even when expression is targeted to the SN through the TH promoter, and most of the studies were not able to show changes in motor function. Interestingly however, when a transgenic mouse model which expresses A30P alpha-synuclein together with A53T alpha-synuclein was analysed, neurons in the brain were shown to be more susceptible to neurotoxicity caused by the neurotoxin MPTP [240]. The study also showed a reduction in dopamine within the SN and signs of locomotor impairment were evident, suggesting that double transgenic mice were able to display phenotypic and neurochemical changes often seen in PD patients.

1.5.1.3.3. E46K mutated alpha-synuclein mouse models

Unlike the A53T and A30P mutations, the E46K mutation has not been as widely used in mouse models of PD. There has been one paper which has examined the neuropathology caused by an E46K mutant alpha-synuclein transgene driven by a prion promoter [241]. In the study, transgenic mice contained intracytoplasmic inclusions which, contrary to those mostly seen in A53T or A30P mice, resembled more accurately Lewy bodies seen in human PD patient; the inclusions were detergent insoluble and hyperphosphorylated, with a core and halo as seen in PD patients and can be found in the cell bodies. Intracytoplasmic inclusions were seen within the perikarya and neurites of neurons in the spinal cord, brainstem, thalamus and motor cortex, although not in the hippocampus. As with the A53T and A30P mice, E46K transgenic mice also displayed signs of motor impairment, in particular reduced ambulation, although this tended to occur at a later stage than that seen in other mutated alpha-synuclein mouse models.

To summarise the different established alpha-synuclein mutant mouse models currently available, the follow table provides a brief overview of the mouse models and their characteristics:

Reference	Human a-syn	Promoter	Genetic Background	Expression levels	Neuropathology	Motor phenotype/ Cognitive dysfunction
[220, 242]	WT	PDGF-β	C57Bl/6 x DBA/2	10–80% of human control	↓ striatal TH (levels, activity); ↓ DA levels; ↓ TH fibres; glia+, ubiquitin+	middle age onset mild ↓ rotarod
[221]	WT	PDGF-β	C57Bl/6 x DBA/2	--	↓ dopaminergic terminals	Early motor dysfunction (pole test)
[235]	WT, A30P	mu Thy-1	C57Bl/6	two-fold end. a-syn	I: SN, STR, HPC, Cx, B	none
[237]	WT, A30P	mu Thy-1	C57BL/6	~two fold expression: a-syn	I: A, B, Cx, H, SC, SN, STR; B: TS amyloid staining; hyperphosphorylation of deficits in probe trial in a-syn in cytosol in SC and phospho-Ser129 staining in A and Cx;	Old age onset: ↓ fear response (freezing and active avoidance), deficits in probe trial in Morris water maze
[236]	WT, A30P	mu Thy-1	C57Bl/6 x DBA/2	10-fold human levels	--	--
[238]	WT, A30P	mu Thy-1	C57BL/6	--	Phospho129 a-syn: H, Cx, A, B, SC	Impaired fear conditioning
[229]	A53T	mu Thy-1	C57Bl/6	--	motor neurons degeneration; I: T, B, C, SC; ubiquitin+	early onset, severe (rotarod)
[243]	Y39C	mu Thy-1	FVB/N	2.5-fold of expression in WT	Cx: I, phospho-Ser129 staining, ubiquitin+, apoptosis.	Old age onset: ↓
[232]	WT, A53T	mouse prion	C57Bl/C3H	2.5- to 30-fold end. a-syn	I: SC, B, C, Th, STR; GFAP+	middle age onset, hunched back, freezing, paralysis (fatal)
[231]	WT, A53T	Mouse prion	FVB/N	5- to 20-fold end. a-syn	altered neuronal morphology, diffuse accumulation of a-syn	↓ stride length, grip strength; ↓ vertical activity; ↓ rotarod
[233]	WT, A30P, A53T	mouse prion	C3H/HeJ x C57Bl/6J	4–15 times > non Tg	I: M, C, B, SC; GFAP+, ubiquitin+	late onset, reduced ambulation, ataxia dystonia (fatal)
[241]	WT, A53T, E46K	Mouse prion	C57Bl/C3H	75% of human A53T a-syn	I: SC, B, Th, Motor Cx	reduced ambulation
[239]	WT, A30P, A53T	hamster prion	C57Bl/6J x SJL	5- to15-fold end. a-syn	GFAP (HPC)	young/middle age onset ↓ rotarod, tremor, dystonia, (fatal)

[234]	WT, A30P, A53T	rat TH	Swiss Webster x C57blk6/DBA	--	I: STR, OB > C Ubiquitinated a-syn	--
[240]	WT, A30P + A53T	rat TH	C57Bl/6	30–50% of mouse a-syn	↓ DAT density; ↓ DA, DOPAC, HVA	middle age onset, mild; ↓ locomotor activity and coordination
[224]	a-syn (1-120)	rat TH	C57Bl/6	--	I: SN, OB ↓Striatal DA and metabolite levels	Progressive ↓ motor activity
[244]	a-syn (1-120)	rat TH	C57Bl/6	-	↓ STR DA levels	-
[225]	a-syn (1-120)	rat TH	C57Bl/6	Hum a-syn < endogenous a-syn	↓ 50% of DA neurons in SNpc	Impaired gait; late ↓ rotarod
[226]	a-syn (1-130)	rat TH	C57Bl/6	1.44 time > non Tg	↓ DA neurons in SNpc, ↓ DA,	↓ spontaneous motor activities
[245]	a-syn (1-120)	CamKII-α1	C57Bl/6	-	A-syn in temporal Ctx, perirhinal Ctx, H	↓ NOR; errors ↑ in Barnes maze.
[246]	WT	proteolipid	C57Bl/6 x DBA/2	0.1–1.2 ng/µg	insoluble oligodendroglial inclusions	none (rotarod, locomotor activity)

Table 2. Overview of alpha-synuclein related mutant mouse models. This table contains data from the review papers Fernagut et al., 2004, Magen et al., 2011 and Crabtree et al 2012 [247-249]. Abbreviations: I, inclusions; A, amygdala; B, brainstem; C, cerebellum; Cx, cortex; H, hippocampus; M, midbrain; OB, olfactory bulb; SC, spinal cord; SN, substantia nigra; STR, striatum; T, telencephalon; Th, thalamus; end. a-syn, endogenous levels of a-syn

1.5.2. DLB-related mouse models

In contrast to the extensive literature on animal models specific to PD, DLB, the second most common for synucleinopathy, is much less explored. Whilst there have been a few synuclein related mutations that have been confirmed to be linked to DLB, such

as E46K alpha-synuclein or even V70M and P123H beta-synuclein, there is currently only one known mouse model, which has shown DLB-related brain pathology. This model, which involves the alpha-synuclein mutant A53T was developed by Lim et al., [250]. The mouse model expresses an inducible A53T mutant alpha-synuclein transgene controlled by the CamKIIα promoter. In this particular E46K model, alpha-synuclein immunoreactivity was found in the midbrain, which includes the cingulate cortex, hippocampus and mamillary body, and to a lesser extent the brain stem and spinal cord of E46K transgenic mice. The presence of alpha-synuclein containing insoluble intracytoplasmic inclusions were found within the perikarya and neurites of neurons in the hippocampus and neocortex. Many of these inclusions were shown to be ubiquitinated and hyperphosphorylated, with a granular appearance, very similar to the Lewy bodies found within the brains of PD or DLB patients. The hippocampus in particular seemed to be affected and neuronal loss could be seen in the CA2/3 region of the hippocampus as well as the dentate gyrus. This was accompanied by impairment in memory, which was determined by fear conditioning memory tests.

These particular results seem to correlate with neurobiology and symptoms seen typical in DLB patients [17]. The A53T mutation, although it is well known as a PD-linked gene, was found in one patient who was thought to have probable DLB, although it is unclear whether the patient did have DLB [251]. Most A53T mouse models typically show predominantly PD-relate neuropathology, such as impairment in motor function and dopaminergic neuronal loss, however the CamKIIα A53T mutated alpha-synuclein model is one of the few studies that use animals which strongly overexpress alpha-synuclein within midbrain and cortical brain regions, which represents DLB pathology more closely than other models.

1.5.3. Final remarks

While the vast majority of the synucleinopathy-related transgenic mouse models available exhibit a phenotype typically seen in PD, there are very few which are able to replicate the distribution of alpha-synuclein accumulation in DLB pathology, as well as DLB-related memory function. The further development of DLB-specific alpha-synuclein mouse model would therefore provide further information on the pathology that occurs within DLB in particular, which may be useful in researching treatments for DLB patients.

1.6. Mice behavioural tests

Patients with neurodegenerative diseases such as PD, AD or HD display a variety of symptoms which can include reduced mobility, mood disturbance, cognitive impairment and memory loss [252-254]. These alterations in behaviour caused by cellular dysfunction and neuronal loss can be investigated using mice models, which can be achieved through the use of behavioural tests. A large variety of mouse behavioural tests have so far been developed to detect the various behavioural changes exhibited by the mice models. As part of my project I shall be employing some of these behavioural tests to determine changes in memory in the mice mode of DLB. Therefore, in this section I shall be discussing the advantages and disadvantages of some of the major behavioural tests available which are used to examine anxiety, motor and memory function in mice, some of which I shall also be using to detect behavioural changes in my mouse models later on.

1.6.1. Motor Tests

Motor behavioural tests were developed to examine alteration in the mobility of mouse models [255]. Motor tests such as the open field test, where mice are allowed to freely explore an open space for a predetermined length of time, and the rotarod, where mice are placed onto an accelerating revolving rod and are timed until they are no longer able to keep up with the speed and fall off (Figure 9), have been shown to be sensitive to changes in fine movement and general activity, and so have been used with mouse models of PD or HD, where motor impairments are prominent [211, 256, 257].

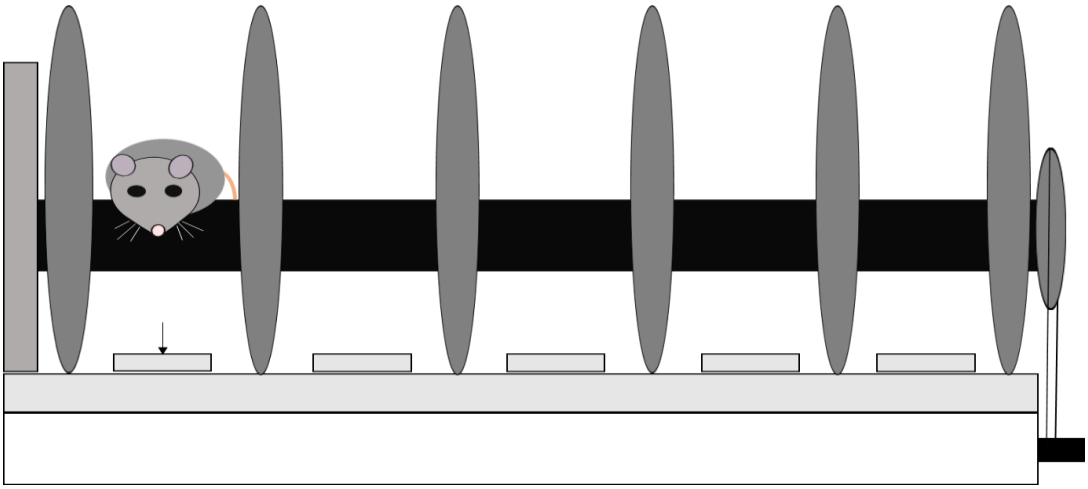

Figure 9. The rotarod test used as a test for motor function. The mouse is placed on the motorised rotating bar (in black), with large circular separators either side (grey). When mice fall off the bar, they depress a pressure pad (arrowed) which stops the timer.

1.6.1.1. Comparison of motor tests

Both the open field test and the rotarod can be used to detect impairment in movement, where the open field test analysed general movement, such as the speed and distance travelled, whereas the rotarod is able to test finer movement and balance, and so may be more appropriate for PD or HD which are predominately movement disorders.

Both of the tests have both been employed in PD-related mouse models, where impairment could be detected [211, 258]. Using the open field test, both the distance travelled, and resting time have been found to be altered in PD mouse models. Certain mice models of PD also showed that mice showed differences in thigmotaxis behaviour, which refers to their tendency to stay close to the walls of the open field area [259]; when mice spends more time close to the wall of the arena it suggests an increase in anxiety level arena. The rotarod has also been often used in mouse models of PD, with many PD mouse models showing significant impairment in the rotarod test,

showing a shorter latency time between the test starting and falling off the rotarod [260].

The open field test is a comparatively simple test which does not require specialised rotarod equipment. However, the rotarod test may give a more accurate reading of the fine motor ability of the mice, as the mice are forced to stay on the rotating rod or else, they will fall off, whilst in the open field test lack of motivation might be a hindrance, as their natural tendency to explore the environment is required. While the rotarod may be useful, the test requires the mice to get used to the equipment, which may be an issue for severely impaired mice which fall off straight away, which may not be such an issue with the open field test [255]. Both the open field and the rotarod are also subject to a large degree of variance, and there are several factors which could contribute to the results, which include for example genetic background of the mice, age of the mice or the surrounding environment, which should be taken into account [261].

1.6.2. Anxiety Tests

Whilst some experiments utilise the open field test as a test of anxiety level, there are two other tests which are often used to investigate anxiety in mice are the marble burying test, where mice are presented with marbles in a cage containing only sawdust [262] and the elevated plus maze, a test which comprises of cross-shaped arena, which two arms exposed and the other two arms covered [263]. In the elevated plus maze, the less anxious the mice are, the more time they will explore the exposed open arm, whereas mice that are anxious will remain in the enclosed arms, [264].

1.6.2.1. Comparison of anxiety tests

Both the marble burying test and the elevated plus maze have been used in mouse models of diseases such as AD or PD to evaluate the emotional state of the mice [265, 266]. The two tests have often used in experiments with anxiolytic drugs, to determine the improvement of anxiety-related symptoms using those drugs [262, 267, 268].

Both the marble burying test and the elevated plus maze require careful handling of the mice before and during the trial, which is important due to the nature of the test; reducing unnecessary stress from the environment or the researcher may impact the analysis of the anxiety tests [264].

Whilst the marble buying test is a simpler test which does not need specialised equipment it does have a major limitation. The accuracy of the marble burying test to distinguish anxiety related symptoms is unclear, as whilst certain papers have found that the test is sensitive to the effects on anxiolytic drugs some certain papers have found that the marble burying test is a better test for generally digging behaviour rather than anxiety related behaviour [269]. Therefore, using the marble burying test with other anxiety tests such as the elevated plus maze would provide more accurate information on the emotion state of the mice.

1.6.3. Memory Tests

The increasing prevalence of dementia means there is an increasing need for reliable tests for dementia-like symptoms in mouse models. As there are many different types of memory, batteries of tests have been created to probe specific forms of memory, for example the olfactory memory test and novel object recognition (NOR) test can both be used to detect deficits in recognition memory test, whereas the Morris water maze and Barnes maze have been used to determine changes in special memory.

1.6.3.1. Comparison of mouse memory tests

Loss of spatial memory is a key aspect in dementia associated with AD or DLB. The water Morris maze and the Barnes maze are similar tests, during which mice are tasked to find and then memorise a specific location within an arena, across several trial sessions. The Morris water maze is one of the most well-known spatial memory tests for rodents used in research and has been used for many years [270, 271]. In this test, mice are lowered into a large circular pool of water, which is filled with enough water so that it forces the mouse to swim. Within the pool there is a small, predetermined area, where a raised platform is situated, which the mice will have to swim to. The test is concluded if they reach the raised platform, on which they are able to rest. The Barnes maze test on the other hand does not involve water. In the Barnes maze, mice are placed on a large circular board, which has holes cut out around the circumference of the board [224]. Under one of these holes is a small pocket which contains food pellets. Mice are placed on the apparatus and are left to explore the maze until they find the hole with the food pellet. the cold water provides a strong motivation for the mice to keep searching for the platform. The test therefore relying only on pellet rewards and the mouse's natural tendency to move away from exposed regions. The Barnes maze test is therefore thought to be less stress-inducing than the Morris water maze [272], which may provide more reliable results.

Another type of memory that is often affected in DLB pathology is recognition memory. There are a few tests used to examine recognition memory, such as the olfactory memory test and the NOR test. Olfactory memory tests use the mouse's sense of smell to explore the environment and test their memory. As one of their predominant senses, the processing of odour cues is important for all rodents, which they rely on to identify food or social cues [273]. This use of olfactory and the mouse's natural

tendency to use scent when foraging for food cues can therefore make olfactory based memory tests suitable when using certain mouse models of dementia. The olfactory system is highly sensitive in rodents and their sense of smell is therefore important for their ability to recognise objects [274]. This sense of smell therefore has been utilised to measure changes in memory. The novel object recognition test on the other hand examines the mice's ability to remember and recognise 3D objects, which they explore by either sniffing, touching, or biting. The test can be used as both a test of short-term and long-term memory, by altering the interval between the familiarisation and choice phase [275]. In this test, there are several factors to consider, for example the choice of the object is a crucial aspect, which could potentially cause unintentional choice bias with the mice [276]. Mice have an innate preference for different objects; therefore it is important to try to minimise any bias from affecting the data. This can be achieved by balancing the objects used, so that each group receives both objected in the familiarisation stage, this would theoretically highlight any major interests for one particular object. The choice of both the familiar and the novel object is also important; to allow the subject mice to recognise a specific object, choosing two objects that are different shape, texture, and to a lesser extent colour is necessary [276]. With all memory function tests, handling of the mice is an important factor, as tests which require less handling throughout the test, such as the marble burying maze, often reduce the stress in the subject mice [277]. Another important factor in memory function tests is the stimuli which encourages participation in the test, whether by adverse stimuli in the Morris water maze, which may in fact prevent accurate results, or by food rewards, which may require food intake reduction for it to reliable [278]. In addition, variance among mice strains might also result in mice from different strains performing worse than others [279]. Therefore, using multiple tests as part of a battery

of behavioural tests might provide more accurate information on the cognitive function of the mice.

1.7. Aims of Project

Research previously undertaken by my research group has studied the neurodegeneration associated with DLB by generating a DLB-specific mouse model; a part of my project will involve further characterising this CamS120 DLB mouse model. In addition, cell work in our research group have highlighted the involvement of beta-synuclein in DLB neuropathology, showing specifically an increase autophagic response in DLB patients and DLB cell culture models. My project will look at exploring these two main areas of research further.

1.7.1. Aim 1: Characterisation of the DLB-specific CamS120 mouse model

The first aim of my project is to determine the accuracy of the DLB mouse model (CamS120 model), by examining changes in behaviour and synuclein protein accumulation. I shall be examining the expression of the transgene in the CamS120 mice model, which expresses truncated alpha-synuclein within the forebrain region, and to analyse the associated memory impairment.

1.7.2. Aim 2: Examine mitochondrial dysfunction in alpha-synuclein related models

The second aim of my project is to determine whether alterations in mitochondrial function can be detected in the CamS120 mice and alpha-synuclein overexpressing cell models. In particular, I shall be examining changes in mitochondrial dynamics in the CamS120 mice, as well as exploring changes in mitochondrial membrane potential and mitophagy markers in the alpha-synuclein overexpressing cells.

1.7.3. Aim 3: Examine the role of beta-synuclein in DLB related models

The third aim of my project is to determine changes in beta-synuclein in CamS120 mice model, and to further explore the effect of both wildtype and mutant beta-

synuclein on mitochondrial function, such as changes in mitochondrial dynamics and mitochondrial membrane potential.

Chapter Two: Methods and Materials

2.1. CamS120 mice

2.1.1. Generation of CamS120 mice

The generation of the CamS120 mice was achieved using the CamS line described in Hall et al, 2015 [245]. Briefly, a vector comprising of a CamKII promoter followed by 1-120 amino acid alpha-synuclein polypeptide with a poly A tail was generate. Pseudo pregnant females were produced by inducing ovulation and eggs were dissected out of the females. Linear DNA was microinjected into the pronucleus of oocytes and inserted into pregnant mice. Offspring from these mice were then bred with alpha-synuclein null mice, C57BL6/OlaHsd (Harlan Laboratory) crossed with C57Bl/6J wild-type mice. Mice taken from litter 1 were genotyped, and heterozygous mice were chosen and crossed back with C57BL/6J wildtype mice, which produced a mouse line used in this project. Mice were kept in a temperature and humidity controlled room, with 12-hour light/dark cycle. Food and water were available *ad libitum*. They were kept in small animal holding room in cages with a total maximum of 8 mice in one cage, with a constant level of humidity (55% ± 10%) and temperature (21°C ± 2°C). At 1 month, 3 months, 6 months, 12 months and 15 months, CamS120 mice either underwent behavioural testing, or they were euthanised by cervical dislocation and their brain tissue collected (Figure 10).

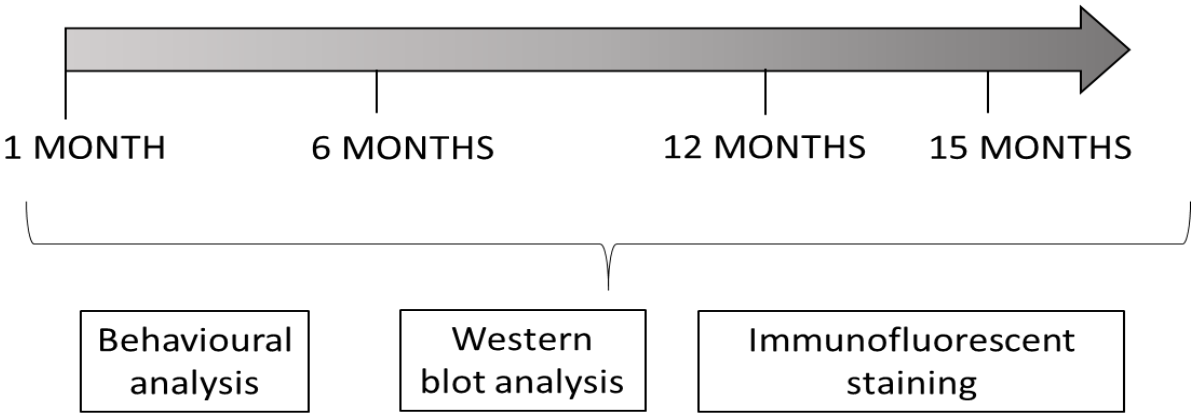

Figure 10. Time course for experimentations with CamS120 mice. CamS120 mice were tested at 1, 6, 12 and 15 months old, and are analysed using behavioural tests, western blot and immunofluorescent staining techniques for changes in behaviour and relevant protein levels.

2.1.2. Genotyping

PCR was used for genotyping of mice. Mice were identified by ear notching, and the ear notch biopsies were retained for genotyping. Using proteinase K, DNA was extracted from the ear notches, then amplified using specific primers (Table 3) to identify the presence of both endogenous mouse alpha-synuclein and the truncated human alpha-synuclein transgene. The DNA strands were separated by electrophoresis, and the resulting band was identified using Gel Red dye (Cambridge Bioscience; 1:10000 dilution), viewed under UV light, with reference to a DNA ladder. Littermate mice were allocated from mice that were identified as negative for human truncated alpha-synuclein, but positive for endogenous alpha-synuclein.

CamKIIα (human alpha-synuclein) primers	Forward	GGCACACTGCAAACTGAAAC
	Reverse	GGCTCCTTCTTCATTCTTGCCC
Endogenous alpha-synuclein primers	Forward	GCAGTGAGGCTTATGAAATGC
	Reverse	GCTTCAGGCTCATAGTCTTGG

Table 3. Genotyping primers. List of forward and reverse primers used for detecting both human truncated alpha-synuclein and endogenous alpha-synuclein gene when genotyping CamS120 mice.

2.1.3. Behavioural tests

At the appropriate age point, mice were put through various behavioural tests: the marble burying test, open field, and the novel object recognition test. In all tests, mice were acclimatised to the room for 30 minutes prior to testing. For each behavioural test, the ceiling lights were turned off and a standing lamp, directed towards the behavioural testing arena, to provide a dim light was turned on. Mice typically have a resting phase, which occurs during the light phase and an active phase which occurs during the night phase. The behavioural testing in this project took place during the light phase of the diurnal cycle, when they were in their resting phase.

2.1.3.1. Marble Burying Test

The marble burying test is a simple test, detecting anxiety, motivation or movement disturbances in mice [262]. Individual cages were set up for each mouse, which contained sawdust at least 2mm deep. On top of the sawdust, 15-20 equally spaced marbles were placed in a grid-like formation. The lighting in the room was adjusted so there was a dim light. The mice were then placed in their appropriate cages and left undisturbed for one hour. After one hour, the mice were returned to their home cage, and the marbles were examined. The percentage of marbles that had been buried, compared with prior to the trial, was calculated for each animal (Figure 11).

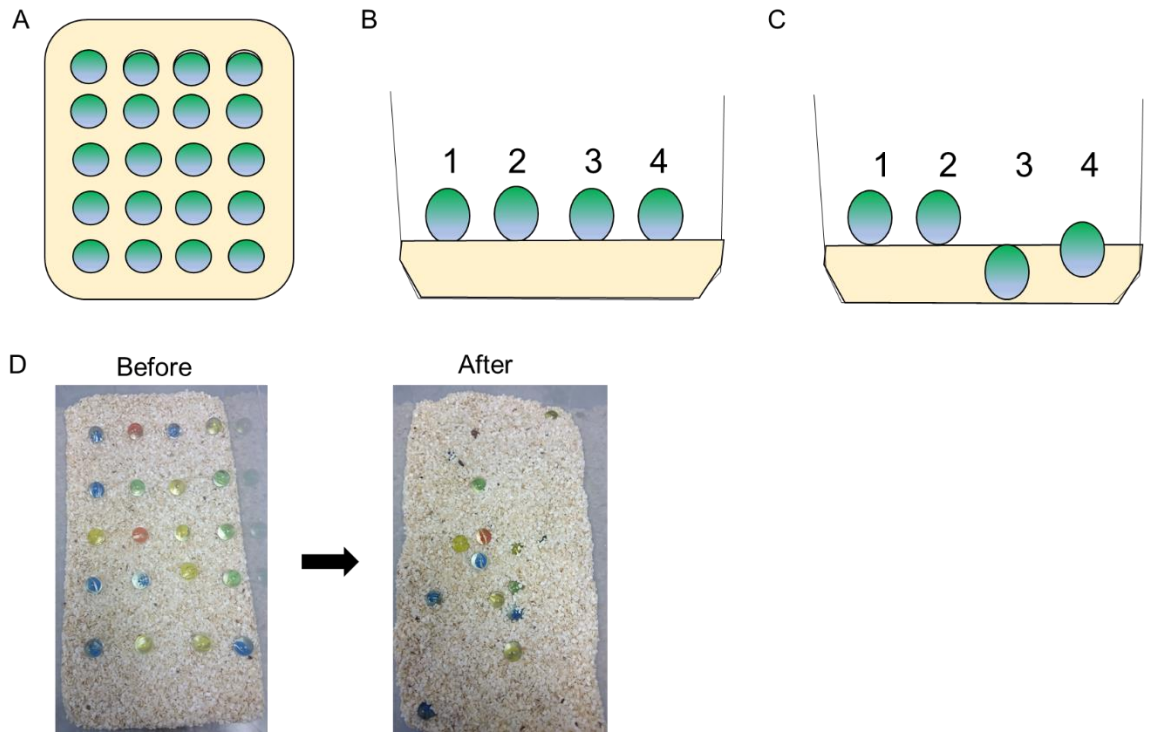

Figure 11. Marble burying test analysis. A diagram representation of the marbles arranged in a 5x4 grid is shown in a cage filled only with sawdust (A). A side-view of the cage shows the initial arrangement of the marbles (B), and an example of the arrangement of the marbles after the test was completed (C). In the example above, marbles 1 and 2 were not buried, marble 3 was fully buried and marble 4 would be counted as being 2/3 buried. Representative photos of the marble burying test performed by a CamS120 mouse were taken before and after the test (D).

2.1.3.2. Open Field Test

This test measures the general locomotor activity of the mice [261]. Mice were placed into an empty square arena measuring 400mm x 400mm x 400mm. The mouse's path was tracked by a camera located above the arena and the outline of the mouse showing the position and orientation of the mouse within the box was recorded automatically using BIO-OR 1.1.6. software (BIOSEB, France). The parameters of interest included distance travelled, average speed, resting time and rearing. Mice were allowed to explore the arena for a maximum of 5 minutes. Mice were given a habituation session, where they were placed in the arena the day prior to the test, so that the mice would become more familiar with the box, in an attempt to reduce anxiety

caused by a novel environment. Whilst this may possibly give an indicator of the general locomotive behavioural of the mouse, such as how much the mice will tend to move around naturally, the data collected on the second day would not be a reliable indicator of the mouse's anxiolytic response.

2.1.3.3. NOR Test

The NOR test examines the visual and recognition memory in mice.[280] The test was performed as reported in [245]. The mice were tested within the same arena as described before in the open field test. One day prior to the test the mice were placed into individual cages, containing only sawdust and a metal wire lid. After acclimation to the room, each mouse was allowed to explore the empty square arena for five minutes. They were then returned to their home cage. On the test day, two identical objects were placed in the centre of the arena, and the mice were allowed to explore them for five minutes. After an inter-trial interval of one hour, one of the two identical objects were exchanged for a novel object. Mice were allowed to explore these objects for five minutes. Mice were then returned back to their home cages. The objects used in my experiments included a red phone box, a metal big ben tower, a T75 cell culture flask filled with sawdust and glass angel decorations. Data representing the time spent exploring the object was collected automatically by the BIO-OR 1.1.6. software (BIOSEB, France). During the test, exploration time was counted as when the mice sniffs, bites or touches the object, although climbing onto the objects was not counted. The ability to discriminate the objects is defined by the discrimination index, or sometimes known as preference ratio, which is calculated using the following equation:

$$\frac{\text{Time spent exploring novel object (sec)} - \text{time spent exploring familiar object (sec)}}{\text{Total exploration time of both objects (sec)}}$$

In the NOR test, which is thought to be hippocampal dependant abnormal mice will tend to explore both the novel object and the familiar object to a similar extent, [281]. This calculation can be used to determine the recognition memory of the test mice. Therefore, mice which do not explore the novel object more than the familiar object in the test will receive a negative D.I. score, which is indicative of poor recognition memory.

This test has been recently used with a separate mouse model, . A recent publication recently published by [282]data collected using the BIOSEB BIO-OR equipment. The rTg(tauP301L)4510mice express a mutant form of the human tau gene (P301L), conditionally expressed under the CamKIIα promoter. The expression of the tauP301L transgene was induced when in the absence of doxycycline. Using the BIO-OR software, alteration in recognition memory could be detected. The rTg(tauP301L)4510 is a well-documented mouse model of frontal temporal dementia and memory impairment has often been reported; these results therefore added further evidence to this, as well as showing the suitability of the NOR test to detect changes in memory.

2.1.4. Fluorescent immunohistochemistry

Control and CamS120 mice (at 1, 6, 12 and 15 months old) were transcardially perfused with 0.9% saline and fixed in 4% paraformaldehyde (PFA). The brain was isolated, post-fixed in 4% PFA overnight, and then immersed in sucrose with sodium azide. It was then sectioned at 30µm thick using a cryostat (Leica). Obtained sections were stored in phosphate buffered saline (PBS) and 0.03% triton (PBS-T) with 0.01% sodium azide at +4^{o}C until processed further. For the staining, sections were then washed in PBS, blocked in 5% normal goat serum (NGS) with PBS-T for two hours.

Sections were then incubated in primary antibody overnight. The following day, sections were washed in PBS, incubated with secondary antibody for two hours, washed in PBS again and then finally mounted onto Superfrost Plus microscope slides with Permafluor (Fisher) mounting medium. A control group with no primary-antibody added was also performed alongside the experiment (Figure 12). Primary and secondary antibodies used for this study are presented in Table 4 and 5 (see section 2.4). Due to technical errors, semi-quantitative analysis of the immunofluorescence images was not possible; however this would be important for proper analysis of the data, as it would confirm changes seen in the western blot.

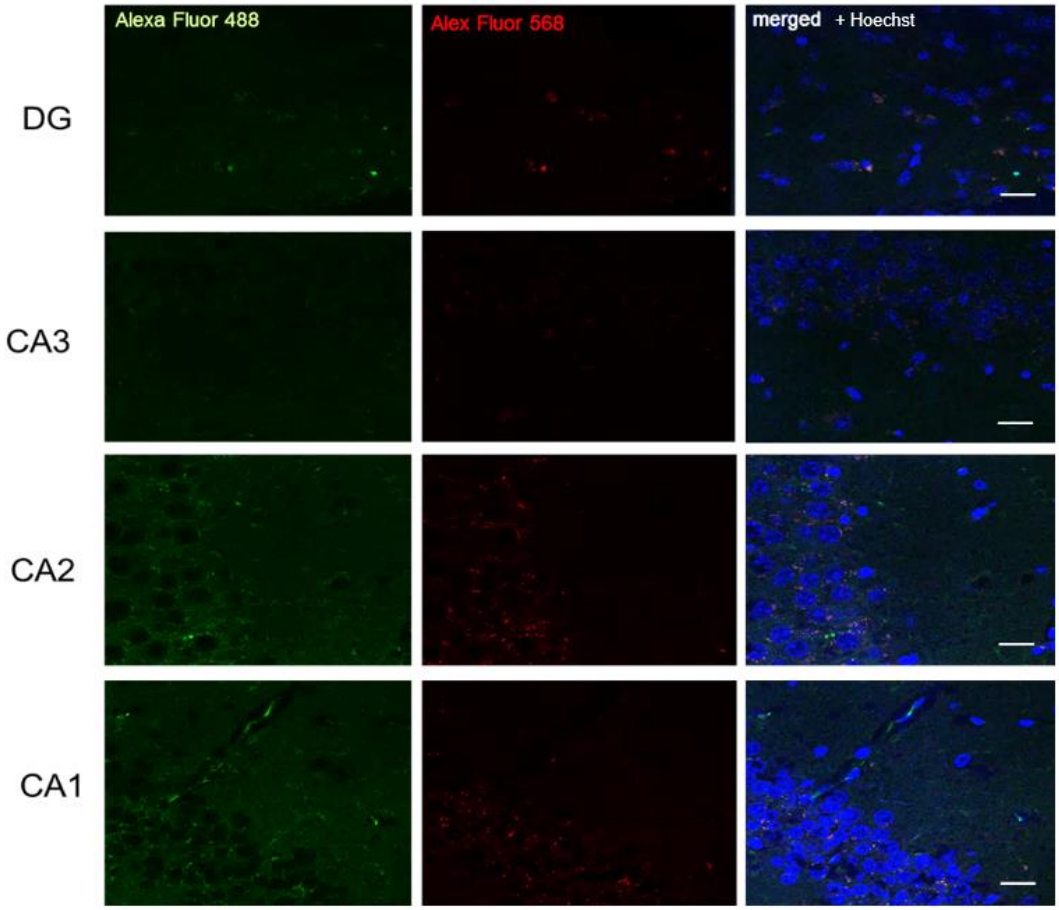

Figure 12. No primary antibody control in CamS120 mice. CamS120 mice were stained only with the secondary antibody and imaged on the confocal. All four subregions were tested: dentate gyrus, CA3, CA2 and CA1. The secondary antibody used were Alexa-Fluor 488 (green) and Alex-Fluor 568 (red). Scale = 20µm.

Specificity of the staining was controlled by the omission of primary and/or secondary antibodies with the rest of the protocol done as usual. No staining was observed in either the green or red channels.

2.1.5. Western blot

Hippocampi were dissected from control and CamS120 mice at 1, 6, 12 and 15 months old. The hippocampal tissues were then frozen and stored at -80^{o}C until needed, at which point the hippocampi were homogenised in ten times volume of PBS-T. The homogenate was spun down, and the supernatant was kept. Protein concentration was then calculated using the BCA assay (Thermofisher BCA assay). Concentrations

of BSA protein was used to produce a standard curve. When a copper based solution was added to several already known concentration of BSA protein (0mg, 0.2 mg, 0.4mg, 0.8mg and 1mg), which resulted in a protein concentration-dependant colour change. A plate reader was used to calculate the absorbance, which allowed the generation of concentration curve for the BSA standards. The absorbance measured for the samples were then compared to the BSA curve, and the approximate protein concentration of the sample was calculated. The lysates were then mixed in with 2x Laemmeli buffer (comprised of: 1M Tris-HCl, SDS, glycerol, β-mercaptoethanol and bromophenol blue), and then run on a 12.5% acrylamide gel. After separation, samples were then transferred to a PVDF membrane, activated using ethanol prior to use. This was done using a semi-dry transfer method, where a membrane gel sandwich is made, and placed into the semi-dry transfer tank between two oppositely charged electrode. A protein ladder was used to calculate the approximate protein band size. To process for synuclein, the membrane was fixed with 0.4% PFA first. Otherwise, the membrane was blocked with 5% milk in Tris buffered solution with 0.05% tween (TBS-T) and then incubated with primary antibody overnight at +4^{o}C. Following which, the membrane was washed in TBS-T, incubated with an HRP-conjugated secondary antibody, determined by the host species of the primary antibody, and then after further washing, the membrane was incubated with ECL western blot substrate before being developed. The Syngene PXi6 Gel and Blot analysing system was used to develop the membranes and to collect the resulting blots. The blots were analysed using ImageJ, standardising values to that of GAPDH or beta-actin, which acts as a loading control. In all experiments, three to four mice per group were used. The primary and secondary antibodies used are listed in Tables 4 and 5 (see section 2.4).

2.2. Cell Culture

2.2.1. Maintenance of stable cell line

The human-derived neuroblastoma cell line BE(2)-M17 cells (Gibco), referred hereafter as M17, were grown, and maintained in Dulbecco's Modified Eagle Medium (DMEM), which contains with high L-glutamine levels, combined with10% Fetal Bovine Serum (FBS) + 5% penicillin/streptomycin. M17 are a multipotential cell line, and express choline acetyltransferase, acetylcholinesterase, and dopamine-β-hydroxylase enzymes, suggesting they have properties of cholinergic neurons but also dopaminergic and adrenergic neurons [283], as such they may be useful for studying diseases that can affect multiple types of neurons, such as in DLB. Stable M17 cells overexpressing full-length alpha-synuclein (aFL), full-length beta-synuclein (bFL) and V70M mutated beta-synuclein (V70M) were maintained and used in cell experiments. Each of the transfected stable cell lines were maintained in 10% FBS in DMEM, containing 200µg/ml G418 antibiotic. Cells were incubated at 37^{o}C with 5% CO2 and were split once the cells reach around 70% confluency.

2.2.2. Immunocytochemistry

Once cells reached around 60-70% confluency, cells were counted using Trypan Blue on a Cell Countess; calculation were made for 10000 cells, which were plated in triplicate on poly-l lysine layered coverslips in a 6-well plate. The cells were washed in 1xPBS and then fixed with 4% PFA for 10 minutes at room temperature. The cells were then washed in PBS, permeabilised in 0.03% triton in PBS (PBS-T) for 10 minutes, washed and then primary antibodies in PBS-T were applied overnight at +4^{o}C. The cells were then washed the next day, incubated in secondary antibodies for 1 hour at room temperature. They were then finally washed in PBS and then the coverslips were removed from the 6 well plate and placed onto a histological slide,

using mounting medium. The slides were then sealed using nail varnish and left to dry. Once dried, the slides were then imaged and processed on the confocal microscope (Leica SP8 confocal microscope). Due to technical errors, semi-quantitative analysis of the immunofluorescence images was not possible; however this would be important for proper analysis of the data, as it would confirm changes seen in the western blot.

2.2.3. Western Blot

Cells were plated into a 6-well plate and left to grow in the incubator (+37^{o}C) overnight. Once they had reach 70% confluency, cells were then harvested the next day using a cells scraper and then transferred to Eppendorf tubes. Cells were then spun at 5000rpm for 1 minute and the supernatant was removed, and the pellet frozen at -80^{o}C. The cells were lysed in TBS-T and suspended in 2xLB. The sample was then loaded onto a 12.5% acrylamide gel and transferred to a PVDF membrane using the same method used with the CamS120 mice. Membranes were analysed using the Syngene PXi6 Gel and Blot analysing system membranes and to collect the resulting blots. The blots were analysed using ImageJ, standardising values to that of GAPDH which acts as a loading control. It should be noted however that protein concentrations were not determined using the BSA assay before western blotting and therefore fluctuations in protein amounts have occurred, which often prevents proper quantifications, which and statistical analysis. Any observed changes in protein amounts therefore should be treated with caution.

2.2.4. Flow cytometry

Flow cytometry was used to determine changes in mitochondrial membrane potential and ROS production within our cell line.

2.2.4.1. Mitochondria membrane potential

The effect of synuclein proteins on mitochondrial functionality, specifically the maintenance of the mitochondrial membrane potential was investigate using flow cytometry. In the case of the mitochondrial membrane potential, the fluorophore Tetramethylrhodamine, Methyl Ester, Perchlorate (TMRM) was used, which is a dye that enters the mitochondria of only healthy cells, if the mitochondrial membrane is normal. If the mitochondrial membrane potential is disrupted, the dye does not enter the mitochondria. The uncoupling agent, carbonyl cyanide 4-(trifluoromethoxy)phenylhydrazone (FCCP), was used as a negative control, as the uncoupler prevents the dye from entering and remaining within the mitochondria, so that fewer mitochondria contain the dye resulting in a reduction of the overall fluorescence. M17, aFL, bFL and V70M cells were collected, washed with PBS + 5% FBS then incubated for 10 minutes with either HBSS, TMRM or FCCP, in triplicates: M17 + HBSS (control), M17 + FCCP +TMRM (FCCP), M17 + TMRM (TMRM), alpha FL + TMRM (aFL), beta FL + TMRM (bFL), V70M + TMRM (V70M).

Cells were spun at 0.4x1000g for 5 minutes and then resuspended in flow fluid. The suspension was then analysed using flow cytometry (BD Accuri C6 flow cytometer). The average fluorescence for each sample was calculated, with a maximum event count of 10,000 cells.

2.2.4.2. Reactive Oxygen Species

When mitochondrial become damaged, reactive oxygen species are often released from the mitochondria into the cell, which leads to cell death [284]. One such ROS molecule is H_2O_2, which is commonly detected by the dye dichloro-dihydro-fluorescein diacetate (DCFH-DA). DCFH-DA is internalised into the cells, where it is broken down into further metabolites, in particular DCFH carboxylate anions. These anions are

oxidised by ROS to generate a fluorescent product, which can then be detected using either confocal microscopy or flow cytometry. M17 cells, aFL overexpressing cells, bFL overexpressing cells and V70M mutant overexpressing cells were stained with DCFH-DA and processed using flow cytometry. Cells were prepared in triplicates in 6-well plates, then washed in PBS, harvested using trypsin and incubated in 500µl of 10µM DCFH-DA at 37^{o}C for 30 minutes. Cells were then analysed using the flow cytometer. For this experiment, Aria II flow cytometer was used. The FITC channel was used to detect the fluorescence of the dye. A control group was also run at the same time by measuring the fluorescence emitted by M17 control cells without dye, to determine the background fluorescence of the cells. The average fluorescence for each sample was calculated, with a maximum event count of 10,000 cells.

2.2.4.3. Gating in Flow Cytometry

In order to only include the most appropriate cells which are thought to correlate to the healthy dye-containing cells, gating of cells was done (Figure 13). This allowed the detection of debris or large artefacts which do not represent healthy cells, which could be then disregarded in the analysis.

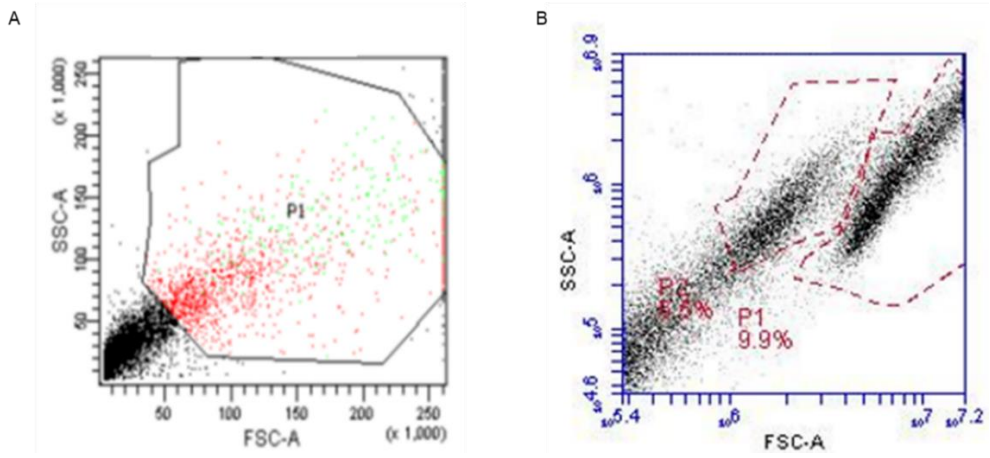

Figure 13. Gating for the flow cytometry experiments. The gating for the flow cytometry experiments to detect changes in ROS (A) and mitochondrial membrane

potential (B). Side scatter (SSC-A) and forward scatter (FSC-A) data are shown. As an example, the gating for only M17 control cells is shown here.

Populations were determined as above. Analysis of changes in ROS production showed a strong presence of debris, as shown by the dense group of cells at the bottom of the scatter plot (Figure 13A). It was therefore hard to distinguish the debris from the normal cells and so a wide area was used to catch all possible healthy cells. Gating was the same for each cell group, in order to reduce inaccuracies that might occur. On the other hand, analysis into changes in mitochondrial membrane permeability (Figure 13B) showed two possible population (labelled P1 and P2), however P2 was the population thought to correspond to the healthy cells with the TMRM dye, due to the higher density and intensity of the TMRM dye. The presence of the P1 population was unexpected in the experiments, however they may correlate with unhealthy cells that

2.3. Confocal microscopy

Both cells and animal tissues stained with fluorescent antibodies were analysed using confocal microscopy. Images were collected using a Leica SP8 TCS confocal microscope at X63 magnification. When using the confocal for mice tissues, the focus was on the hippocampus region, where images of the various hippocampal subregions (dentate gyrus, CA3-1) are taken.

2.4. Primary and secondary antibodies

Information regarding the primary and secondary antibodies used in the experiments are listed below:

Antibodies used (+ Species reactivity)	Supplier	Dilution	Technique
Syn204 (Mouse)	Abcam	1:150	Immunofluorescence
C-20 alpha-synuclein (Rabbit)	Santa Cruz Bio-technology	1:1500	Immunofluorescence
Syn1 (Mouse)	BD Biosciences	1:200	Western blot
5G4 antibody (Mouse)	Millipore	1:500	Immunofluorescence
Beta-synuclein (Rabbit)	Atlas antibodies	1:1000	Immunofluorescence/ Western blot
TOMM20 (Rabbit) *	Atlas Antibodies	1:1000	Immunofluorescence/ Western blot
DLP1 (Mouse)	BD Biosciences	1:1000	Western blot
		1:500	Immunofluorescence
OPA1 (Mouse)	Abcam	1:750	Immunofluorescence/ Western blot
LC3A/B (Rabbit)	Cell Signalling Technology	1:500	Immunofluorescence
		1:1000	Western blot
Lamp2 (mouse)	Abcam	1:500	Immunofluorescence

Table 4. Primary antibodies. Information regarding the primary antibodies used in the immunofluorescence and western blot experiments are listed. Manufactures and dilutions are included. * TOMM20 antibody is also known as Tom20 and is referred to as such henceforth.

Secondary Antibodies used (+ Species reactivity and supplier)	Dilution	Technique
Alexa Fluor-488 Goat anti- mouse (Invitrogen)	1:1000	Immunofluorescence
Alexa Fluor-488 Goat anti- rabbit (Invitrogen)		
Alexa Fluor-594 Goat anti – mouse (Invitrogen)		
Alexa Fluor 594 Goat anti- rabbit (Invitrogen)		
Goat HRP- conjugated anti-mouse IgG (Thermofisher)	1:10000	Western blot
Goat HRP- conjugated anti-rabbit IgG (Thermofisher)		

Table 5. Secondary antibodies. Information on the secondary antibodies used in the immunofluorescence and western blot experiments are listed above.

2.5. Statistics

For mouse behavioural experiments and western blot experiments , data is represented as the mean +/- the standard error of the mean (SEM). Unpaired t-test was performed for these statistical analyses, using the software GraphPad Prism version 5.01. Statistical tests for cell culture western blot and flow cytometry experiments with more than two groups were performed using 2-way ANOVA, using a Bonferroni post-hoc test. Statistical significance is defined using an alpha level of 0.05.

Chapter Three: Results I – Characterisation of the DLB-specific CamS120 mouse model

Whilst there are currently many available mouse models for other neurodegenerative diseases such as Alzheimer's disease and Parkinson's disease, both of which have been extensively reviewed [248, 285], there are currently very few models of DLB. DLB presents a specific set of symptoms, different from other neurodegenerative diseases [17]. In my project a novel mouse model of DLB was closely examined in order to determine its appropriateness and accuracy. The mouse model, named CamS120, is a transgenic mouse line, generated on a C57BL/6J wildtype background, and expresses both a mouse endogenous form of alpha-synuclein, as well as a C-terminally truncated form of human alpha-synuclein. Whilst full-length alpha-synuclein consists of 140 amino acids, the truncated form contains only 120 amino acids. The effect of post-translational modifications of the protein alpha-synuclein, such as nitration, phosphorylation and ubiquitination, has previously been investigated [286], and were found to have an intensifying effect on alpha-synuclein aggregation. Truncation of alpha-synuclein is another post-translation modification which is known to increase the aggregating properties of alpha-synuclein [224, 287], and the resulting alpha-synuclein protein fragment has been found within aggregates isolated from post-mortem DLB brain tissues [48].

3.1. CamS120 genotyping

To confirm that the CamS120 mice do contain the transgene within their DNA, CamS120 mice were ear notched and the DNA extracted from the ear notches was amplified using two set of primers specific to the human truncated alpha-synuclein and the mouse endogenous full-length alpha-synuclein.

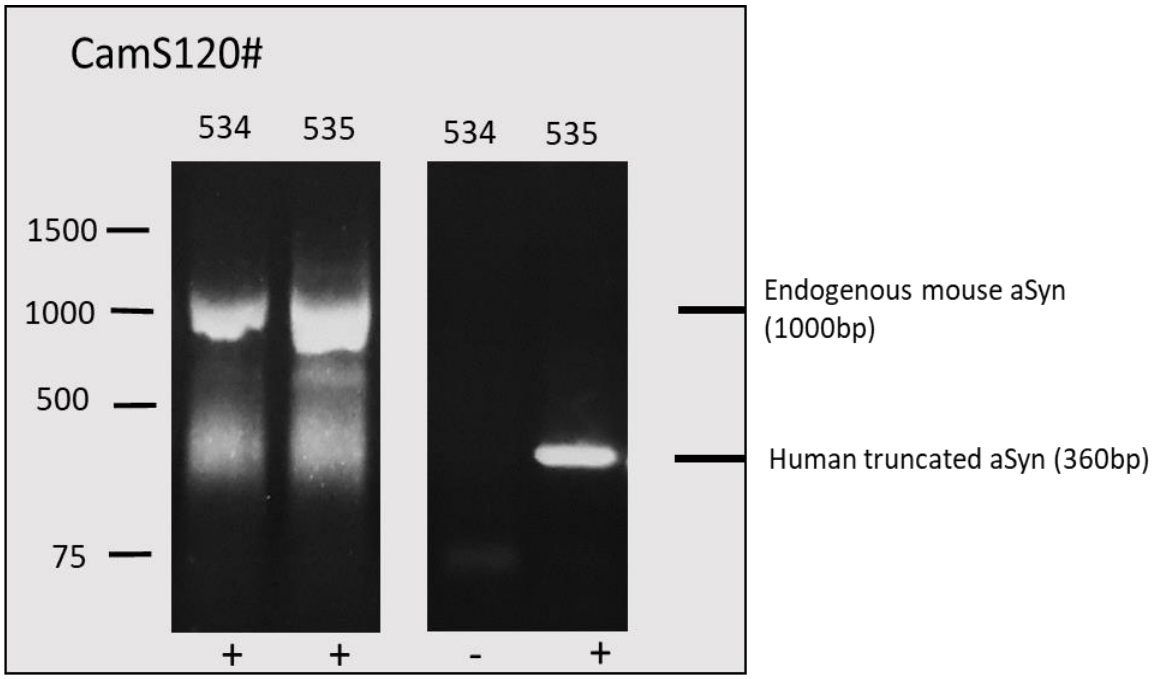

Figure 14. Genotyping of CamS120 mice. DNA of CamS120 mice was extracted and primers for human truncated alpha-synuclein (detects band at around 360bp) and endogenous full-length mouse alpha-synuclein (detects band at around 1000bp) were used to determine the presence of alpha-synuclein. aSyn = alpha-synuclein

In the above figure (Figure 14), genotyping of two mice are shown as an example of identifying control and CamS120 mice. When the PCR product was separated, mouse endogenous alpha-synuclein was found to form a band at around 1000bp, whereas the human truncated alpha-synuclein transgene formed a band at 360bp. Whilst full-length alpha-synuclein is comprised of 420bp, the DNA amplified also contains introns, meaning the band detected consists of more base pairs.

Mice that were positive for both endogenous and the human truncated alpha-synuclein were classified as CamS120 mice, and mice that were positive only for endogenous alpha-synuclein were grouped together to form a control group.

3.2 Alpha-synuclein in CamS120 mouse model

3.2.1. Human alpha-synuclein (Syn204)

Syn204 is an antibody used to detect human alpha-synuclein. This antibody was chosen specifically for its species reactivity, as it detects only human alpha-synuclein and not mouse alpha-synuclein, with a recognition epitope before the C-terminal 20 amino acids of the protein, ensuring sufficient recognition of the truncated product

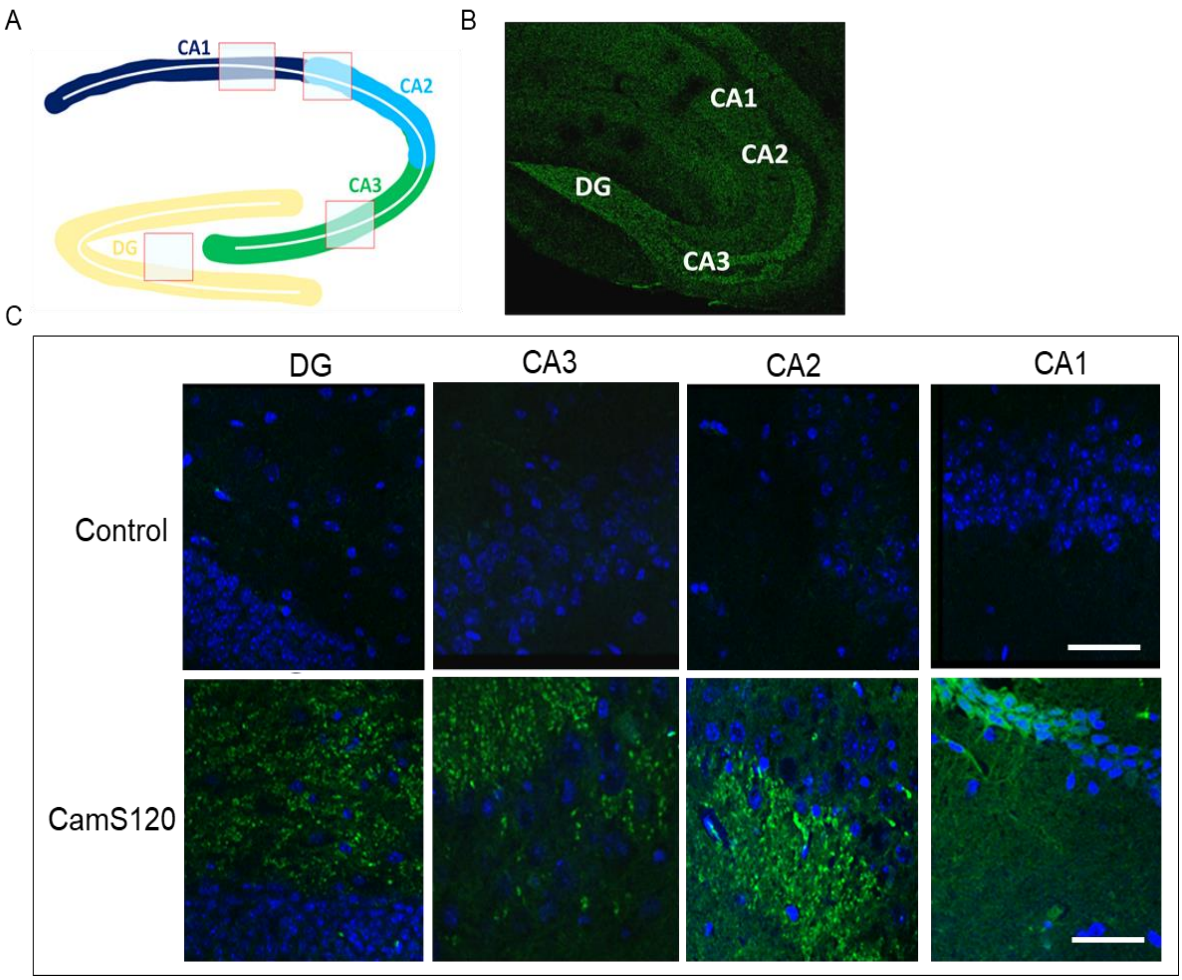

Figure 15. Human alpha-synuclein expression in the hippocampus. Using fluorescent immunostaining, the hippocampus of Control and CamS120 mice were stained using Syn204 antibody (green). An illustration of the general structure of the hippocampus is shown (A). An overview of the hippocampus was taken at X10 magnification of 6 months control and CamS120 mice (B). The differential expression of Syn204 between different hippocampus subregions (dentate gyrus, CA3, CA2 and CA1) was examined with higher magnification (X63 magnification) for both control and CamS120 mice at 12 months old (C). Hoechst staining in blue, as a nuclear marker. Scale bar = 20µm. N=3.

Fluorescent immunostaining for Syn204 in the hippocampus in our CamS120 mice has shown that human alpha-synuclein was found throughout the hippocampus in the transgenic mice, whereas the control mice did not have this characteristic Syn204 staining. Syn204 staining could be seen in the dentate gyrus, CA3 and CA2 regions but staining was weaker in the CA1 region (Figure 15B). Syn204 staining had a diffuse distribution within the hilus and the inner granular layer of the dentate gyrus. The distribution of Syn204 continues to other regions of the hippocampus, with abundant staining in the CA3 and CA2 regions. Syn204 punctate were found mostly in the stratum radiatum region, below the pyramidal cell layer where staining was also seen (Figure 15C).

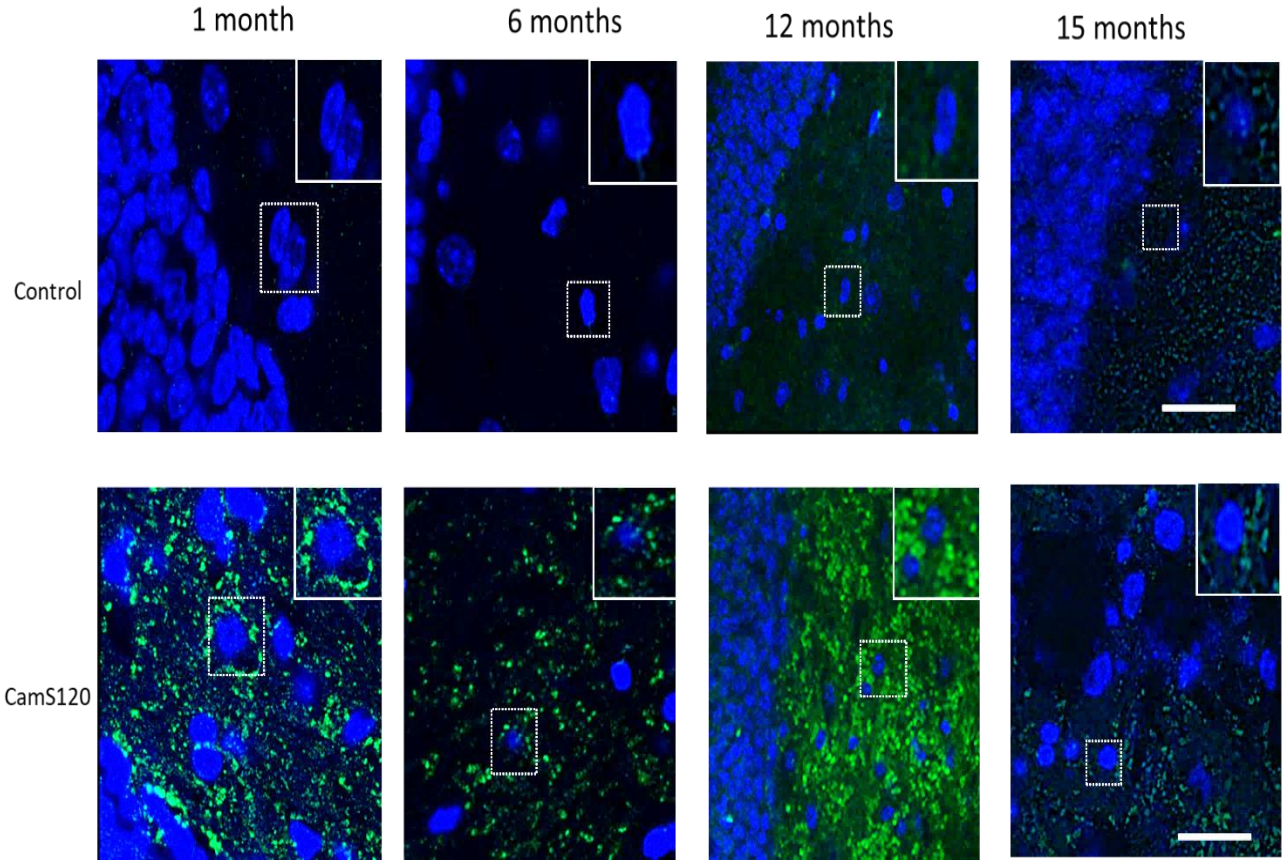

Figure 16. Syn204 staining in the hippocampus of 1, 6, 12 and 15 months mice. Immunofluorescent images were taken of Syn204 staining (green) in the dentate gyrus subregion of the hippocampus of all 4 age groups (1 month, 6 months, 12 months, 15 months). Hoechst staining in blue, as a nuclear marker. Scale bar = 20µm. Magnification X63. N=3.

Immunofluorescent staining with Syn204 staining at all four time points, 1, 6, 12 and 15 months, showed that human alpha-synuclein is present in mice of all time points (Figure 16).

CamS120 mice were then analysed for human alpha-synuclein protein levels using western blot.

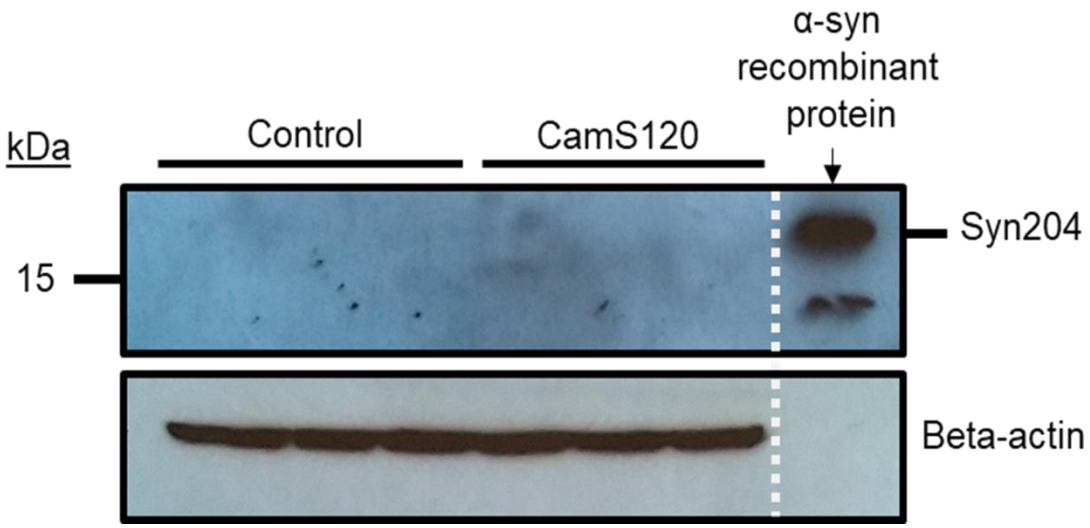

Figure 17. Human alpha-synuclein protein levels could not be detected using western blot. One month control and CamS120 mice were probed with Syn204 antibody. Alpha-synuclein recombinant protein was loaded as a positive control. N=3.

Western blot analysis of hippocampal lysates of 1 month control and CamS120 mice did not show any bands corresponding to human alpha-synuclein as detected by the humans-specific antibody Syn204 (Figure 17). To provide a positive control, human alpha-synuclein recombinant protein was loaded to determine whether the Syn204 antibody was able to detect human alpha-synuclein protein. Results showed that Syn204 was able to sufficiently detect the presence of human alpha-synuclein protein but was not able to detect human alpha-synuclein in hippocampi from CamS120 mice.

3.2.2. Endogenous alpha-synuclein

Whilst human truncated alpha-synuclein could not be detected using western blot, endogenous mouse alpha-synuclein was detected using the antibody Syn1, which detects both mouse and human alpha-synuclein.

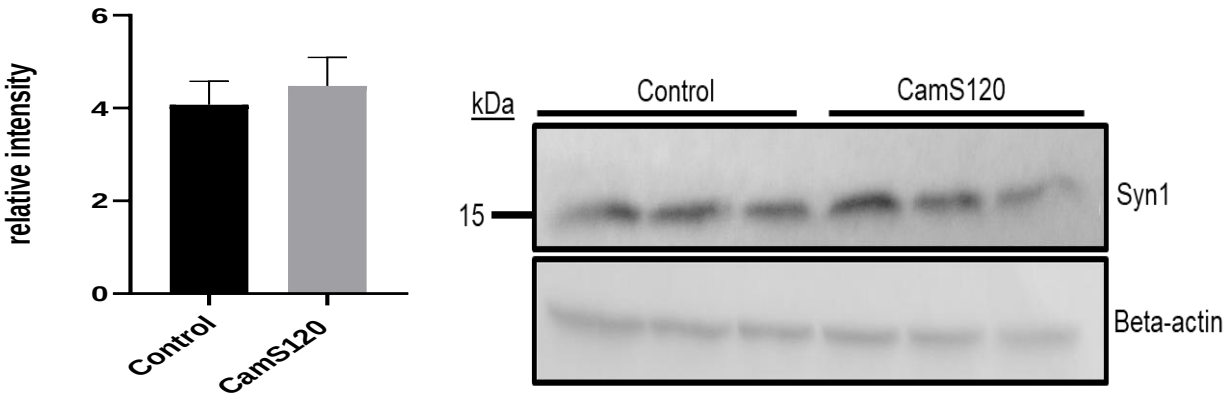

Figure 18. No change in endogenous alpha-synuclein in CamS120 mice. Hippocampi lysates taken from 1 month CamS120 were probed with Syn1 antibody. Data is shown as mean ± SEM. N=3.

Using western blot, 1 month CamS120 mice did not show any changes in endogenous alpha-synuclein levels, as detected by the Syn1 antibody (Figure 18). Western blot data however shows that endogenous alpha-synuclein is present within both control and CamS120 mice. The bands seen in Figure 18 correspond to full-length alpha-synuclein and so can be attributed to mouse endogenous alpha-synuclein. This suggests that the presence of human alpha-synuclein does not necessarily affect the levels of endogenous mouse alpha-synuclein.

3.2.3. Aggregated alpha-synuclein

The defining feature of many neurodegenerative diseases is the presence of aggregating proteins. In DLB, monomers of the protein alpha-synuclein aggregate together to form oligomers, fibrils and eventually Lewy bodies. To determine whether our mouse model displays these oligomeric forms of alpha-synuclein, sections from

15 months old mice were stained for the antibody 5G4, which is an antibody used to detect the oligomeric form of alpha-synuclein.

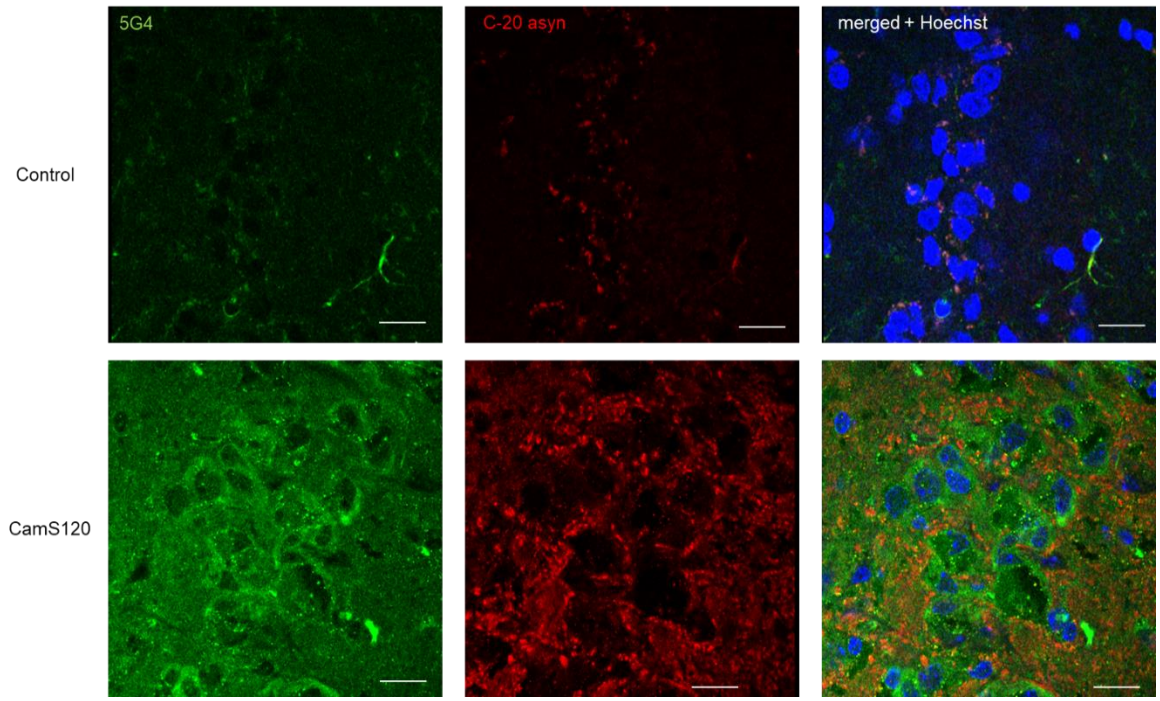

Figure 19. 5G4 immunofluorescence in the hippocampus of 15 month mice. Immunofluorescent images were taken of 5G4 staining in the CA3 subregion of the hippocampus in 15 months mice. Tissues were stained with 5G4 antibody (green) and C-20 alpha-synuclein antibody (red). Scale = 20µm. Magnification X63. N=2

In this experiment, monomeric alpha-synuclein was determined by the antibody C-20. 5G4 staining showed the possible present of insoluble protein in the 15 months CamS120 mice (Figure 19). It can be seen mostly in the cytoplasm outside the nucleus. Strong staining of 5G4 was seen especially around the cell bodies in the pyramidal cell layer. The distribution of the monomeric form of alpha-synuclein was more widespread throughout the CA3 subregion. Whilst monomeric alpha-synuclein was more abundantly expressed throughout, 5G4 staining was present in cells also containing C-20 alpha-synuclein staining.

3.3. Behavioural abnormalities in CamS120 mice

As cognitive and behavioural deficits are core symptoms found in DLB patients, mice models of DLB should ideally show signs of cognitive impairment. In DLB, one of the key areas affected is the hippocampus, which is directly involved in spatial memory and long term memory. My aim was to determine whether the CamS120 mouse model displays any hippocampal dependent memory impairment, like that seen in DLB patients. The NOR test was used to detect changes in recognition memory. To determine whether the effects were due to memory alone, two additional tests, the marble burying test and the open field test, were performed alongside the NOR test to determine if the transgenic mice display sufficient movement capabilities and low stress levels respectively. I used CamS120 mice at 1, 6, 12 and 15 months of age, to identify the specific age points showing recognition memory deficit using the aforementioned behavioural tests.

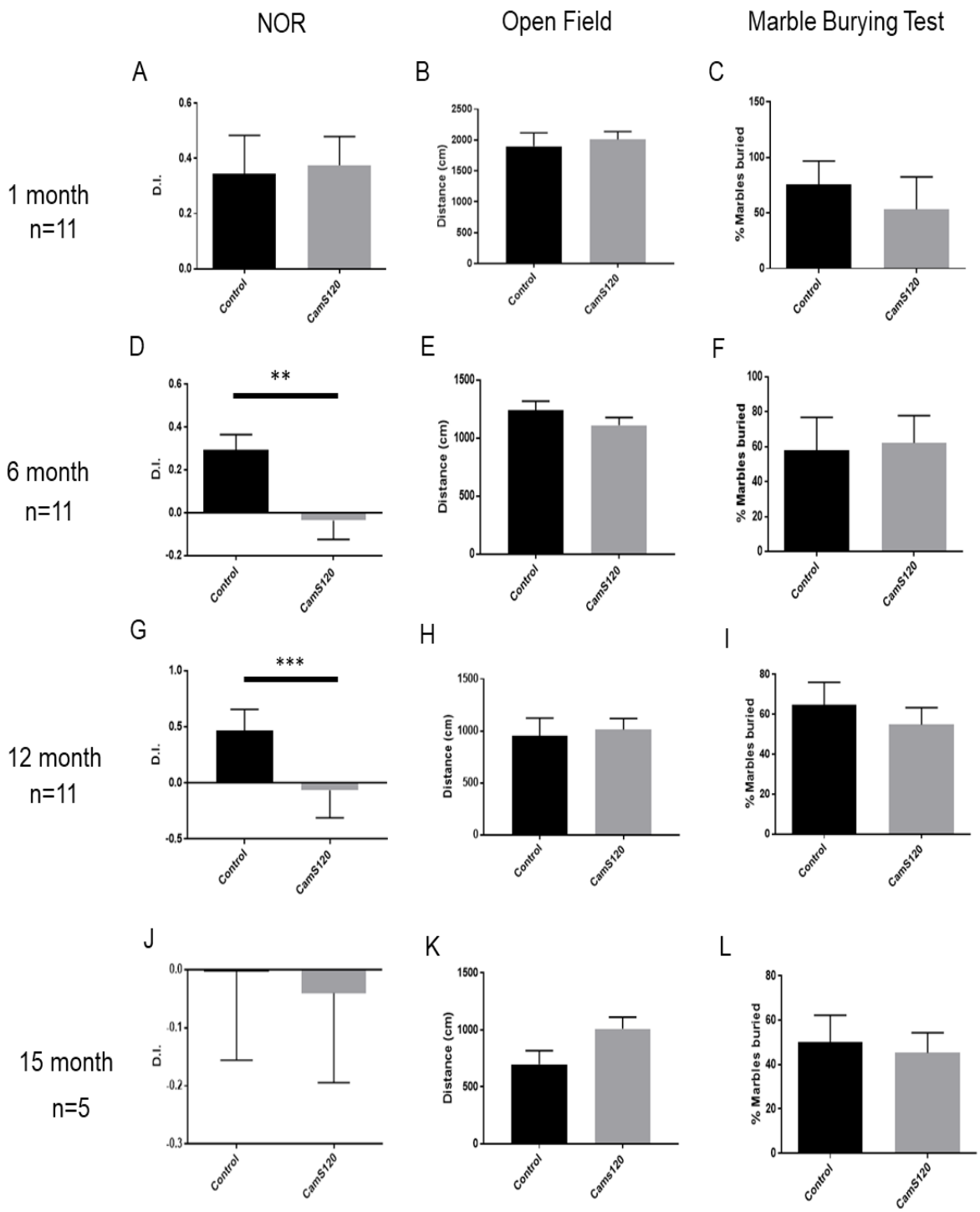

Figure 20. Key behavioural changes in 1 month, 6 months, 12 months and 15 months CamS120 mice. Control and CamS120 mice were tested at 1 month, 6 months, 12 months and 15 months in the NOR test (A,D,G,J respectively), open field test (B,E,H,K respectively) and the marble burying test (C,F, I, L respectively). Data is shown as mean ± SEM. ** $p<0.01$ *** $p<0.001$.

In 1 month old animals, no significant alterations in memory, anxiety or motor activity (Figure 20A) were detected. Both the control and transgenic group achieved similar D.I. scores, indicating equal recognition of the novel and the familiar object. In 6 months old mice, however, I saw for the first time a significant change in the D.I. score, which saw a decrease in the CamS120 transgenic mice ability to recognise a novel object compared to control mice (Figure 20D). This trend continued to be present at 12 months of age, which saw a more pronounced decrease in D.I. score with the CamS120 compared to their age matched controls (Figure 20G). However, at 15 months, both controls and CamS120 mice showed negative D.I. scores, indicating poor recognition memory for both the CamS120 mice and the control mice (Figure 20J).

In these experiments I have seen that our CamS120 mice displayed no changes in cognitive ability at 1 month of age. At this age, both the CamS120 and the age matched control were very mobile, averaging a total distance travelled of more than 1.5m (Figure 20B) and managed to bury around 25% of the marbles (Figure 20C). The results from both the open field and marble burying test show that at this stage the CamS120 transgenic mice were not anxious and displayed normal movement behaviour. CamS120 mice tested at 6, 12 and 15 months also showed little changes in marble burying compared to controls (Figure 20F, I and L). The same was also seen in 6, 12 and 15 months mice when examining their movements in the open field test (Figure 20E, H and K) with no significant difference in the distance the control and CamS120 mice travelled.

Additional parameters were recorded to characterise further movement patterns of CamS120 mice. The table below shows some of these for each test:

		1 month (n=11)		6 months (n=11)		12 months (n=11)		15 months (n=5)	
Test	Parameter	Control	CamS120	Control	CamS120	Control	CamS120	Control	CamS120
Open Field	Speed (cm/s)	3.67	3.91	2.60	2.45	2.28	2.34	1.90	2.30
	Time travelled (s)	264.34	279.91	252.41	243.41	227.68	231.65	191.68	227.68
Marble burying test	2/3 buried (%)	75.56	53.33	57.78	62.22	64.74	54.85	17.19	16.25
NOR	Total exploration time (s)	8.45	8.45	18.42	24.64	29.68	21.40	27.32	23.82
	Nº of explorations	10.38	9.23	11.01	13.10	25.38	12.24	20.75	17.25

Table 6. Additional behavioural changes in CamS120 mice. In addition to the total distance travelled, further parameters tests in the open field included the speed of travel and the length of time travelling were calculated. In the marble burying test, as well as the overall number of marbles buried, the number of marbles that were at least 2/3 buried into the sawdust was also measured. Additional parameters in the NOR include the total length of time mice explored the two objects, the distance travelled around the entire arena, and the number of times the mice went to explore or interact with the objects. Data is shown as the mean value.

These values show that the 15 years old mice in particular, both control and CamS120, spent less time exploring the arena in the open field test, and buried fewer marbles compared to the 1 month, 6 months and 12 months mice. However, the 15 months mice also display longer object exploration times and made the greatest number of explorations, i.e., they made more visits to explore the object.

.

3.4. Final Discussion for Chapter 3

There are very few mouse models that accurately model DLB disease neuropathology. As most synucleinopathy-related models focus on PD, they very often focus on motor abilities. In my project, a novel DLB-specific mouse model was explored. The mouse model used here expresses a truncated form of human alpha-synuclein under the CamKIIα promoter, which allows the distribution of the alpha-synuclein transgene to be focused onto brain regions specifically involved with cognitive functions, such as the frontal cortex and hippocampus. The CamS120 mouse line was derived from a transgenic truncated 1-120 alpha-synuclein mouse line originally described by Hall et al., 2015, which, as described in the section 2.1.1, were bred on an alpha-synuclein null background. The mouse line was then crossed with wildtype C57BL/6J mice, which lead to a mixture of mice being positive or negative for endogenous alpha-synuclein. There have been some reports that human alpha-synuclein pathology is exacerbated in the absence of endogenous alpha-synuclein [288, 289]. Reintroducing endogenous alpha-synuclein into the CamS120 mice was done to gain insight into the importance of endogenous alpha-synuclein in the CamS120 mouse, where truncated alpha-synuclein is expressed, and to see if any behavioural and biochemical changes could be seen in mice positive for endogenous alpha-synuclein and the human alpha-synuclein protein.

As a transgenic mouse model, it is important to show not only the presence of the transgene within their DNA, but also an increase of the protein compared to the control group. Some alpha-synuclein related animal models have shown a substantial increase in alpha-synuclein, with some showing a 2-fold increase [236, 243]. Using immunofluorescence, CamS120 mice model showed strong staining of human alpha-synuclein at all age points, within the hippocampus, in particular within the dentate

gyrus and surrounding the CA3 and CA2 regions. Whilst the CamS120 mice showed a strong positive band for CamKIIα primers when genotyping and a clear increase in diffuse alpha-synuclein protein levels using immunohistochemistry, quantifying alpha-synuclein total proteins levels using western blot was not possible. When analysing alpha-synuclein protein levels using western blot, the whole hippocampi were dissected out of their brains, homogenised and the proteins separated, however for unclear reasons probing for Syn204 has been found to be unsuccessful, with little or no signal seen. However, the presence of monomeric alpha-synuclein using Syn1 antibody which is immunoreactive for both human and mouse alpha-synuclein protein has been seen using western blot. With CamS120 mice, the transgene is truncated, producing a 120aa alpha-synuclein protein, which should be detected as a lower molecular weight than the full-length alpha-synuclein. This, however, was not seen either using western blot. This suggests that perhaps the alpha-synuclein levels, although clearly present in immunofluorescence images in certain subregions of the hippocampus, are not high enough to be detected using the western blot technique. This was unexpected, as previous papers initially examining the mouse model have shown an increase in Syn204 staining [245]. It is possible that as subsequent generations were produced, the expression of the truncated SNCA gene was reduced. As expected, the CamKIIα promoter drove the expression of the transgene to the dentate gyrus, CA3 and CA2 region, however there was no expression of alpha-synuclein in the CA1 region of the hippocampus. In AD, the CA1 region is one of the most affected subregions of hippocampus, and there are reports that the CA1 region may also be affected in DLB too, although possibly not to the same extent as other hippocampal subregions [65]. This does suggest that the model may not fully simulate the hippocampal pathology seen in patients. Despite this though, the results collected

showed that the CamS120 mice displayed a significant impairment in recognition memory, with no accompanying changes in motor function or anxiety, suggesting that pathology in the DG, CA3 or CA2 are involved in the deficit recognition memory seen in the CamS120 mice.

This memory deficit was initially seen in the 6 months old but was more pronounced in the 12 months mice. A significant drop however in D.I. score was seen at 15 months. From the behavioural results, 1 month old mice displayed no problems in recognition memory. They also showed no deficits in general movement and anxiety, as quantified by the open field test and marble burying test, respectively. In contrast, at both 6 months and 12 months, the CamS120 mice scored a negative D.I. score, with a more pronounced decrease in the D.I. at 12 months old mice. In the NOR test, normal control mice should be able to remember the objects presented in the familiarisation stage and will therefore on the whole tend to explore the object that they had not seen before during the testing stage, thus resulting in a positive D.I. score. The negative score seen with the 6 and 12 months old CamS120 mice showed that they spent less time exploring the novel object, and the majority of the time was spent examining the familiar object. This suggests that the mice were most likely not able to recognise the familiar object as well, and so preferentially explored the familiar object again. Objects were paired together for their difference in shape, texture and colour so that they were not too identical in shape. This however presents an issue with the innate preference for one object over another, which might mean that the mice will spend longer on an object which it prefers, or conversely avoids an object it fears. In order to minimise this issue, objects were randomised between the mice, so that within the individual testing groups, mice were presented with either of the two available objects used during the familiarisation stage, to determine any discrepancies within the group. Additionally, it

is also possible that mice may display preference to a particular side of the arena, which will favour the object in that half of the arena. To take this into account, the two objects were always placed in the centre of the arena and during the testing stage half of the mice will have the novel object on the left and the other half on the right. These measures were put in place in an attempt to prevent bias from affecting the average D.I. scores. When performing the novel object recognition test, other protocols for the test have often set a threshold for the total time exploring the object [290]. A threshold of 20 seconds for the total time exploring the objects in the test stage of the test is often used. However, as shown in Table 1, the total exploration average of the 1 month mice was only 8 seconds. The three other time points tested had almost all on average explored the objects for over 20 seconds. At 1 month of age, the mice were put into the behavioural testing arena for the first time. The same mice were then used for the subsequent time points. It may be possible therefore that the 1 month mice might spend more time exploring the arena in comparison to the objects, especially since at that age they tend to be more energetic. Enforcing an exploration time threshold ensures that the D.I. score better reflects the ability of the mice to recognise and discriminate objects. A small total exploration time suggests that the mice have either limited interest in the objects or that the objects were generating a stressful response [276].

Analysis into the CamS120 mice using immunofluorescence showed a relatively little difference in immunopositive staining in the 15 months mice, which correlates to the strong decrease in D.I. score for both control and CamS120 mice at 15 months. The results suggest that whilst CamS120 mice still display a negative D.I. score indicative of poorer memory ability, the control mice themselves may have perhaps developed

age related memory impairment, therefore showing a comparable discrimination ability to CamS120 mice.

The presence of oligomeric alpha-synuclein is a defining feature in DLB and is often regarded as the main toxic species responsible for cell death and not Lewy bodies, as was once thought. This has been confirmed by multiple cell studies which show that expressing alpha-synuclein oligomers leads to significant cellular dysfunction [291]. This is supported by the fact that not all PD patients show the presence of alpha-synuclein containing Lewy bodies, despite showing certain behavioural and motor dysfunction symptoms [292]. In the CamS120 mouse model, oligomeric alpha-synuclein staining could been seen in the cytoplasm only, substantially more so than control mice, suggesting there may be limited oligomeric human alpha-synuclein within the cytoplasm of certain pyramidal cells within the CA3 region. The antibody used to detect oligomeric alpha-synuclein 5G4 in my experiments however has some limitations, as it does not specifically detect alpha-synuclein but rather oligomeric protein in general. Whilst the 5G4 antibody is thought to be able to detect alpha-synuclein using western blot techniques, probing western blots with 5G4 was not successful. Typically, the presence of oligomeric alpha-synuclein is confirmed by isolating aggregates from brain tissue using sequential centrifugation. In this method, lysates are centrifuged, and the resulting supernatants are resuspended in increasing concentrations of detergent, with a final resuspension into urea. This then results in a pellet containing urea-soluble aggregates, which can then be detected using western blot [293]. However, due to the fact that human alpha-synuclein protein level is too low in the CamS120 mice to detect using western blot normally, the sequential centrifugation technique cannot be used to detect insoluble aggregates in the CamS120 mice. Instead, the presence of oligomeric alpha-synuclein could have been

confirmed through the use of the enzyme Proteinase K (PK). PK is able to digest soluble oligomers and so has been used in neurodegenerative disease research [294, 295]. Once applied to the brain tissue, only insoluble protein oligomers should remain, therefore confirming that any immunopositive staining seen using the 5G4 antibody are insoluble oligomeric proteins.

In summary, CamS120 transgenic mice showed human alpha-synuclein staining within the dentate gyrus and CA3-2 subregions of the hippocampus proper, accompanied by possible deficits in recognition memory. Although quantification of alpha-synuclein using western blot could not be confirmed, these results do suggest that the mouse model is most likely able to replicate the overexpression of alpha-synuclein, however to confirm these behavioural changes it would be necessary to establish whether the CamS120 mice do show the presence of human truncated alpha-synuclein using western blot.

Chapter Four: Results II – Mitochondrial dysfunction in alpha-synuclein related models

Alterations in mitochondrial morphology and function are key pathological processes seen in many neurodegenerative diseases. Studies show mitochondria function is often impaired in neurodegenerative diseases such as DLB, which can include a reduction in the total mitochondrial mass, impairment in ATP production and cell metabolism processes [296]. The mitochondrial population integrity is regulated through different pathways, such as mitochondrial dynamics. There are two processes in particular involved in the regulation of mitochondria dynamics: mitochondrial fission and mitochondrial fusion [155, 156]. When stimulated, mitochondrial fission causes a single mitochondrion to divide, whereas mitochondrial fusion causes mitochondria to fuse together. Both mitochondrial fission and fusion consists of several steps, involving proteins found on both the outer and inner mitochondrial membranes. During mitochondrial fusion, both the inner and outer mitochondrial membranes fuse together to form a larger elongated mitochondrion. In mitochondrial fission, mitochondrial fission proteins enclose mitochondria, lysing the mitochondrial membranes, causing mitochondria to become fragmented. Both of these two mitochondrial processes have a direct effect on mitochondrial morphology and overall mitochondrial mass, and often work in tandem, allowing a balance between fission and fusion which enables a degree of control over the mitochondrial population, the process of which is reviewed by [297]. Abnormalities in these processes have been implicated in many neurodegenerative diseases, including PD, HD and AD [298-300]. Research into DLB has also established a link between DLB and mitochondrial dysfunction [301]. Using both a cell model which overexpresses full-length alpha-synuclein, and the novel mouse model CamS120, changes in mitochondrial dynamics were examined using various

mitochondrial markers, including Drp1, Opa1 and Tom20. Although ideally a cell model expressing the truncated form of alpha-synuclein, to match the CamS120 mouse model, would have been used, stably transfected alpha-synuclein full length mice were already available, and due to lack of available time, I was not able to generate a 120 amino acid truncated stable cell line. This does mean that direct comparison between the cell model and the CamS120 mouse model is not possible.

4.1 Distribution of mitochondrial population in alpha-synuclein overexpressing models

4.1.1. Cell model

BE(2)-M17 cells stably transfected with full-length alpha-synuclein (aFL cells) were stained with Tom20 antibody.

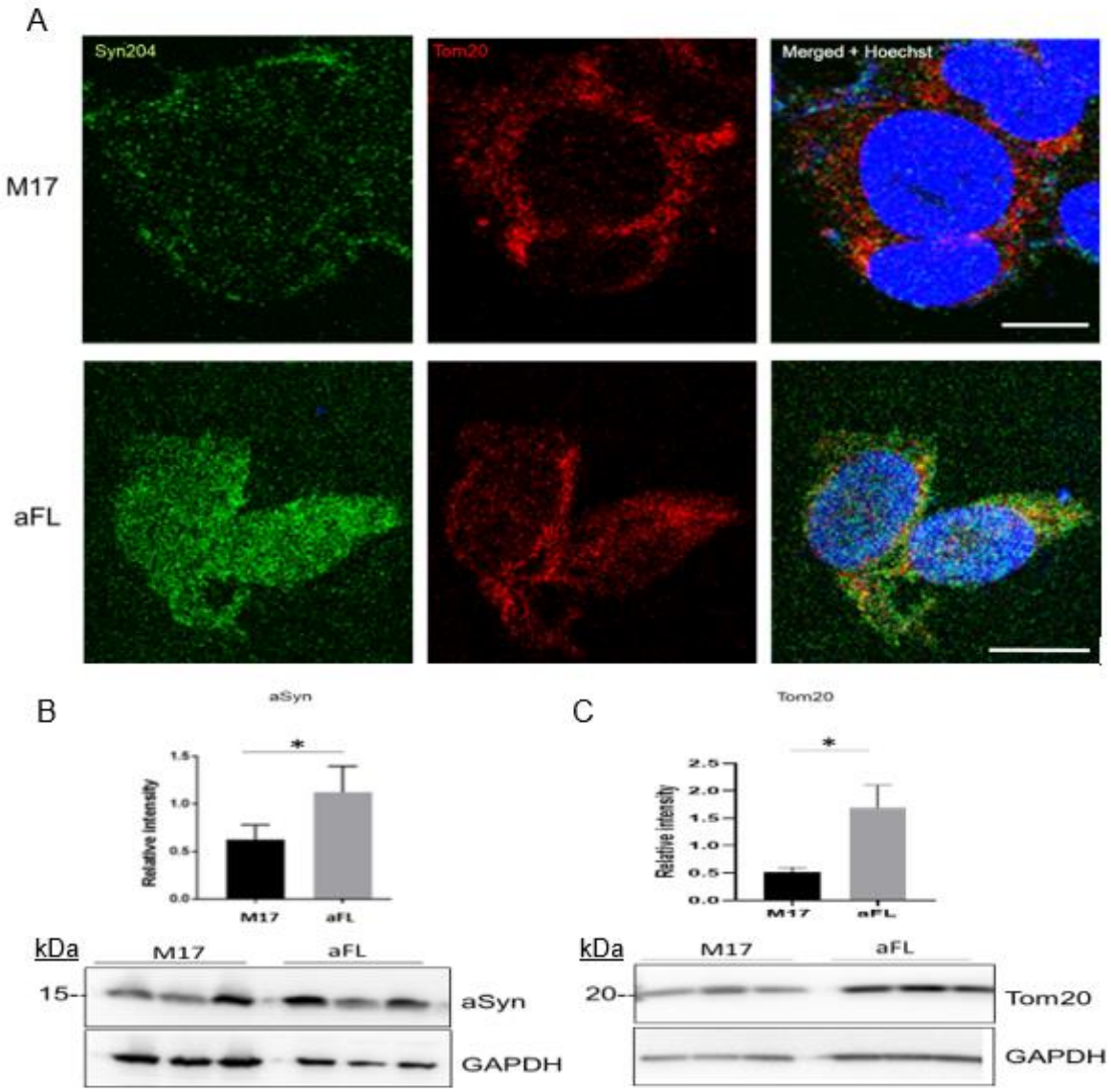

Figure 21. Full-length wildtype alpha-synuclein overexpression alters Tom20 expression. M17 control and alpha-synuclein overexpressing cells were double stained with Tom20 (red) and Syn204 (green) antibody, N=3 (A). Western blotting of M17 and aFL cells lysates were probed with alpha-synuclein and Tom20 antibodies. (B) and Tom20 (C). * $p<0.05$. Western blot data is represented as mean ± SEM. Scale bar = 10 µm. Magnification X63. N=3.

Using immunocytochemistry and western blot, aFL overexpressing cells showed an increase in alpha-synuclein in comparison to M17 controls (Figure 21B). Tom20 is a general mitochondrial protein, and so can identify the total mitochondrial mass. Staining shows that mitochondria labelled with Tom20 were confined to the perinuclear and cytoplasmic regions (Figure 21A). No overall morphological changes in

distribution of Tom20 staining in aFL overexpressing cells were detected. Overexpression of alpha-synuclein however did appear to affect Tom20 protein levels, with elevated Tom20 levels seen (Figure 21C).

4.1.2. CamS120 model

Next, I asked whether changes in the mitochondrial mass in the hippocampus of CamS120 can be observed in similar manner to the cell model described in 4.1.1. CamS120 mice at 12 and 15 months were selected due to the changes seen in the behavioural tests, as 12 months mice showed the strongest memory impairment, and at 15 months old mice show interesting changes after symptoms appear. Therefore I used these particular ages to analyse mitochondrial markers using immunohistochemistry and western blot.

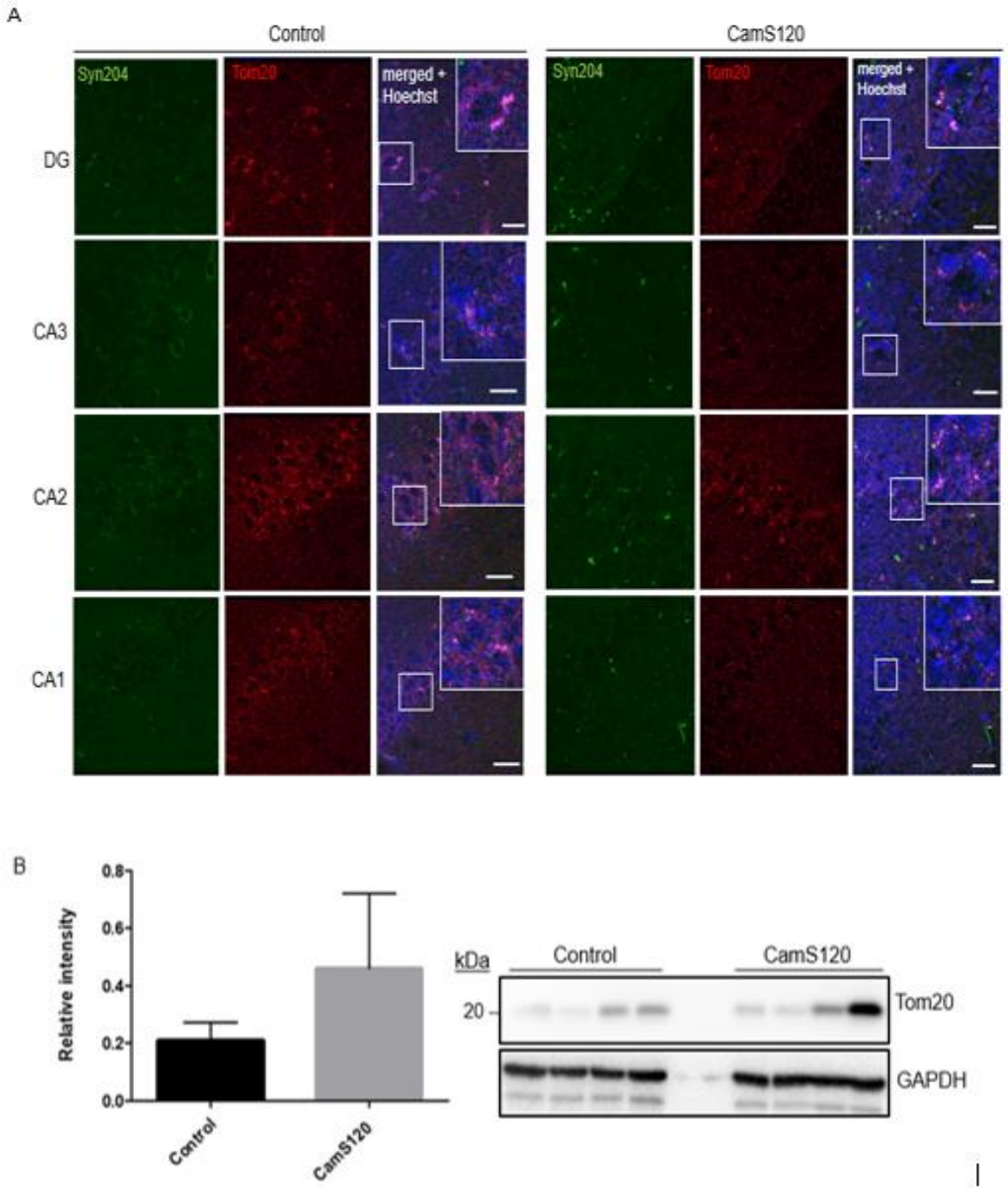

Figure 22. Analysis of 12 month CamS120 mice showed there was a slight, but not significant, increase in Tom20. Hippocampal sections were stained for Tom20 (red) and Syn204 (green) using immunofluorescence N=3 (A). Hippocampi lysates taken from 12 months mice were then analysed for Tom20 protein levels (B). Western blot data is represented as mean ± SEM. Scale bar = 20µm. Magnification X63. N=4.

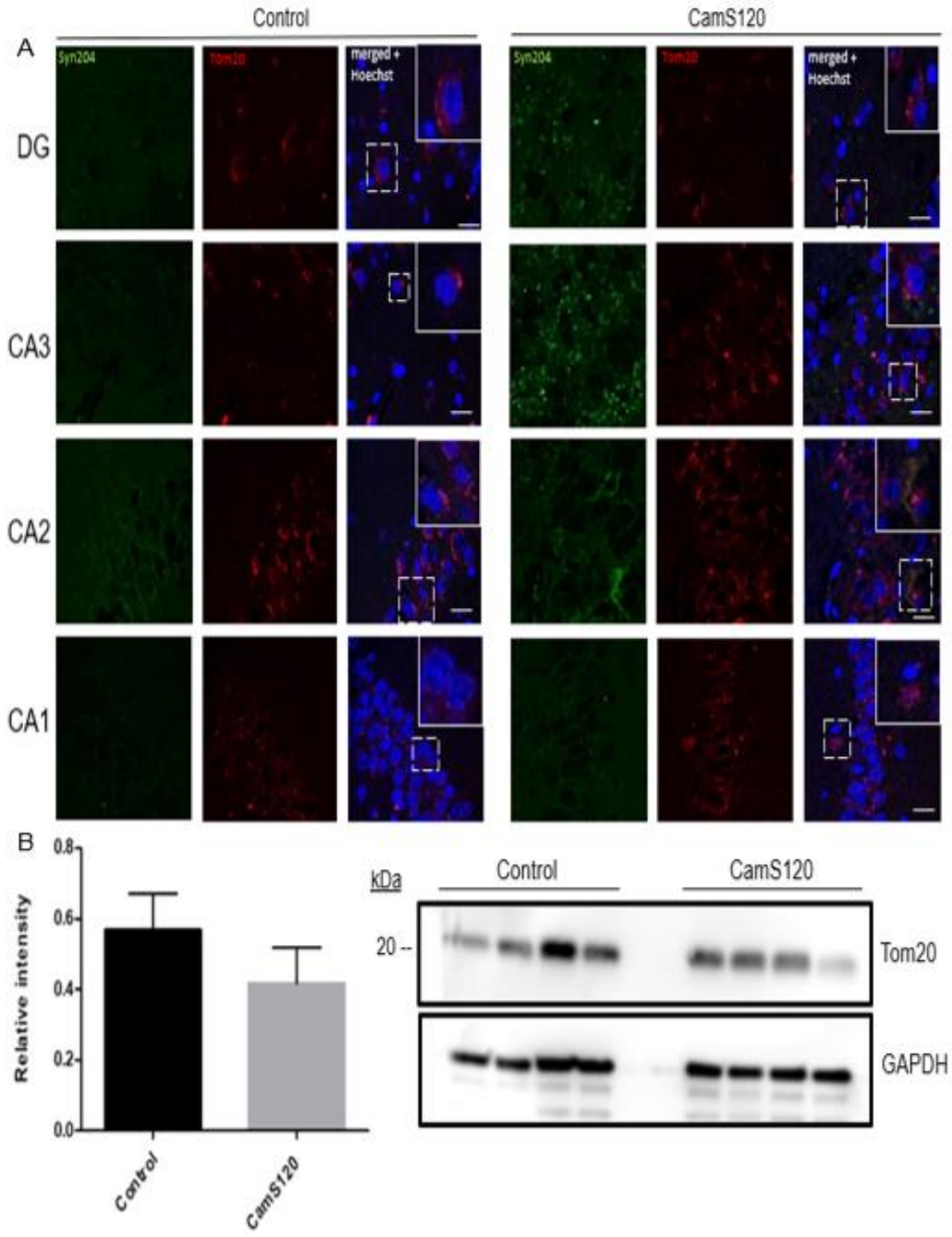

Figure 23. 15 months CamS120 mice show no significant changes in Tom20 levels. Hippocampi sections were stained for Tom20 (red) and Syn204 (green) using immunohistochemistry techniques, N=3 (A), and hippocampal lysates were probed for Tom20 protein using western blot (B). Western blot data is represented as mean ± SEM. Scale bar = 20µm. Magnification X63. N=4.

When examining immunohistochemical distribution of Tom20 in 12 months CamS120 mice, abundant staining was observed around nuclei, showing that in both control and CamS120 mice, mitochondria were mainly clustered within the perinuclear region of the cell, throughout all four regions of the hippocampus (Figure 22A). No significant changes could be seen in morphological distribution of mitochondria; however this was not easily observable using this immunohistochemical technique. Hippocampal lysates of 12 months mice were then prepared in order to examine Tom20 protein levels. No significant changes were seen in the 12 months CamS120 mice (Figure 22B). A similar level of Tom20 protein distribution was seen in 15 months CamS120, with strong Tom20 staining found around the nuclei area of the cells (Figure 23A). Again, there were no significant changes in the Tom20 protein level of hippocampal lysates from 15 months old mice (Figure 23B).

4.2. Mitochondrial dynamics in alpha-synuclein related models

Mitochondrial fission and fusion both involve proteins such as Drp1 or Opa1. Using antibodies which recognise these proteins, I examined whether there were any changes in mitochondrial dynamics in our models of alpha-synuclein overexpression.

4.2.1. Mitochondrial fission

4.2.1.1. BE(2)-M17 cell model

M17 control cells and aFL-overexpressing cells were double stained with Drp1 and Tom20 and examined using the confocal microscope.

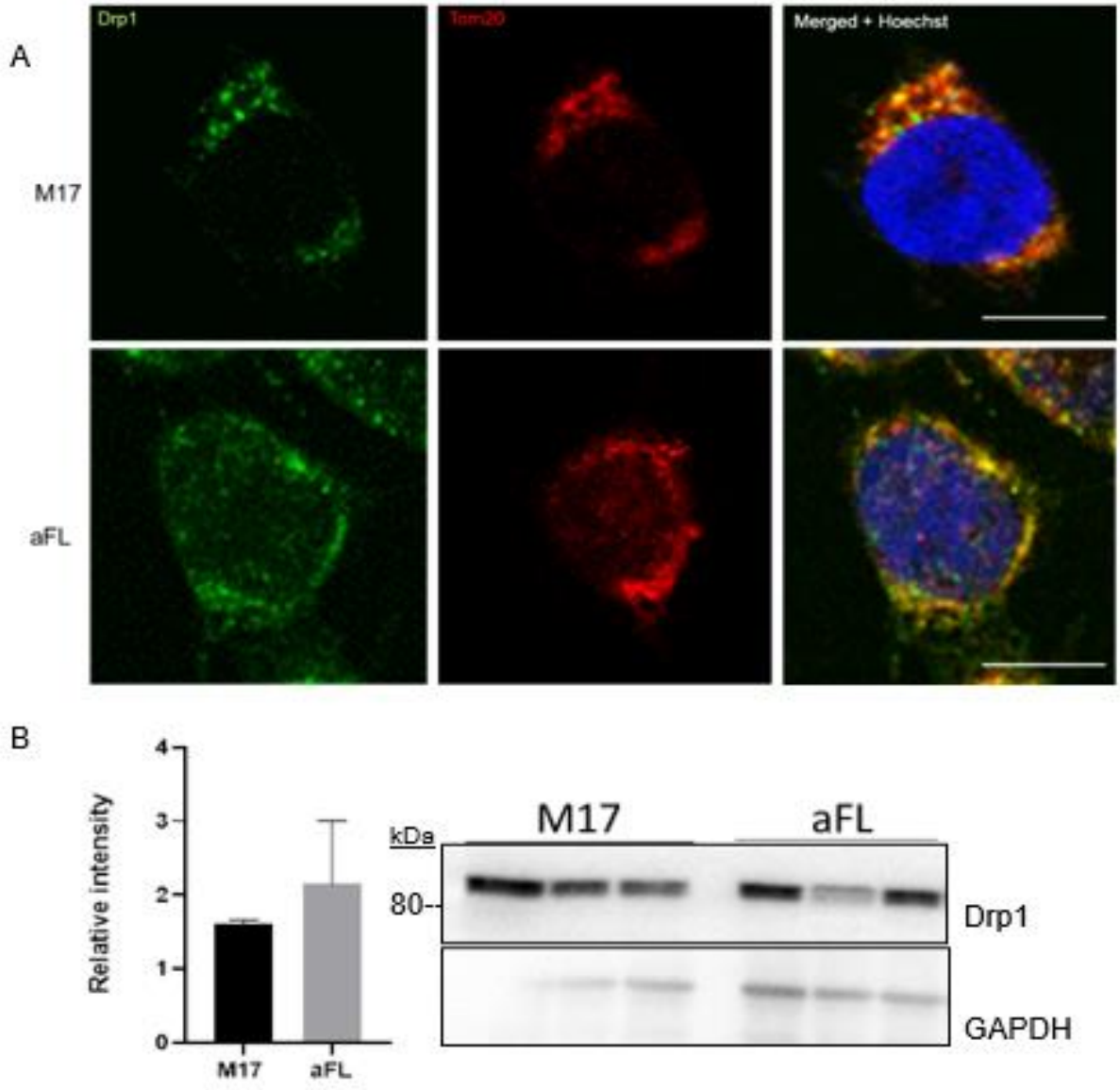

Figure 24. Alpha- synuclein overexpressing cells do not show an increase in Drp1. M17 and aFL cells were double stained with Drp1 (green) and Tom20 (red), N=3 (A). M17 and aFL lysates were analysed for Drp1 protein levels (B). An insignificant increase in Drp1 was seen (p=0.5564). Western blot data is represented as mean ± SEM. Scale = 10µm. Magnification X63. N=3.

aFL cells were stained for Drp1, which is a marker of mitochondrial fission. Staining was prevalent in both M17 and aFL cells, but Drp1 staining seemed stronger in the aFL cells than the control M17 cells (Figure 24A). Using western blot, Drp1 levels were not changed in aFL cells (Figure 24B).

4.2.1.2. CamS120 mice

Hippocampal samples from 12 and 15 months CamS120 mice were stained with the mitochondrial fission protein Drp1.

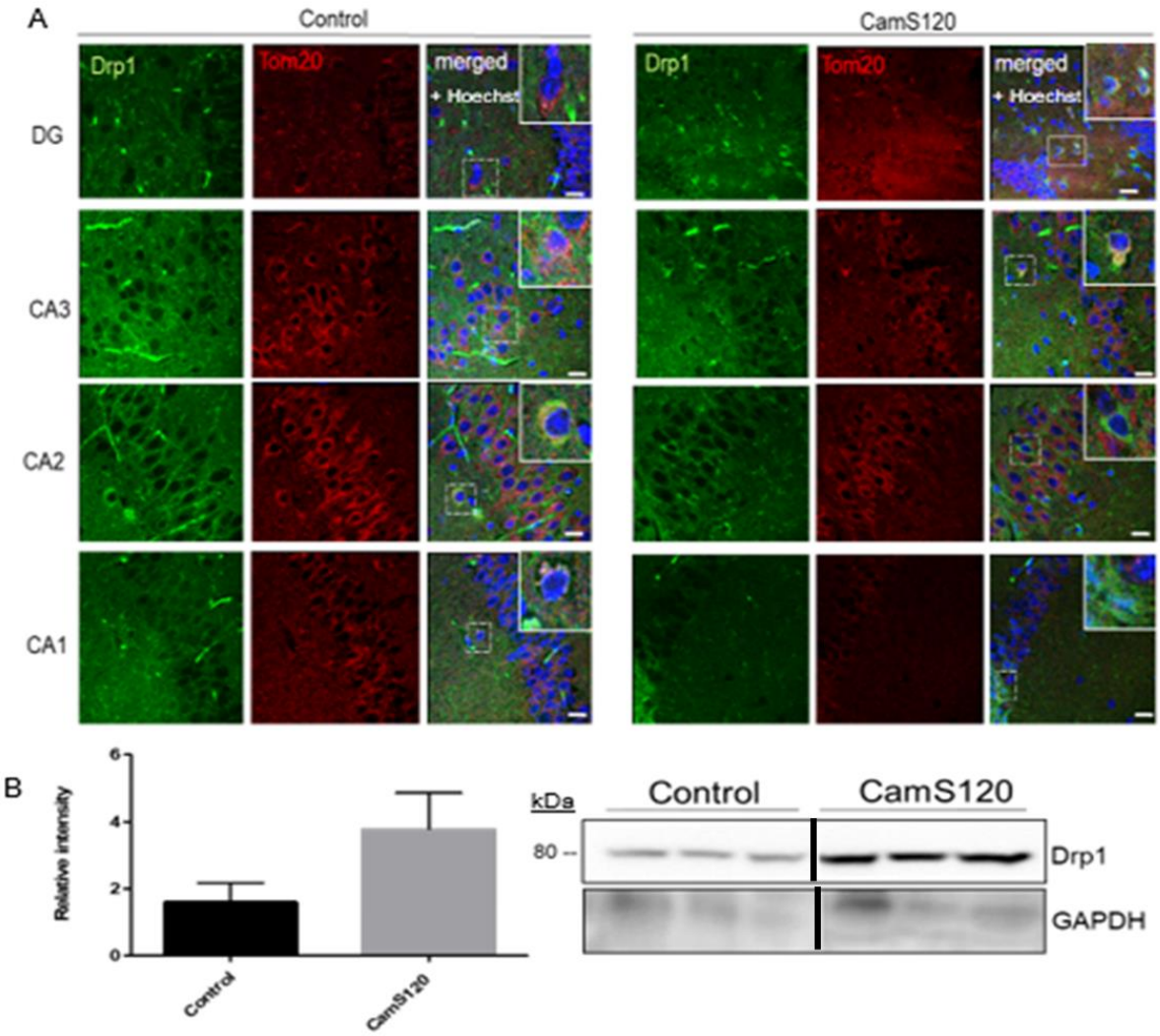

Figure 25. 12 months CamS120 mice show no significant change in mitochondrial fission. Hippocampal sections were double stained with Drp1 (green) and Tom20 (red). N=3 (A). Hippocampi from 12 months CamS120 mice were stained for the mitochondrial fission protein Drp1 (B). Scale = 20µm. Western blot data is represented as mean ± SEM. Magnification X63. N=3.

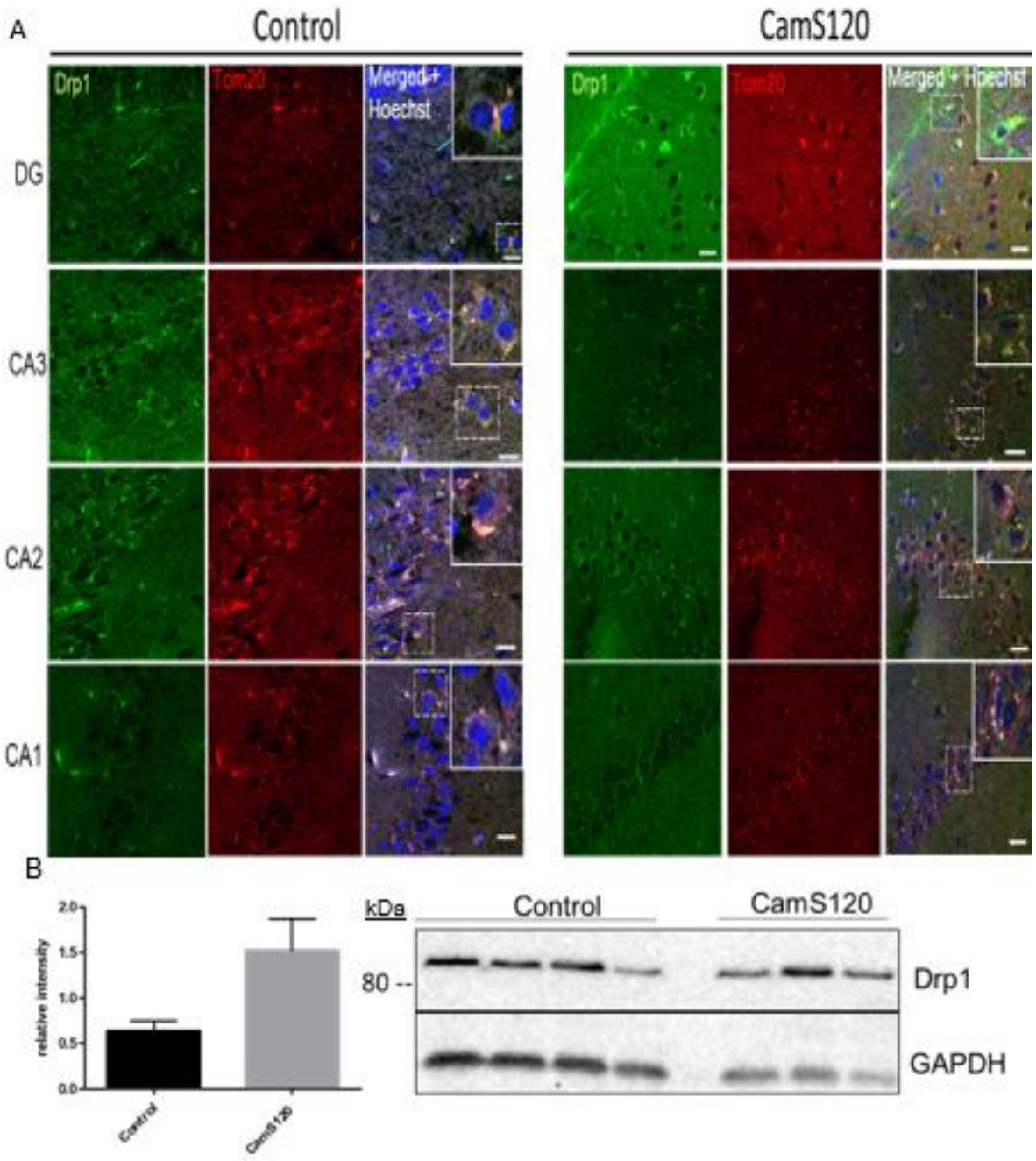

Figure 26. 15 months CamS120 mice show no significant change in mitochondrial fission. Hippocampal sections were double stained with Drp1 (green) and Tom20 (red) N=3 (A). Hippocampi from 15 months CamS120 mice were analysed for the mitochondrial fission protein Drp1 (B). Scale = 20µm. Western blot data is represented as mean ± SEM. Magnification X63. N=3/4.

Drp1 and Tom20 staining was detected in both the 12 months and 15 months CamS120 mice. Both Drp1 and Tom20 were found in close proximity, in the cytoplasm

surrounding the nucleus in both the 12 months (Figure 25) and 15 months (Figure 26) CamS120 mice. Using immunohistochemistry, there was visually very little change in Drp1 in both age groups. Across the hippocampal regions in the 12 and 15 months mice, Drp1 staining was more intense in the dentate gyrus, but there was not as such staining in Drp1 staining in the CA3, CA2 and CA1 regions (Figure 25A, 26A). However, any changes in staining with these mice were subtle and this was further confirmed by western blot (Figure 25B, 26B), which showed there was no significant changes in Drp1 protein levels in both the 12 months and 15 months CamS120 mice. The western blot showing changes in Drp1 levels in 12 months, were cut as there was technical error with one of the samples and so that one was removed from analysis, however these samples were run on the same blot, and so the remaining mouse tissue can still be compared.

4.2.2. Mitochondrial fusion

4.2.2.1. BE(2)-M17 cell model

Having seen a change in mitochondrial fission in the cell model where alpha-synuclein is overexpressed, I tested for changes in mitochondrial fusion in the same cell model.

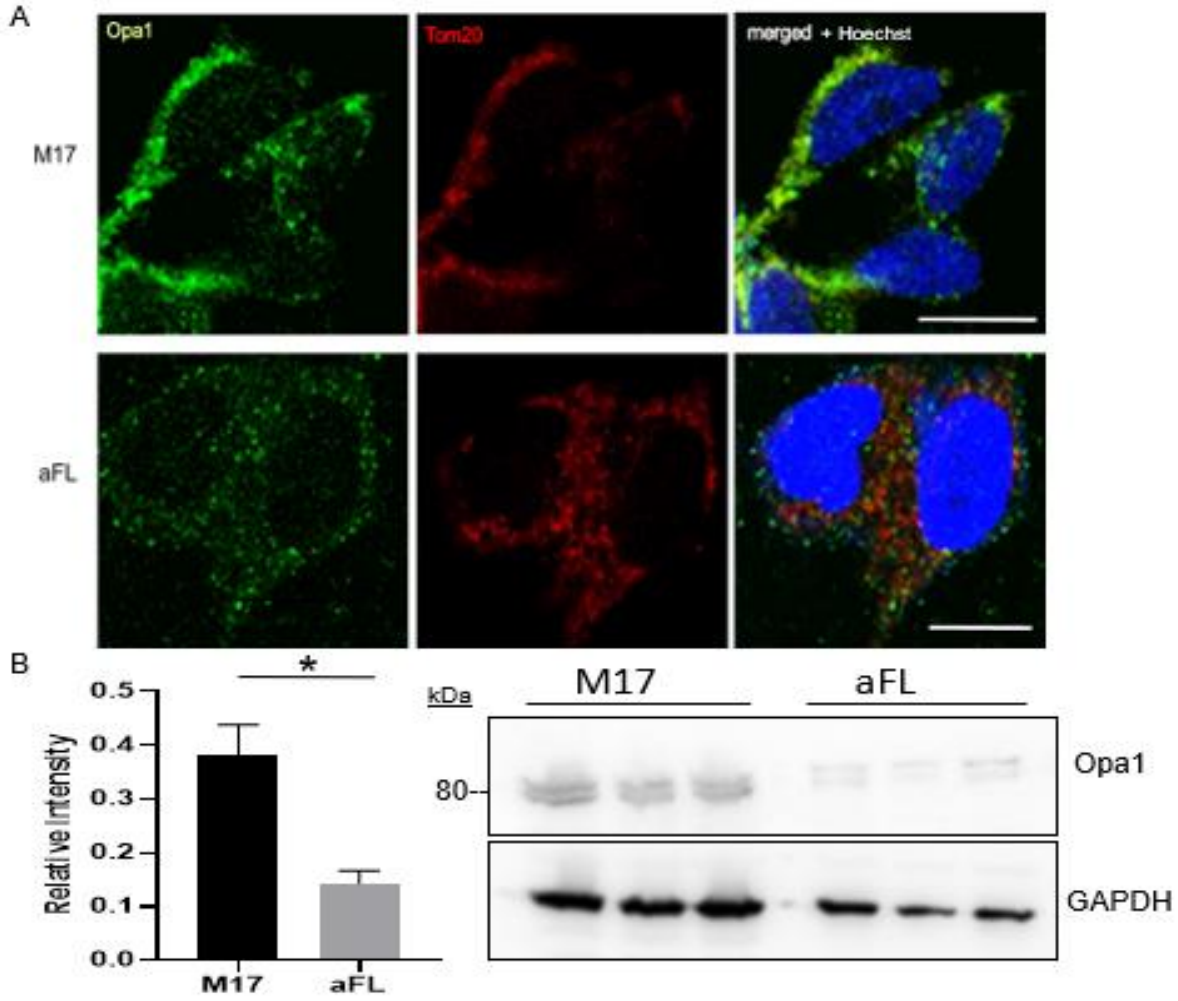

Figure 27. AFL overexpressing cells show a decrease in Opa1 staining. M17 control and aFL cells were double stained with Opa1 (green) and Tom20 (red), N=3 (A). M17 and aFL cells were analysed from Opa1 protein levels using western blot (B). Western blot data is represented as mean ± SEM. Scale = 10µm. Magnification X63. * $p<0.05$. N=3.

AFL overexpressing cells were stained with the mitochondrial fusion protein antibody Opa1 and Tom20 (Figure 27A). Opa1 staining could be seen in the M17 cells and were seen as punctates in the cytoplasm outside the nucleus. When analysing the Opa1 levels using western blot, Opa1 levels appeared to be reduced in aFL cells (Figure 27B).

4.2.2.2. CamS120 mouse model

Staining for changes in Opa1 protein levels was then done using 12 months and 15 months CamS120 mice.

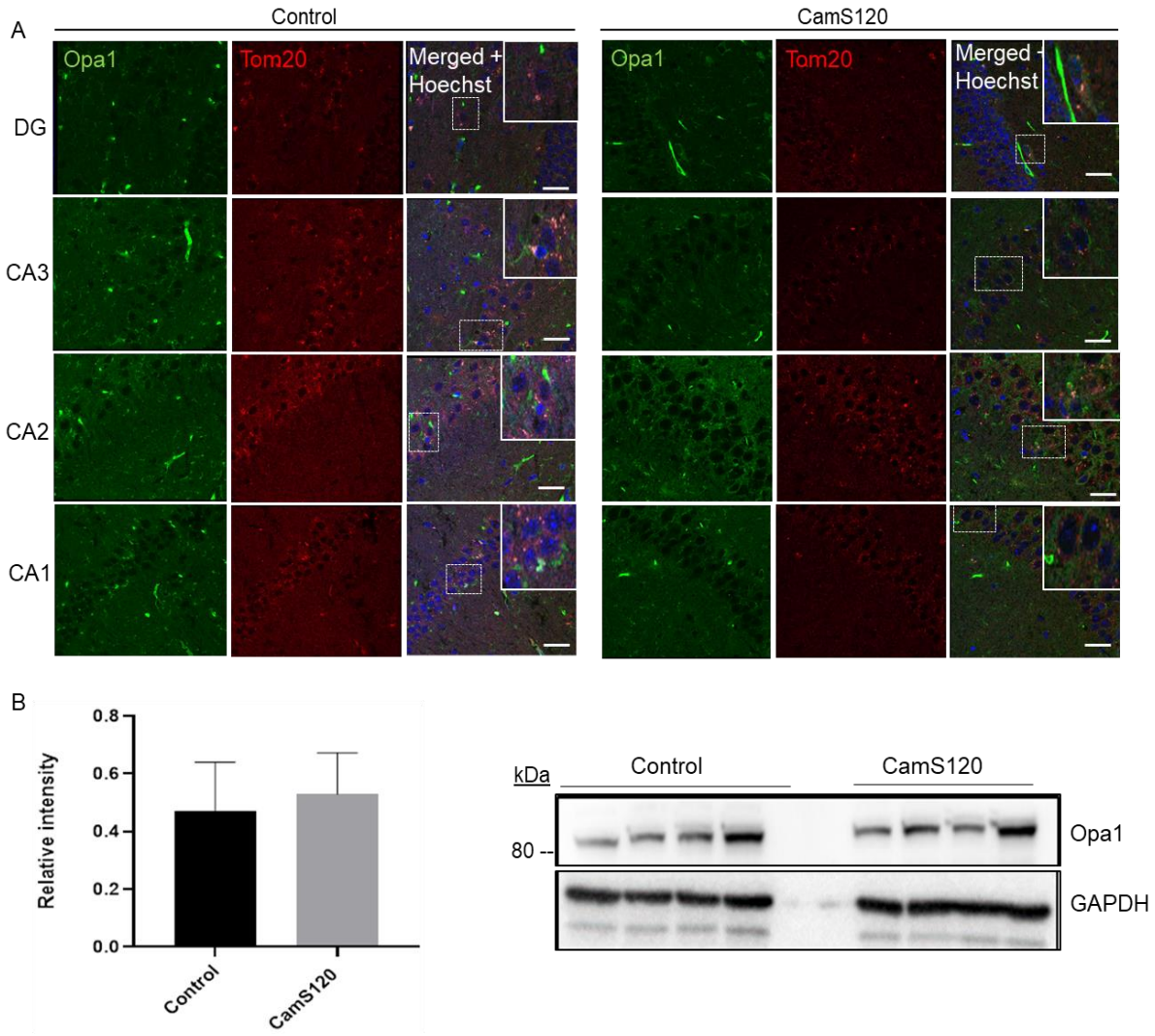

Figure 28. 12 months CamS120 mice show no significant change in mitochondrial fusion. Hippocampal brain sections were immunostained for Opa1 (green) and Tom20 (red), N=3 (A). Opa1 protein levels were analysed using western blot (B). Western blot data is represented as mean ± SEM. Scale = 20µm. Magnification X63. N=4.

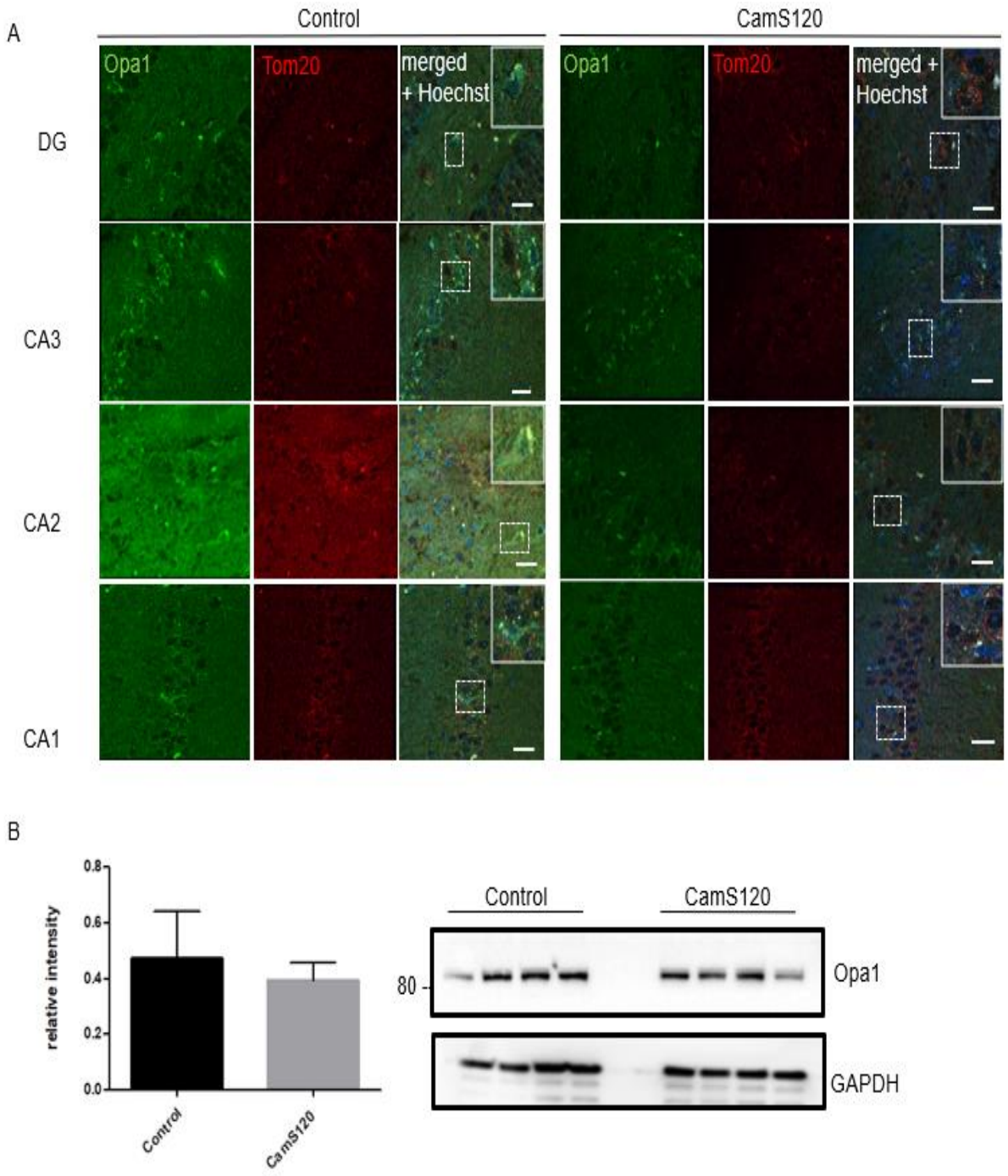

Figure 29. 15 months CamS120 mice show no significant change in mitochondrial fission. Hippocampal sections from the mice from 15 months mice were double stained for Opa1 (green) and Tom20 (red) N=4 (A) Hippocampal lysates were analysed for Opa1 protein levels using western blot (B). Western blot data is represented as mean ± SEM. Magnification X63. Scale = 20µm. N=4.

In the cell model, a possible decrease in Opa1 staining could be seen. However, this was not seen in the mouse model. Both 12 months (Figure 28) and 15 months old

(Figure 29) control and CamS120 mice showed Opa1 staining in all four regions, with strong staining in the CA3 especially. Western blot analysis showed that at both ages, there was no significant changes in Opa1 protein levels in CamS120 mice at either 12 months or 15 months.

4.3. Changes in mitochondrial membrane potential in aFL cells

The maintenance of the mitochondrial membrane potential is necessary for the normal function of healthy mitochondria. To detect membrane potential, I have used TMRM dye, which can only permeate through the mitochondrial membrane of active mitochondria and can then be detected by the FL-2A channel on the flow cytometer.

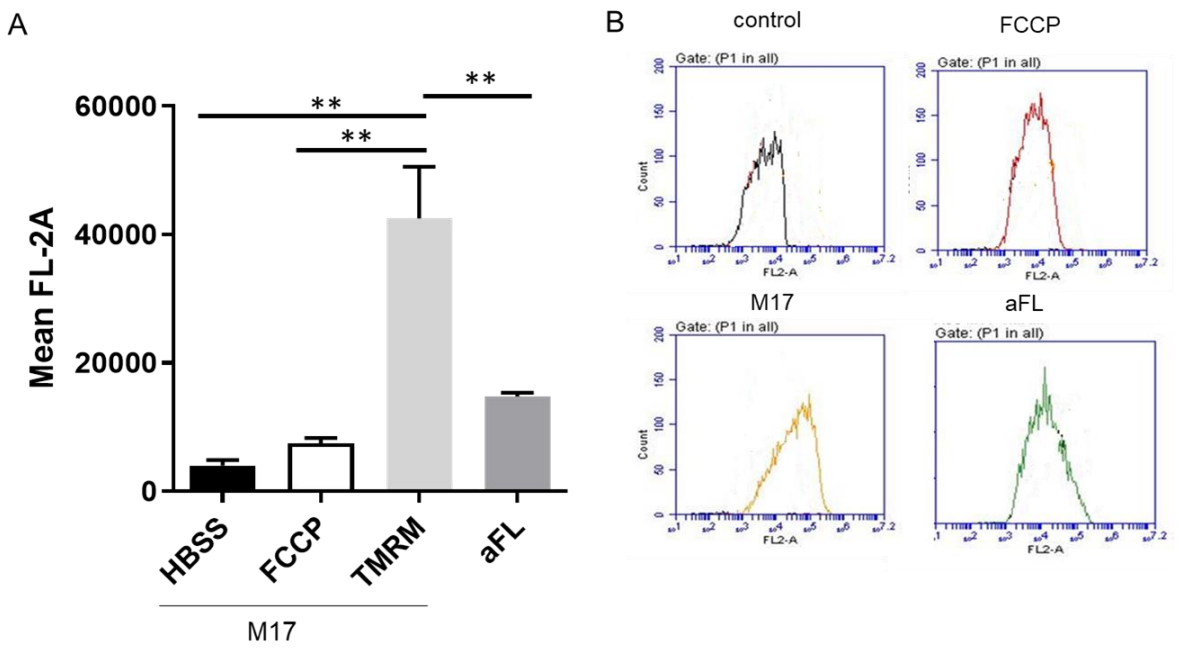

Figure 30. Full-length alpha-synuclein cells show abnormalities in the mitochondrial membrane potential. Wildtype M17 cells and alpha-synuclein overexpressing cells (aFL) were stained with the dye TMRM. The cells were then analysed using flow cytometry and the fluorescence (FL-2A) was detected. Data is represented as mean ± SEM (A). Wildtype M17 cells were stained with TMRM and used as a control (labelled TMRM). The mitochondrial uncoupler FCCP was added to M17 cells in addition to TMRM as a positive control (labelled FCCP). M17 cells with no dye added was also done to determine auto-fluorescence of the cells (labelled control). Average cell counts are represented as a histogram (B). Cell types were performed in triplicates. ** $p<0.01$

The fluorescence from M17 control (with only TMRM) cells was significantly stronger than that from the M17 FCCP control (Figure 30A). The aFL cells were tested alongside M17. As was seen in the FCCP control, the cells overexpressing alpha-synuclein saw a significant decrease in fluorescence signal, in comparison to the M17 cells. This can be seen in the average events histograms (Figure 30B), which showed that a shift to the left in fluorescence can be seen in aFL cells compared to M17 cells.

4.4. Reactive oxygen species generation in aFL cells

When mitochondria undergo cell death, mitochondria release ROS such as Cytochrome C and H_2O_2. DCFH-DA is a dye which binds to intermediates of H_2O_2. Attached to a fluorophore, the dye is detected by the FITC channel

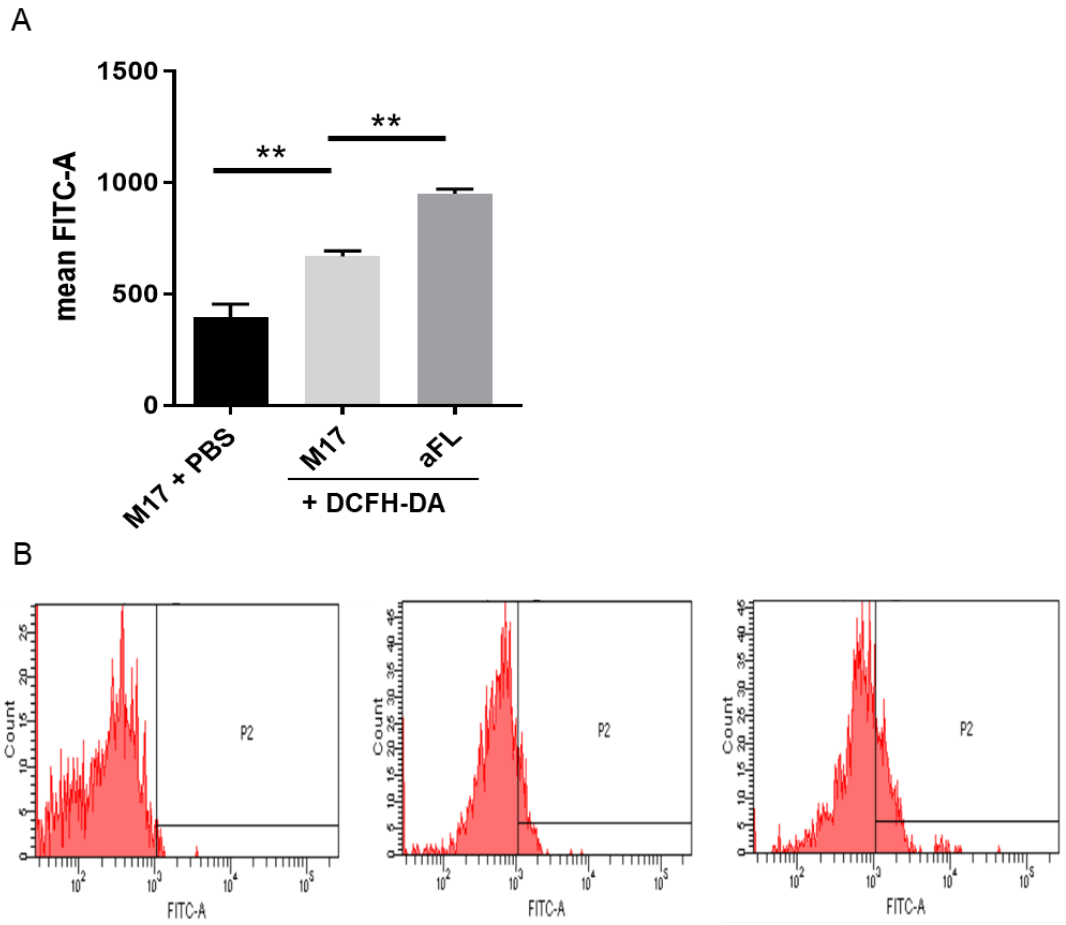

Figure 31. AFL overexpressing cells contain a higher level of ROS. M17 wildtype and aFL overexpressing cells were stained with the dye DCFH-DA and then analysed on the flow cytometer. M17 cells without dye were examined as the control group. Cell

types were performed in triplicates. Data is represented as mean ± SEM (A). Events count graphs for each sample were produced, showing the number of events counted for specific FITC fluorescence (B). ** p< 0.01.

M17 cells were found to have a significantly higher fluorescence compared to the M17 cells without DCFH-DA dye added control group. In addition, aFL cells were also found to have significantly higher fluorescence compared to the M17 cells (Figure 31A). This can be seen in the average events histograms (Figure 31B), where a noticeable shift in fluorescence can be seen across all three groups tested.

4.5. Mitochondrial interactions with autophagy proteins

Mitophagy is the specific process by which damaged mitochondria are degraded by the autophagy system and is often disrupted in neurodegenerative diseases such as PD and DLB [302, 303]. To see whether this may also be the case in our cell model , I co-stained them with Tom20 and either LC3 (Figure 32) or Lamp2 (Figure 33).

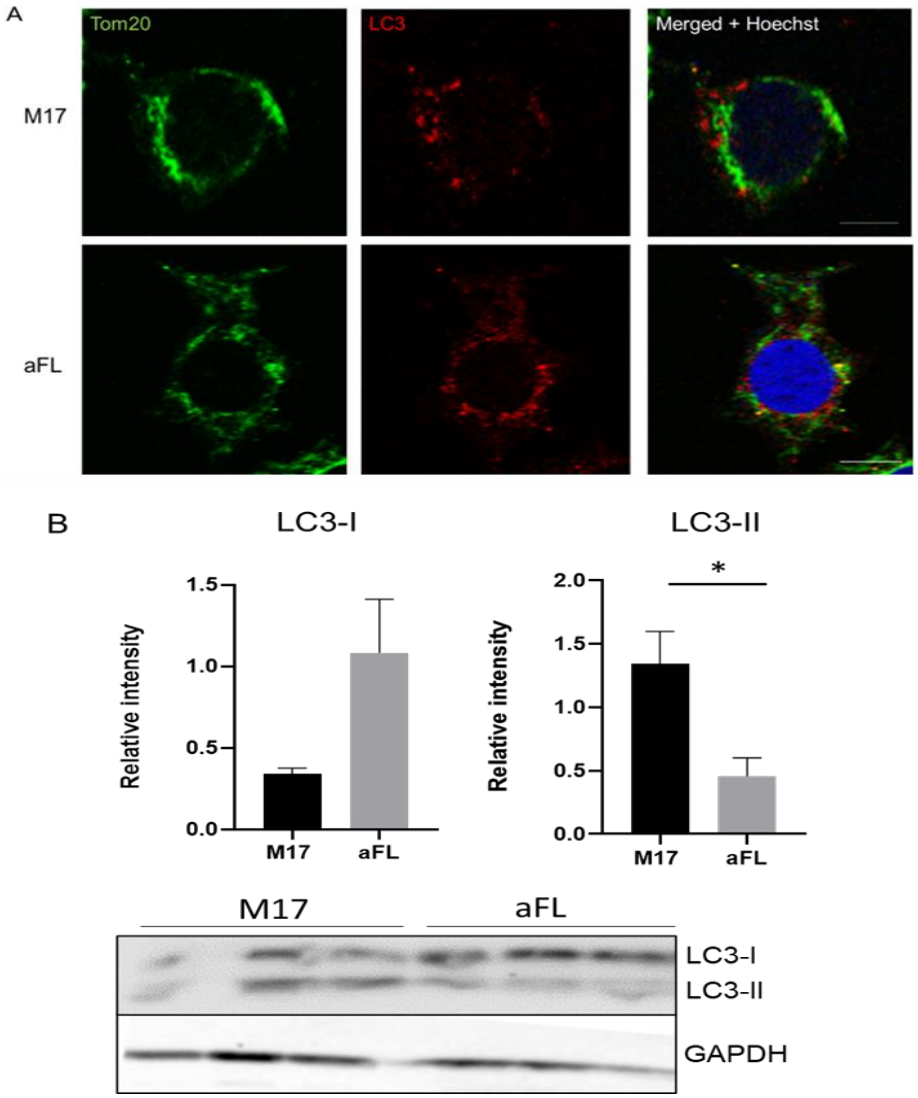

Figure 32. AFL overexpressing cells show an increase in the localisation between LC3 and Tom20. M17 and aFL cells were double stained with LC3A/B (red) and Tom20 (green) antibody. AFL cells were probed for LC3 using western blot. N=3 (B). Western blot data is represented as mean ± SEM. * $p<0.05$ Scale = 10µm. Magnification X63. N=3.

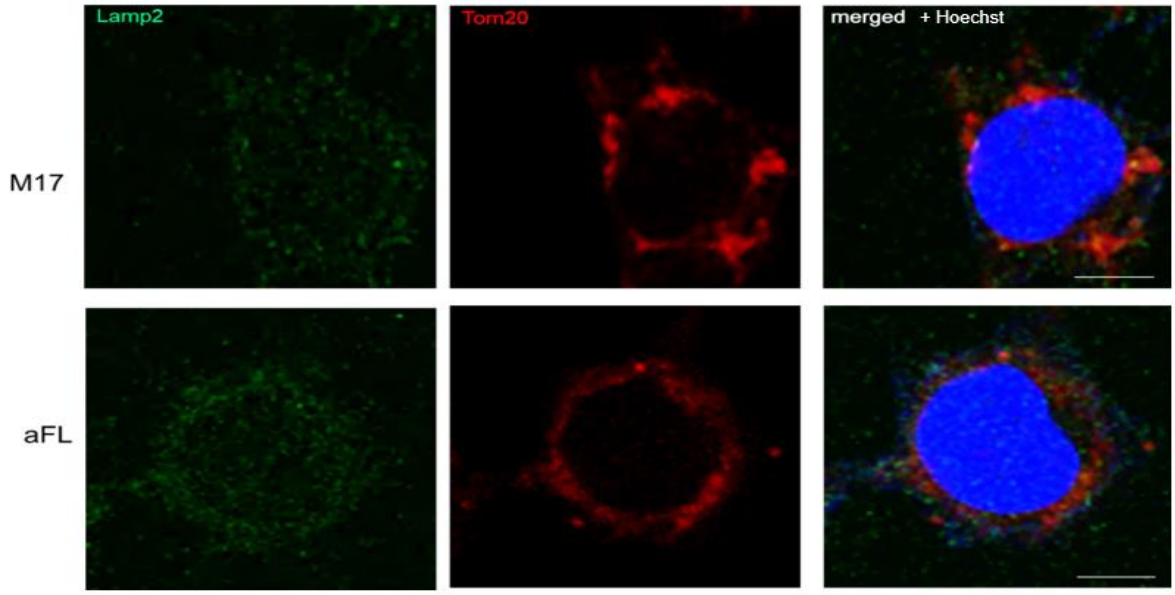

Figure 33. Lamp2 staining show no difference between aFL and M17 controls. M17 and aFL cells were double stained with Lamp2 (green) and Tom20 (red). Scale = 10µm. Magnification was X63. N=3.

LC3 punctates could be seen in both M17 and aFL cells and were localised in the cytoplasm, outside of the nucleus. Overall, there appears to be an increase in LC3 punctates in aFL cells (Figure 32). Lamp2 staining was weak, but stronger staining was seen in the cytoplasm, outside the nucleus (Figure 33). With aFL cells, the Lamp2 staining appeared more closely clustered within the perinuclear region, and so staining seemed very slightly stronger. LC3 protein levels were also measured with western blot (Figure 32B). Two distinct bands could be seen, and an increase in the band corresponding to LC3-I was also seen, whereas conversely a decrease was seen in the band corresponding to LC3-II protein. The western blot therefore possibly indicates a lack of proper autophagosome formation, as LC3-I protein is converted to LC3-II upon autophagosome formation.

It is worth noting that these experiments however were trial experiments to begin exploring changes in mitophagy in aFL cells, and as such would need to be repeated to confirm such a change.

4.6. Final discussion for Chapter 4

Mitochondrial dysfunction is a key characteristic in neurodegenerative diseases such as PD and AD. Here, using cell and animal models related to the neurodegenerative disease DLB, changes in mitochondrial function were analysed. The CamS120 and cell mode reproduced the alpha-synuclein accumulation observed in DLB. The CamS120 mice model showed possible accumulation of alpha-synuclein within the hippocampus of transgenic mice.

The CamS120 mouse model showed little change in the distribution of mitochondrial mass or in mitochondrial dynamics proteins. Changes in mitochondrial dynamics proteins have been reported in other studies [147], which show that increased alpha-synuclein protein can lead to an increase in mitochondrial fission, causing mitochondria to fragment. In addition, a decrease in Opa1 levels suggest that fewer mitochondria are fusing together, resulting in shorter mitochondrial overall. Whether the overall increase in Tom20 in aFL cells is directly due to the decrease in Opa1 levels is unclear.

The modest changes in mitochondrial dynamics in the mouse model however may possibly be in response to the limited production of the truncated alpha-synuclein, suggesting that that the CamS120 mice is perhaps not a strong enough model to show significant changes in mitochondrial dynamic proteins. To complement the mouse model and to verify whether the lack of overall mitochondrial alteration in CamS120

mice is due to the nature of truncation or level of expression, it would have also been interesting to prepare a stable cell model which expresses a truncated version of alpha-synuclein.

To determine the mitochondrial quality, the mitochondrial membrane potential and ROS production were tested, both of which are highly controlled mitochondrial processes. Since the cell model appears to be more sensitive to changes in mitochondrial function so far, only the cell model was tested for changes in mitochondrial membrane potential and ROS production. In other alpha-synuclein models, mitochondrial membrane potential has been shown to become impaired and ROS production increased [304, 305]. These particular changes in mitochondrial function were also seen in the aFL cell model used here.

When mitochondria become damaged, it initiates the process of mitophagy which leads to the degradation and removal of the damaged mitochondria from the cell. In neurodegenerative diseases, including PD and DLB, this process can be disrupted, preventing the degradation and removal of damaged mitochondrial from the cell [306]. An integral part of the mitophagy process is the recruitment of lysosomes to the autophagosomes [307]. The marker Lamp2, a lysosomal associated membrane protein, is often used to analyse lysosomal activity. Immunofluorescent staining with Lamp2 showed a very weak punctate staining, making it hard to determine any significant changes in Lamp2 expression in aFL cells. LC3 staining on the other hand was more successful. An increase in LC3 punctates might reflect an increase in the number of autophagosomes, and thus a higher rate of the autophagy process in the cells. This response might be indicative of an early autophagy response to increased alpha-synuclein overexpression, where autophagosomes are formed in the cytoplasm.

To determine whether there is a convergence between the autophagy and mitochondrial system in our DLB cell model, double staining was done to determine the interaction between mitochondria and LC3 proteins. Using western blot, two distinct bands could be seen using the LC3 antibody, which correlated to either LC3-I or LC3-II. When autophagosomes are formed, LC3-I is converted to LC3-II and so is an indicator of complete autophagosome formation. The data therefore indicates that whilst there appeared to be an increase in LC3 protein levels, there was a decrease in LC3-II, which would imply that there is an impairment in complete autophagosome formation as well as in the proper clearance of autophagosomes by the lysosomal system. Lamp2 staining was however not successful so the involvement of the lysosomes in our cell model could not be confirmed with the data collected. Previous studies using cells overexpressing alpha-synuclein have shown co-localisation between alpha-synuclein protein, autophagy and lysosomal markers, such as LC3 and Lamp2 proteins [111], which shows that increased alpha-synuclein accumulation in cells are able to promote autophagy processes, with increased alpha-synuclein containing autophagosomes. The effect of the accumulation of alpha-synuclein on mitophagy processes has also been examined using cell models, with studies showing that alpha-synuclein interacts with mitochondria and stimulates the mitophagy process [116, 303]. Alpha-synuclein for example was found within Parkin expressing mitophagy vacuoles, showing that toxic alpha-synuclein is sequestered into mitochondria, which stimulates the clearance of these mitochondria through mitophagy [308], which fits with results collected from experiments with my aFL cell model.

Overall, the results collected have shown that the mouse model did not exert any significant effect on mitochondrial function, so it is hard to conclude whether

mitochondrial function is directly related to the behavioural changes seen in the CamS120 mice. Additionally, whilst analysis of the aFL cell model did show some possible changes in mitochondrial function, it is important to note that due to the quality of the blots and the loading controls with the cell culture work that significant results seen here should be treated with caution, and experiments would needed to be repeated to sufficiently determine whether Tom20 protein levels are affected in beta-synuclein expressing cells. The CamS120 mice model often showed large variances between mice in the same group which might add to the lack of significance seen in the results and so increasing the number of mice per group might improve the chances of obtaining a significant result. The question of what happens at the cellular level within the CamS120 mice to cause the possible behavioural deficits seen is still not clear. Due to the inconclusive results seen with the CamS120 mice here however, it is hard therefore to come to a conclusion about the effect of truncated alpha-synuclein on mitochondrial function.

Chapter Five: Results III – Beta-synuclein in DLB

The exact role of the protein beta-synuclein in DLB pathology, how it can prevent alpha-synuclein aggregation or how mutated beta-synuclein can lead to DLB-related symptoms is still not well understood. Research so far has found a connection between beta-synuclein, in particular mutated beta-synuclein, and impairment in cellular dysfunction, such as attenuating autophagy flux [202] and lysosomal function [203]. Comparatively, little is known about the effect of beta-synuclein, mutated beta-synuclein in particular, on mitochondria. In this chapter, I aim to investigate whether wildtype beta-synuclein is altered in our DLB CamS120 mouse model, and the stable alpha-synuclein overexpressing cells, to a similar extent seen in human DLB post-mortem tissue. In addition, I aim to investigate the effect of mutated beta-synuclein in particular on mitochondrial function which as of yet not been explored before, using a V70M mutated beta-synuclein stable cell line.

5.1. Beta-synuclein protein levels in CamS120 mice

In order to find an explanation for the observed changes in the behavioural alterations of the CamS120 mice model, I examined beta-synuclein protein distribution and protein levels using both immunochemistry and western blot. Beta-synuclein levels in the hippocampus of CamS120 mice were detected using the beta-synuclein antibody, which is immunoreactive for both human and mouse beta-synuclein protein.

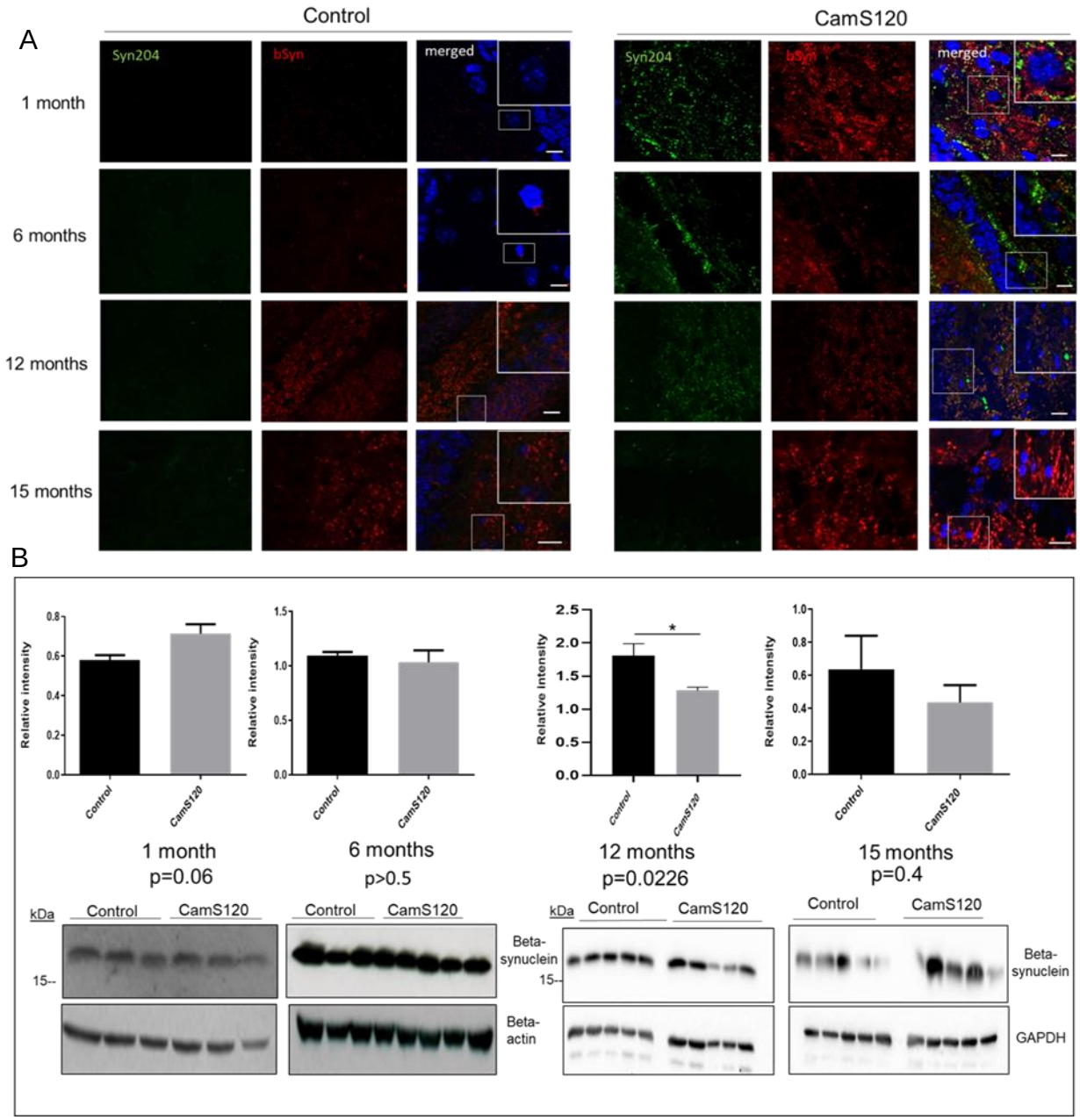

Figure 34. 12 months CamS120 mice show a significant decrease in beta-synuclein levels. The dentate gyrus of 1, 6, 12 and 15 months control and CamS120 were analysed for beta-synuclein (red) and Syn204 (green) N=3 (A). Hippocampal lysates from 1, 6, 12 and 15 months were analysed for beta-synuclein using western blot techniques (B). Scale bar = 20µm. Controls used in western blotting for 1 and 6 months were beta actin. Data is represented as mean ± SEM. N=3 (1 month), N=4 (6 months), N=5 (12 and 15 months).

To correspond with the temporal progression of behavioural changes, 1, 6, 12 and 15 months CamS120 mice were tested for beta-synuclein levels. Immunofluorescent staining showed a diffuse pattern of beta-synuclein protein in all four age groups (Figure 34A), in both control and CamS120 mice. The distribution of beta-synuclein

within the hippocampus of CamS120 mice did not visually appear to change with time, with each age group showing strong beta-synuclein staining within the neuropil in the hilus region, as well as some weaker staining found closely surrounding the cell bodies in the granular layers of the dentate gyrus. In this respect, beta-synuclein staining was found to be in close proximity to alpha-synuclein and co-localisation between the two proteins could be seen throughout the hippocampus, indicated by the appearance of yellow staining. This is indeed expected for these two synaptic proteins. Western blot analysis of whole hippocampal lysates shows no significant changes in beta-synuclein levels in the younger years (1 and 3 months) and 15 months mice, however, a significant decrease in beta-synuclein protein levels was seen in 12 months CamS120 mice (Figure 34B).

5.2. Beta-synuclein levels in aFL cells

Beta-synuclein protein levels were then analysed in alpha-synuclein overexpressing cells (aFL cells) using immunofluorescence and western blot.

.

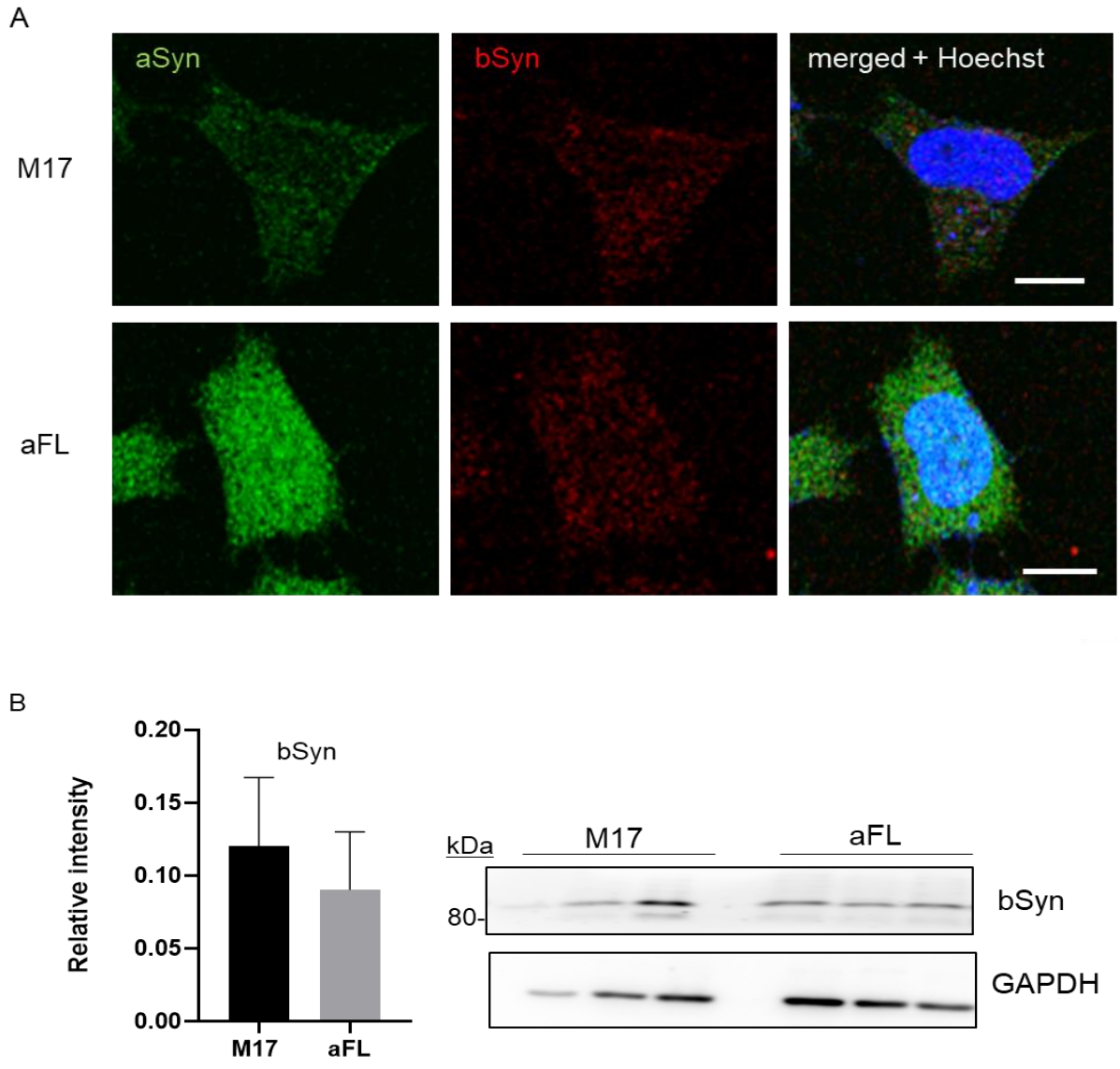

Figure 35. AFL cells show no change in beta-synuclein expression. AFL cells were double stained for both alpha-synuclein (green) and beta-synuclein (red), N=3 (A). M17 and aFL cells were lysed and probed for beta-synuclein levels (B). bSyn = beta-synuclein. Scale bar = 10µm. Western blot data is presented as mean ± SEM. N=3.

First, aFL cells were stained for alpha-synuclein and beta-synuclein. An expected increase in alpha-synuclein was seen, but any changes in beta-synuclein expression (Figure 35A) could not be detected using immunofluorescent imaging techniques. Western blot analysis showed however that there were no changes in beta-synuclein levels detected in aFL cells (Figure 35B).

5.3. Alpha-synuclein expression in beta-synuclein expressing cells

To determine whether beta-synuclein is able to affect alpha-synuclein protein levels, I used cells overexpressing full-length human beta-synuclein (bFL cells) and the DLB-related V70M beta-synuclein mutation (V70M cells) and stained them using alpha-synuclein antibody.

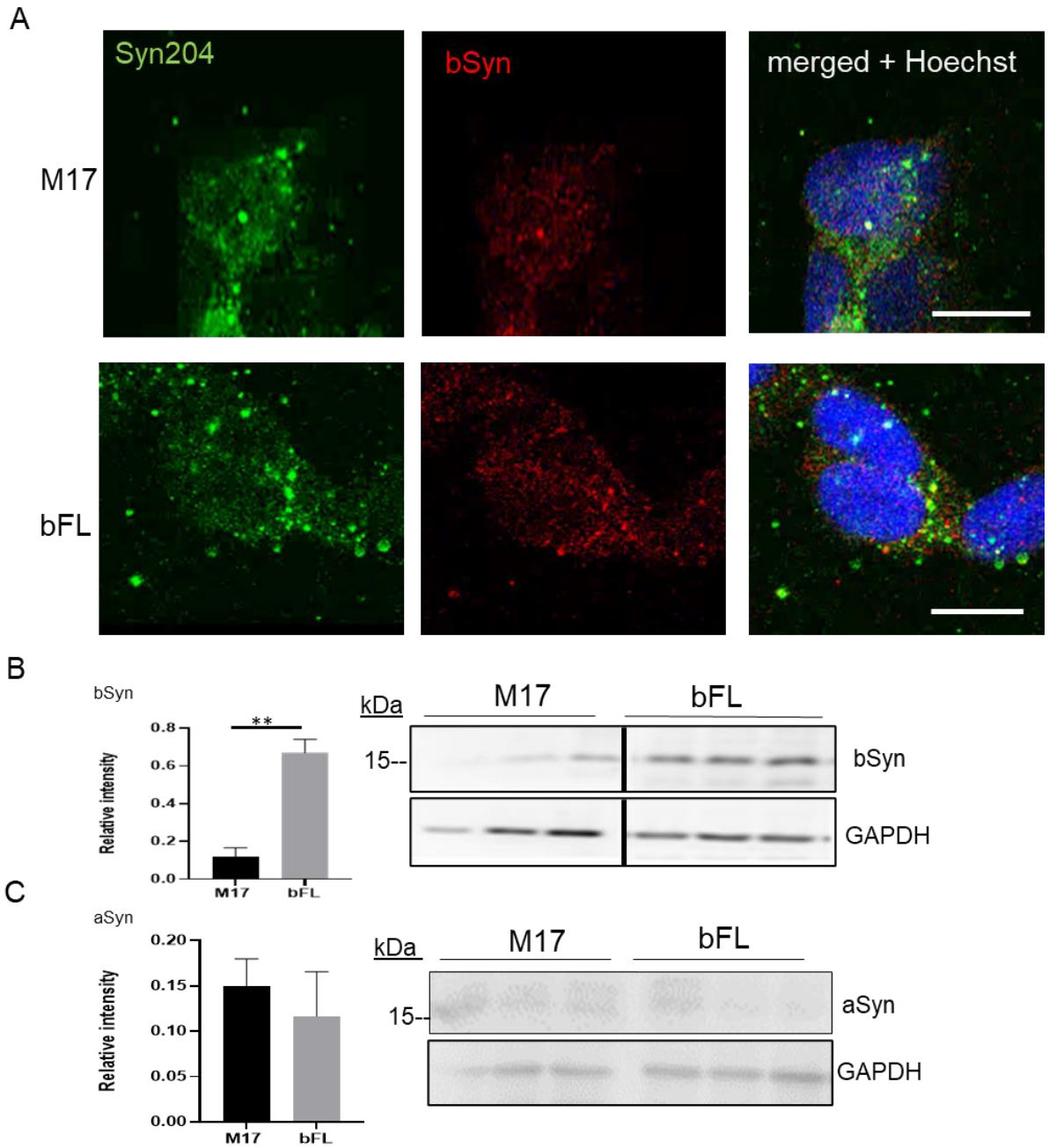

Figure 36. BFL cells show no significant change in alpha-synuclein levels. Cells were double stained for both alpha-synuclein (green) and beta-synuclein (red), N=3 (A). The level of overexpression of beta-synuclein protein in bFL cells was quantified using western blot (B). BFL cells were lysed and probed for alpha-synuclein protein level (C). Scale bar = 10µm. aSyn = alpha-synuclein, bSyn= beta-synuclein. Western blot data is represented as mean ± SEM.** $p<0.01$. N=3. Vertical line indicates that where the image has been cut.

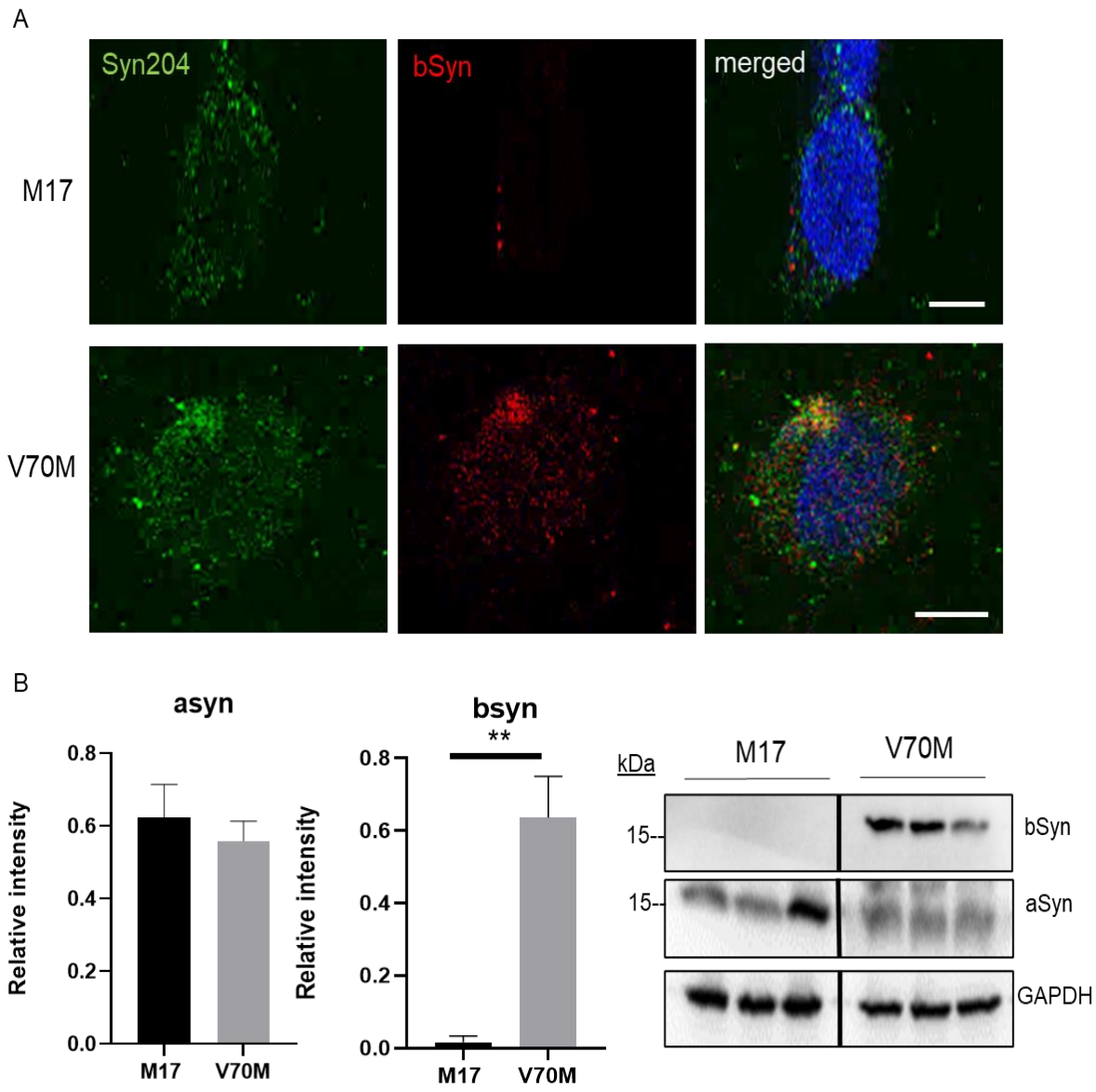

Figure 37. V70M cells show no significant change in alpha-synuclein levels. Cells were double stained for both Syn204 (green) and beta-synuclein (red), N=3 (A). V70M cells were lysed and probed for alpha-synuclein levels. The level of overexpression of beta-synuclein protein within V70M mutated beta-synuclein cells were quantified using western blot (B). Scale bar = 10µm. aSyn = alpha-synuclein, bSyn= beta-synuclein. Western blot data is represented as mean ± SEM.** $p<0.01$. N=3. Vertical line indicates that where the image has been cut.

Using the western blot and immunofluorescence, the presence of beta-synuclein in bFL and V70M was found(Figure 36 and 37 respectively). No apparent changes in endogenous alpha-synuclein protein levels was detected in either bFL (Figure 36C) or V70M overexpressing cells (Figure 37B). Strangely, in the western blot data (Figure

36B), beta-synuclein does not appear to be detected in the M17 cells, whilst in previous blots there is evidence of some, although very low, expression of beta-synuclein in wildtype control cells. The blots on the western blot for bFL and V70M were cropped to focus on beta-synuclein cells, and so non-relevant cells which were run on the same blot are not included. Since the cells were transferred to the same membrane, comparison can still be made.

5.4. Changes in mitochondrial function in beta-synuclein overexpressing cells

It has been previously seen that overexpressing alpha-synuclein in cells can cause changes in mitochondrial function, notably alpha-synuclein has been shown to affect mitochondrial dynamics [309], however there is limited information whether overexpression of beta-synuclein could induce any mitochondrial abnormalities. Therefore, bFL and V70M cells were examined to analyse changes in mitochondrial function, in response to beta-synuclein overexpression.

5.4.1.Tom20 protein levels in bFL and V70M cells

I have started with assessing total mitochondrial mass by analysing Tom20 protein levels in bFL and V70M cells using fluorescent staining and western blot.

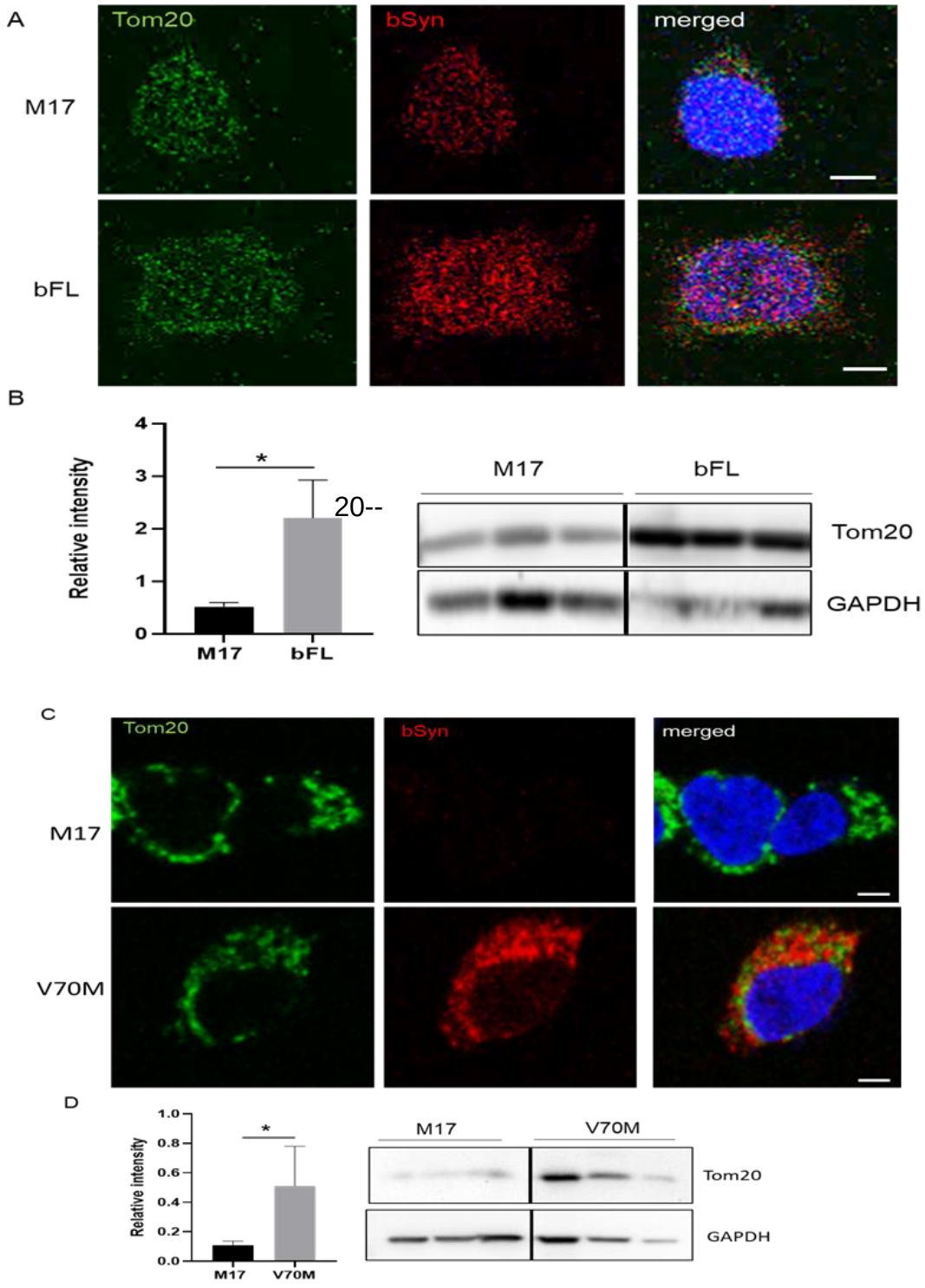

Figure 38. Both bFL and V70M cells show an increase in Tom20 levels. BFL cells (A) and V70M cells (C) were double stained with Tom20 (green) and beta-synuclein (red) N=3. Cell lysates of M17, bFL (B) and V70M (D) cells were probed using Tom20 antibody. Western blot data is represented as mean ± SEM. * $p<0.05$. Scale bar = 10µm. N=3. Vertical line indicates that where the image has been cut.

BFL and V70M cells were double stained with Tom20 and beta-synuclein. Using immunofluorescence, strong punctate Tom20 staining was present within both bFL and V70M which, in the case of V70M cells, were found mostly outside the nuclear region (Figure 38A and C). In bFL cells however, staining could also be seen in nuclear region in bFL cells. Western blot analysis of total Tom20 protein levels suggests that there is an increase of Tom20 in both bFL and V70M cells (Figure 38B and D) The blots on the western blot for bFL and V70M were cropped to focus on beta-synuclein cells, and so non-relevant cells which were run on the same blot are not included. Since the cells were transferred to the same membrane, comparison can still be made.

5.4.2. Changes in mitochondrial dynamics in bFL and V70M

5.4.2.1. Changes in mitochondrial fission

Using fluorescent imaging and western blot, bFL and V70M cells were tested for the mitochondrial fission marker Drp1.

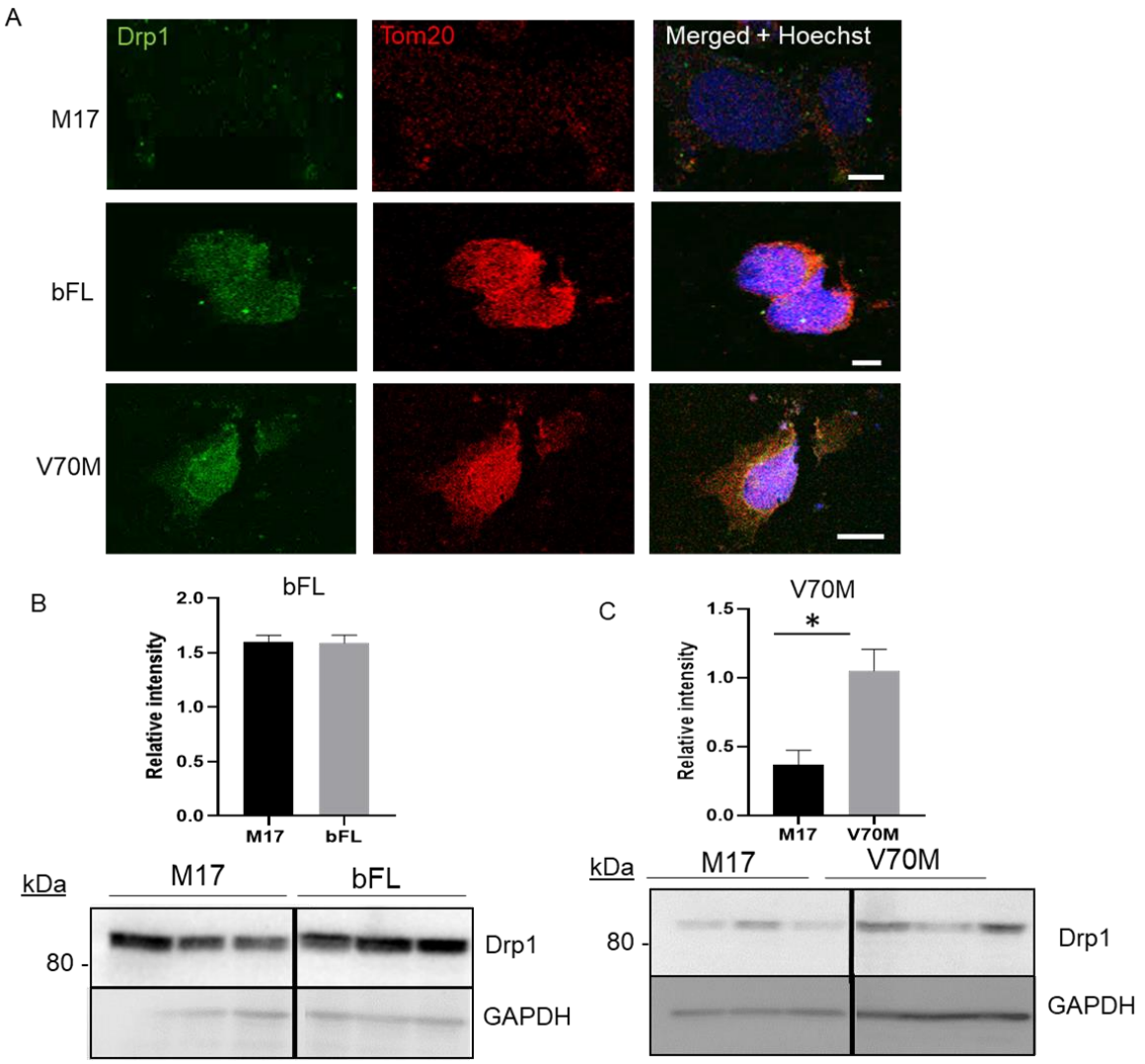

Figure 39. Drp1 levels are not changed in bFL cells but are increased in V70M cells. M17, bFL and V70M cells were double stained for Tom20 (red) and Drp1 (green), N=3 (A). Western blot analysis of bFL (B) and V70M (C) lysates were probed for Drp1. Scale bar = 10µm. Western blot data is represented as mean ± SEM. * $p<0.05$. N=3. Vertical line indicates that where the image has been cut.

The immunocytochemistry results suggests that Drp1 staining can be seen throughout the entire cell in both bFL and V70M (Figure 39A). Using western blot however, only the V70M cells (Figure 39C) appeared to show an increase in Drp1 protein levels, whereas no change was seen in bFL cells (Figure 39B).The blots on the western blot for bFL and V70M were cropped to focus on beta-synuclein cells, and so non-relevant cells which were run on the same blot are not included. Since the cells were transferred to the same membrane, comparison can still be made.

5.4.2.2. Changes in mitochondrial fusion

BFL and V70M cells were then stained with the mitochondrial fusion marker Opa1.

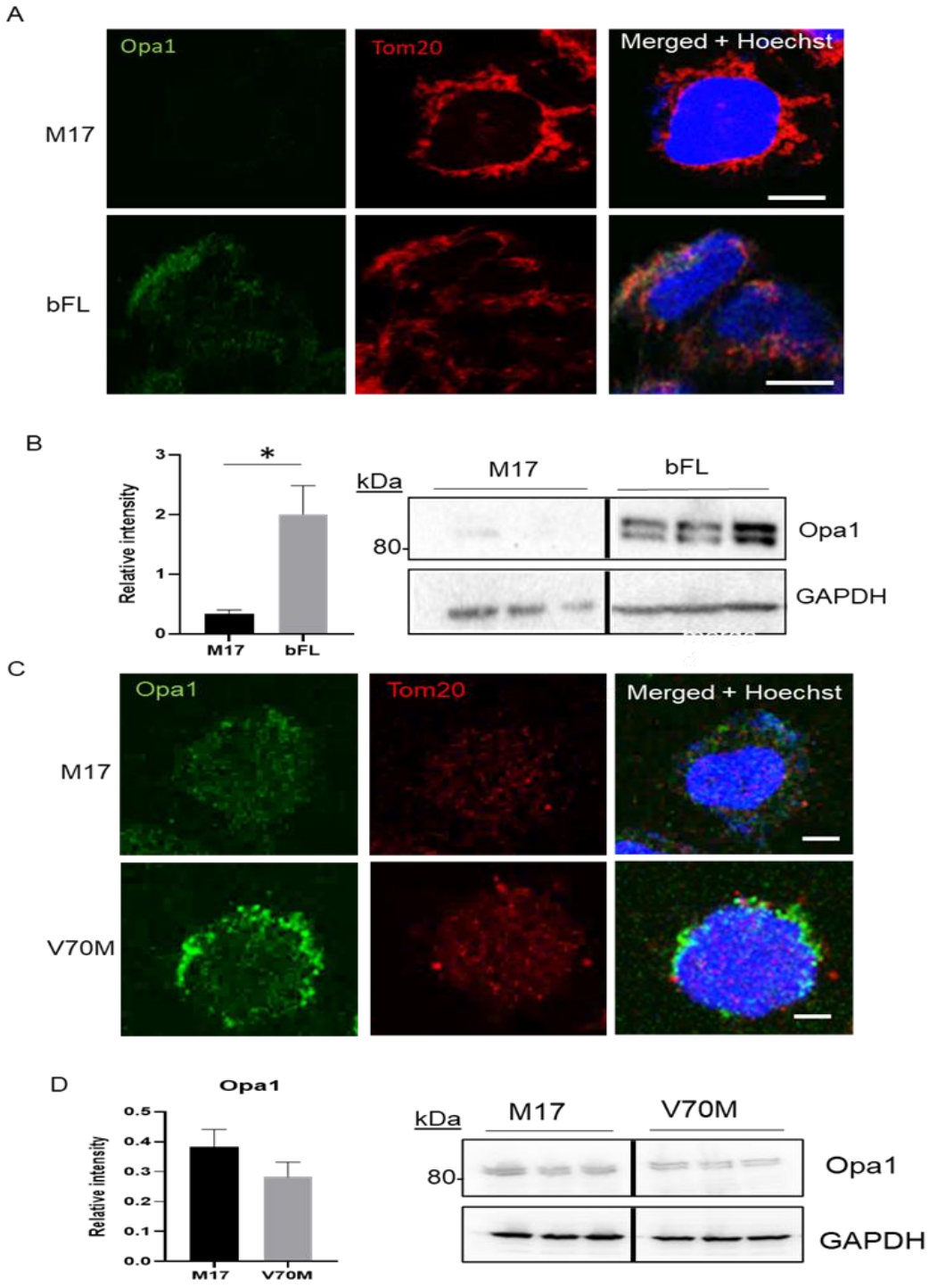

Figure 40. BFL cells showed an increase in Opa1. Both bFL (A) and V70M (C) cells were stained for the mitochondrial fusion protein Opa1 (green) and Tom20 (red) N=3. Lysates from both bFL (B) and V70M (D) cells were analysed for Opa1 protein levels. Scale bar = 10µm. Western blot data is represented as mean ± SEM. N=3. Vertical line indicates that where the image has been cut.

Using immunofluorescent techniques, Opa1 protein levels can be seen in the perinucleus in both bFL and V70M cells(Figure 40A). Western blot data also suggests that there might be an increase in total Opa1 protein levels in bFL cells(Figure 40B). Whilst Opa1 signal could also be seen in the cytoplasm of V70M cells (Figure 40C), with punctate staining in the perinuclear area in particular, no change in total Opa1 protein levels was shown in western blot analysis (Figure 40D). The blots on the western blot for bFL and V70M were cropped to focus on beta-synuclein cells, and so non-relevant cells which were run on the same blot are not included. Since the cells were transferred to the same membrane, comparison can still be made.

5.4.3. Beta-synuclein and mitochondrial membrane potential

The beta-synuclein overexpressing cell model was then tested for changes in the mitochondrial membrane potential using the dye TMRM.

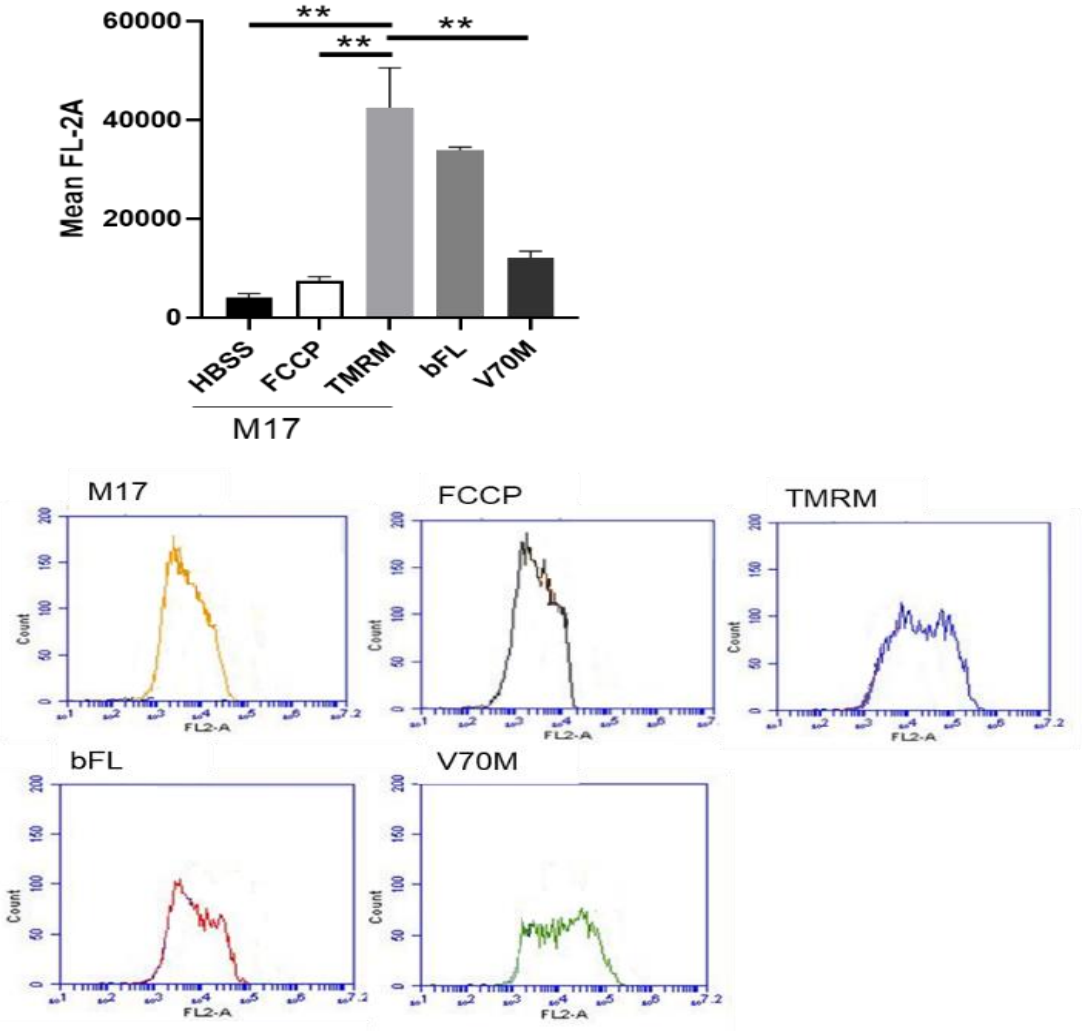

Figure 41. V70M cells show a decrease in mitochondrial membrane potential. M17, bFL and V70M cells were incubated with the dye TMRM, and fluorescent intensity was measured using flow cytometry. M17, bFL and V70M was stained with TMRM, labelled TMRM, bFL and V70M respectively (A). Two controls groups were run alongside these cells; cells incubated without dye (labelled control), and M17 cells incubated with FCCP and TMRM (labelled FCCP). Average event count and fluorescence intensity (FL2-A channel) was measured and represented as a histogram (B). Figure 47A data is represented as mean ± SEM. ** $p<0.01$, *$p<0.05$.

M17 cells incubated with TMRM show a significant increase in fluorescence intensity, in comparison to both the control and FCCP group. This confirms that the change in

fluorescence did not occur due to autofluorescence of the cells. Additionally, the significant increase in fluorescence compared to FCCP, shows that the test is sensitive to alterations in the mitochondrial membrane potential. Results regarding the bFL and V70M cells showed that whilst bFL did not show any changes in fluorescent intensity in comparison to M17 cells, V70M cells showed a significant reduction in FL2A levels, which refers to the total pulse area or light intensity emitted from each cell detected by the lasers in the flow cytometer, comparable to the reduction seen in the FCCP control group (Figure 41A). The average event count for each group is presented in a histogram, where it shows that the peak of the TMRM and bFL histograms are shifted towards the right, corresponding to an increase in fluorescence intensity (Figure 41B).

5.4.4. Beta-synuclein overexpression increases ROS production

Having detected changes in mitochondrial membrane potential following beta-synuclein overexpression, I have then examined if bFL and V70M overexpression would lead to accumulation of ROS using DCFH-DA.

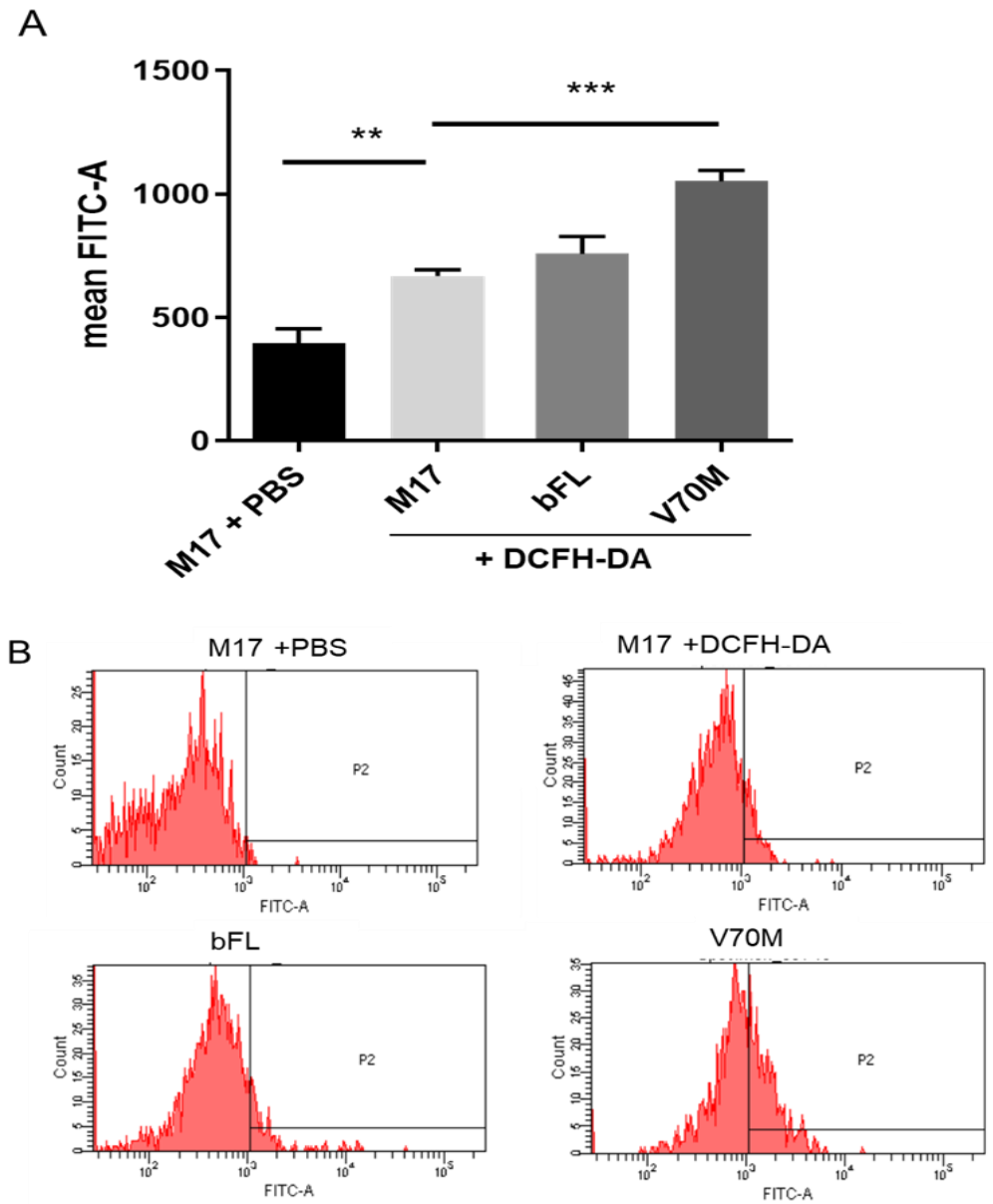

Figure 42. V70M mutant beta-synuclein overexpressing cells show a significant increase in ROS production. M17, BFL and V70M cells were incubated with the dye DCFH-DA and then fluorescent intensity was analysed using flow cytometry (A). A control group was also run, using M17 cells without DCFH-DA dye (labelled control). Average event count and fluorescence intensity (FITC channel) was measured and represented as a histogram (B). Figure 44A data is represented as mean ± SEM. ** $p<0.01$, *** $p<0.001$.

M17 cells were incubated with the dye DCFH-DA. As seen before, M17 control cells produced a significantly higher fluorescence intensity, compared to no dye control cells. No significant change was seen with bFL cells, however V70M showed a significant increase in FITC fluorescence intensity (Figure 42A). Event counts for each cell group were also represented as histograms (Figure 42B), where it can be seen that both M17 and V70M cells showed a noticeable shift to the right, compared to the no dye control group, suggesting an increase in the production of ROS molecules in the cells.

5.5. Final discussion for Chapter 5

Examination of the CamS120 mice model suggested that, a decrease in total beta-synuclein protein levels was seen at only one age point (12 months). A slight decrease appeared to be seen at the oldest age point (15 months), however this was not a significant change, and at that age both the control and CamS120 mice showed a large degree of variance. Whilst it may be possible to suggest that the significant decrease in beta-synuclein might correlate to the increase in alpha-synuclein seen previously in CamS120 mice, the quantification of alpha-synuclein using western blot was not successful and so the precise alpha-synuclein levels could not be calculated, meaning that this possible theory could not be confirmed. This lack of proper alpha-synuclein protein quantification does however suggest that results from the CamS120 should be treated with caution, and as such the changes in beta-synuclein should also be treated with caution, especially since changes in beta-synuclein could not be confirmed using immunofluorescence.

In addition, whilst an experiment comparing all four age points was not done, if proper quantification of alpha-synuclein protein levels had been successful it would be

interesting to confirm whether there is a higher level of alpha-synuclein protein level at the 12 months age point. Since the greatest change in beta-synuclein levels appeared to be at 12 months, this would correlate with the higher levels of alpha-synuclein protein levels, which might suggest an interaction between the two synuclein proteins. Furthermore, when examining the CamS120 mice at 15 months old, the immunostaining for alpha-synuclein showed relatively little change in alpha-synuclein, this might also reflect the absence of any difference in beta-synuclein protein levels at 15 months.

Using the aFL cell model, I saw that despite previously showing a possible increase in alpha-synuclein in aFL cells, there was no morphological evidence for protein aggregation in my cell model. There was also no significant change in the beta-synuclein protein levels in aFL cells, using either western blot or immunofluorescent techniques. The signal seen using immunofluorescent techniques was relatively weak, with a particularly low endogenous expression of beta-synuclein in the control cells, which was unexpected. This made it harder to detect any further significant decrease in beta-synuclein. This may possibly be due to inefficient staining using immunofluorescence, since when detecting beta-synuclein protein levels using western blot, M17 control samples showed a band corresponding to beta-synuclein protein. Therefore, to compare the interaction between alpha-synuclein and beta-synuclein in cells, an additional experiment where full-length alpha-synuclein is transfected into beta-synuclein overexpressing cells might have provided additional information on the ability of beta-synuclein to prevent alpha-synuclein overexpression. If beta-synuclein is able to prevent alpha-synuclein accumulation, a reduction in alpha-synuclein protein would be seen, and this would be in agreement with previous beta-

synuclein research has shown that beta-synuclein is able to prevent alpha-synuclein aggregation in other cell models [190, 193].

Very little research has been done to determine the effect of beta-synuclein, if any, on mitochondrial function. Here, I have started to examine the effect of wildtype and mutation beta-synuclein on mitochondrial dynamics. Previous studies have found a relationship between wildtype beta-synuclein mitochondrial fragmentation [204], however mitochondrial dynamics were not examined. The effect of mutated beta-synuclein has not been extensively studied, with studies examining the mutation P123H only, where P123H mutated beta-synuclein protein was shown to lead to an increased oxidative stress response, although not to the same extent as alpha-synuclein protein, although additional experiments by the same group showed no other changes in mitochondrial function [205]. There have been no previous studies which have examined changes in mitochondrial dynamics proteins in V70M beta-synuclein overexpressing cells.

It is commonly thought that wildtype beta-synuclein is not toxic to cells, and in fact has a more protective effect on alpha-synuclein aggregation [193], therefore it is feasible to assume that close to physiological wildtype beta-synuclein levels will not have a damaging effect on cellular function. V70M mutated beta-synuclein however has been shown to be harmful to cells and a subgroup of DLB patients have been discovered to have the V70M beta-synuclein mutation [199]. Further examination of cells overexpressing full-length beta-synuclein or hippocampal tissue taken from CamS120 using electron microscopy mice might provide additional mitochondrial morphological information.

Analysis into mitochondrial dynamics proteins identified a significant increase in Drp1 level in V70M cells. Although inconclusive from the performed experiments, V70M beta-synuclein might also have an altering effect on mitochondrial fusion process as well. These results would suggest a possible effect of the mutant beta-synuclein on mitochondrial dynamics processes, in particular an inclination to stimulate mitochondrial fission. , and so therefore also suggest that beta-synuclein proteins are potentially able to modulate mitochondrial dynamic processes. Further studies would have to be done to confirm this effect of beta-synuclein.

Using flow cytometry, bFL and V70M cells were further analysed for additional mitochondrial function. The results appeared to indicate that bFL and V70M exerted different effects on mitochondrial membrane potential and ROS production. Only mutated beta-synuclein showed a significant impairment in mitochondrial membrane potential and an increase in ROS production. V70M beta-synuclein results are consistent with those seen in cells overexpressing alpha-synuclein. This would suggest that over-expression of wildtype beta-synuclein does not cause any significant mitochondrial dysfunction, and that beta-synuclein mutation is sufficient to cause mitochondrial disruption, however this impairment was not as strong as that seen with cells overexpressing alpha-synuclein. This result seems to be in alignment with a study which showed that only certain forms of the beta-synuclein protein can cause significant effects on lysosomal function [203], further strengthening the notion that mutated beta-synuclein exerts toxic effect on cytoplasmic mechanisms. This also suggests that mutant beta-synuclein might be sufficient enough to cause other forms of cellular dysfunction seen in DLB pathology, and not just mitochondrial dysfunction,

such as synaptic function for example. The major limitations of all these experiments however, such as lack of proper quantification of beta-synuclein protein levels in beta-synuclein overexpressing cells and insufficient n-numbers, do put the results into question, and if the experiments were to be continued these would have to be thoroughly addressed to confirm these changes, which would have done by ensuring proper controls were used and that protein loading was balanced across groups.

Chapter Six: Final discussion and future work

6.1. Mouse models of DLB

In order to address the first aim of my project, I closely examined the CamS120 mouse model and attempted to assess its usefulness as an accurate model of DLB. Behavioural analysis of the CamS120 mouse model showed signs of impairment in recognition memory (Figure 20), using the NOR test. This decline in recognition memory suggests a hippocampal-specific impairment caused by accumulation of alpha-synuclein within the hippocampus, however running additional hippocampal-dependent memory behavioural tests, such as the Barnes Maze or the water Morris maze, would be necessary to confirm the behavioural data seen here. The changes here however were seen using only one particular memory-related behavioural test. Using additional memory behavioural tests, such as the Barnes Maze or the water Morris maze, which were not available to use at the time, would be necessary to confirm any hippocampal-dependent deficits seen in the CamS120 mice.

Whilst a significant change in recognition memory was seen in 6 months and 12 months old, human alpha-synuclein protein could be seen using immunofluorescent detection at all four age groups in the CamS120 mice (Figure 16). Limited detection using western blot techniques prevented proper quantification of alpha-synuclein in this work (Figure 20), which suggests that human alpha-synuclein expression is not strong enough to be detected when the transgene was expressed in murine alpha-synuclein background. The reason for this was unclear however, as original tests performed by [245] was able to show a strong increase in human alpha-synuclein, suggesting that the limited detection of alpha-synuclein by western blot was due to a reduction of gene expression when the line was further crossed into C57BL/6J mouse strain. Despite this low expression of alpha-synuclein, using the 5G4 antibody which

tests for the presence of oligomeric alpha-synuclein, showed the potential presence of alpha-synuclein aggregates (Figure 19). 5G4 antibody had unfortunately generated rather high levels of background in my experiments, and further work adjusting conditions for the optimal staining would be needed before any conclusions on whether aggregates can be seen in the CamS120 mouse model can be made.

Upon discovering the impairment in recognition memory in 12 months using the NOR test, I began to examine the biological processes that might contribute to the behavioural changes seen. Since the strongest change in behavioural was seen in the 12 months CamS120 mice, I focused on the 12 months in particular for further experiments. I also examine any changes in mitochondrial function in the subsequent age group to investigate fully the lack of behavioural deficits seen in the 15 months age group.

The analysis of the alpha-synuclein full-length overexpressing cell model had identified several possible changes in mitochondrial function, which prompted the examination of the mitochondrial function of the mouse model as well. Mitochondrial function has been shown to be severely affected in DLB pathology [117]. Mouse models of other synucleinopathies, such as PD, have shown increased mitochondrial dysfunction [303]. Due to the scarcity of DLB mouse models, changes in mitochondrial function in DLB models remain poorly studied. Here, I detected no significant alterations in mitochondrial morphology and function, in particular there were no significant changes in either Tom20 (Figure 21) or the mitochondrial dynamic proteins Drp1 (Figures 25-26) or Opa1 protein levels (Figures 28-29). Whilst the overall results with the CamS120 mouse model did not show a significant effect, the 12 months old CamS120 mice showed a trend towards a similar result with a slight increase in Drp1 and decrease in Opa1. A similar result could be seen in 15 months old mice. These insignificant

changes in both mitochondrial dynamic proteins again suggest however that the CamS120 mice do not show strong mitochondrial dysfunction, normally associated with DLB pathology.

Levels of overexpressed protein are important to trigger mitochondrial dysfunction, as our cell model, which overexpresses full-length alpha-synuclein protein showed a disruption in mitochondrial dynamics, including an increase in Drp1 (Figure 24) and a decrease in Opa1 (Figure 27). These two proteins are both key mitochondrial dynamic proteins which are thought to work in tandem to control both the number and morphology of the mitochondrial populations within the cell, which is discussed in a review by [155]. When full-length alpha-synuclein was overexpressed the mitochondrial fusion process was inhibited, while fission was enhanced, which is expected and has been previously reported [147].

The effect of alpha-synuclein protein on mitochondrial dynamics seen here in our cell model is similar to that seen in previous studies examining mitochondrial dynamics and alpha-synuclein expression [309]. In neurodegenerative disease, mitochondria are reported to become much shorter and become fragmented, which is usually as a result of a higher rate of mitochondrial division [310]. How exactly alpha-synuclein affects mitochondria is not entirely certain, although it has been suggested that alpha-synuclein might bind to proteins and lipids found on the OMM, which affects the membrane curvatures of the mitochondria, thereby impairing the mitochondrial fusion process, this particular process has not however been particularly well explored [298].

When examining the mitochondrial population within the hippocampus from frozen brain tissue, determining changes in mitochondrial dynamics may not always be accurate. When mitochondria undergo fusion or fission, mitochondrial dynamic

proteins such as Drp1 translocate from the cytoplasm to the mitochondria, which means that total levels of Drp1 levels may not change overall. To determine a more accurate depiction of changes in mitochondrial fission, isolation of mitochondria from hippocampal tissue might be able to show a more accurate change in Drp1 protein levels to the mitochondria. In addition, focusing on phosphorylated forms of Drp1 instead of total Drp1 protein might also improve accuracy. When Drp1 proteins are recruited to form a multimeric ring around the mitochondrion, they become phosphorylated which allows Drp1 to lyse the OMM leading to division of the mitochondrion. Additionally, confirmation of changes in mitochondrial function should be confirmed using other markers of mitochondrial dynamics, such as Mitofusin 1, which is a marker for mitochondrial fusion

As seen in Table 7 below, CamS120 mice showed certain behavioural abnormalities at 12 months of age only, although only slight alterations in mitochondrial function was seen at that age point.

	CamS120 mice			
	1 months	6 months	12 months	15 months
Beta-synuclein	--	--	(↓)	--
Tom20	--	--	--	--
Drp1	--	--	--	--
Opa1	--	--	--	--
Open field test	--	--	--	--
Marble burying test	--	--	--	--
Novel object recognition	--	↓	↓	--

Table 7. Behavioural and biochemical alterations in CamS120 mice. Results from experiments examining changes in beta-synuclein levels, mitochondrial related protein levels and cognitive function in CamS120 transgenic mice, compared to control mice are listed. Dashed line refers to no significant changes.

It is unclear therefore from the experiments performed here what the exact underlying processes that occur in CamS120 mice are which may contribute to the behavioural deficit seen in the NOR test. Additionally, since conclusive evidence could not be shown that alpha-synuclein proteins are increased in the hippocampus using western blot, it is also difficult to confidently confirm that the changes in behaviour are in response to alpha-synuclein overexpression

While mitochondrial function is the main focus in my project, there are several other possible cellular processes which could contribute to the behavioural impairment seen here; including synaptic dysfunction, neuroinflammation or autophagy disruption. .

While it appears that the CamS120 mouse model is not effective as a model of DLB, there may be other options for modelling DLB in mouse models. While there are almost no mutant mouse models of DLB available, generating and examining a transgenic mouse line which expresses E46K mutated alpha-synuclein, under the CamKII promoter focusing the expression of alpha-synuclein to DLB-relevant regions such as the cortex and hippocampus. Since E46K is one of the few alpha-synuclein mutations which has been confirmed as a DLB-relevant mutation, it might be an interesting alternative to using truncated alpha-synuclein as a model specific to DLB.

6.2. Beta-synuclein and its role in DLB

Beta-synuclein protein has previously been implicated in DLB pathology [311]. Whilst beta-synuclein has not been identified within Lewy bodies and Lewy neurites, there have been studies which show that beta-synuclein is otherwise involved in synucleinopathies, which include the identification of two mutant forms of beta-synuclein in DLB patients (P123H and V70M) [199, 207]. The protein levels of beta-synuclein were examined in our mouse model, where a significant decrease was

discovered in hippocampus lysates (Figure 34). I concluded from these results that beta-synuclein is, although not confirmed in my experiments, may be related to alpha-synuclein expression; theorising that a decrease in beta-synuclein could be in response to the increased alpha-synuclein level.

As beta-synuclein protein is thought to inhibit alpha-synuclein aggregation, it is possible that when beta-synuclein levels are reduced, alpha-synuclein protein accumulation is no longer inhibited by beta-synuclein, which would lead to increased levels of alpha-synuclein protein. This result is in agreement with other studies using DLB post-mortem tissues, which have shown alterations in beta-synuclein protein levels [202, 312].

Using the CamKIIα promoter in the CamS120 mouse line also allowed the production of the transgene in other regions within the mouse's brain which are also thought to be implicated in DLB pathology, such as the frontal cortex, olfactory bulb, amygdala and striatum [313]. Although due to time constraints, analysis was not possible with the CamS120 mice, analysis into the cortex and the olfactory bulb could provide additional information on the various beta-synuclein protein levels between different brain regions normally affected in DLB. Studies into beta-synuclein levels in DLB/PDD post-mortem tissue in our research group, as well as in other research groups [312], have shown that there are differences in beta-synuclein expression within different brain regions, for example within the occipital cortex, hippocampus, and olfactory bulb.

I examined the effect of beta-synuclein itself on cell function, focusing on the effect on mitochondrial function in particular. There are very few studies which have investigated the effect of wildtype beta-synuclein on mitochondrial function. Here, I have begun to explore the effect of both wildtype and the DLB-related V70M beta-

synuclein mutant on mitochondrial function. There have been studies that show that wildtype beta-synuclein may also cause cell dysfunction, however this was not entirely seen with our cell model (Table 8).

	aFL cells	bFL cells	V70M cells
Alpha-synuclein	(↑)	--	--
Beta-synuclein	--	↑	(↑)
Tom20	(↑)	(↑)	(↑)
Drp1	(↑)	--	(↑)
Opa1	(↓)	(↑)	--
Mitochondrial membrane potential	(↓)	--	(↓)
ROS production	(↑)	--	(↑)

Table 8. Overview of alteration of mitochondrial function in the cell model. Results from the mitochondrial related experiments performed with aFL, bFL and V70M cells are listed. Dashed line refers to no significant changes.

The results here instead show that, while it is unclear whether wildtype beta-synuclein showed alterations in mitochondrial structure or function, V70M mutant beta-synuclein seems to have a stronger relation with DLB-related pathology. Results from the V70M cells showed that changes may potentially be found in mitochondrial dynamic proteins (Figure 39-40), ROS production (Figure 42) and mitochondrial membrane potential (Figure 41). These results, if they were to be confirmed, are the first to show the effect of the V70M mutated form of beta-synuclein on mitochondrial function. The results collected here suggest that V70M mutations in beta-synuclein may detrimentally affect certain mitochondrial functions to almost the same extent seen with alpha-synuclein overexpression.

The interaction between beta-synuclein and mitochondrial function is not well studied so far, and there are other possible experiments that could further explore the effects of beta-synuclein. Direct interaction between beta-synuclein, wild-type and mutated, and mitochondrial dynamic proteins using co-immunoprecipitation and proximity ligation assay techniques would address the question of whether beta-synuclein and mitochondrial dynamic proteins co-localise and bind to each other, which might give further information as to whether beta-synuclein can have a direct effect on mitochondrial function. This may especially interesting as it is still unclear whether mutated beta-synuclein can affect cell function directly.

6.3. Concluding remarks

The generation of appropriate and representative animal models is an important tool in DLB research. As part of my project, experiments were conducted in attempt to explore one particular novel model. Through the experiments conducted, I found that the CamS120 mice displayed some aspects of DLB-like phenotype. Whilst it is suspected that the presence of aggregation-prone truncated human alpha-synuclein in hippocampus caused a significant impairment in recognition memory was seen, I found little correlation to changes in mitochondrial function. The lack of quantifiable alpha-synuclein using western blot, low levels of protein expression coupled with the very subtle changes in mitochondrial dynamics protein levels have highlighted the limited usefulness of this mouse model of DLB. As proper quantification of the truncated alpha-synuclein protein levels could not be verified, it is very difficult to ascertain whether the changes in mouse model are actually due to changes in alpha-synuclein protein.

The experiments into our cell model has provided further evidence that overexpression of full-length wildtype alpha-synuclein might be able to cause a major disruption in several different mitochondrial functions within the cell. The impact of these mitochondrial abnormalities might contribute to the pathophysiology which underlies synucleinopathy diseases, as disruption to mitochondrial function can lead to further cell dysfunction by affecting mitophagy processes, synaptic dysfunction and stimulate apoptosis within the cell, leading to neuronal loss and reduce neuronal activity within key regions of the brain leading to cognitive and movement impairment in DLB or PD.

I have found that beta-synuclein levels appear to be decreased in response to alpha-synuclein accumulation and aggregation in the hippocampus of DLB mice. This data would extend our previous findings in human DLB brains [202], where we found that cells devoid of alpha-synuclein aggregates had increased levels of beta-synuclein. This apparent contradiction may indicate temporal progression of alpha-synuclein aggregation, when initial stages see an increase in monomeric-oligomeric alpha-synuclein and a decrease in beta-synuclein, whilst loss of alpha-synuclein function due to the aggregation at late DLB stages results in compensatory increase in beta-synuclein levels. DLB-related mutated beta-synuclein V70M appears to influence mitochondrial function, as changes in mitochondrial potential could be seen in cells overexpressing V70M mutated beta-synuclein. These results in particular suggest that beta-synuclein can play a larger role in DLB pathology than was previously thought, that in its mutant form beta-synuclein can potentially cause mitochondrial dysfunction, and so therefore might be worth further exploring to confirm these results. Tight regulation of beta-synuclein is important, as its decrease promotes alpha-synuclein aggregation ([312]), whilst its increase affects mitochondrial and autophagy function ([202]).

Overall, whilst the results collected may not have given concrete evidence for the changes in mitochondrial function caused by DLB-related proteins, alpha-synuclein and beta-synuclein , my experiments have provided a basis for future experiments which might provide further information on the potential biochemical mechanisms of DLB (Figure 43).

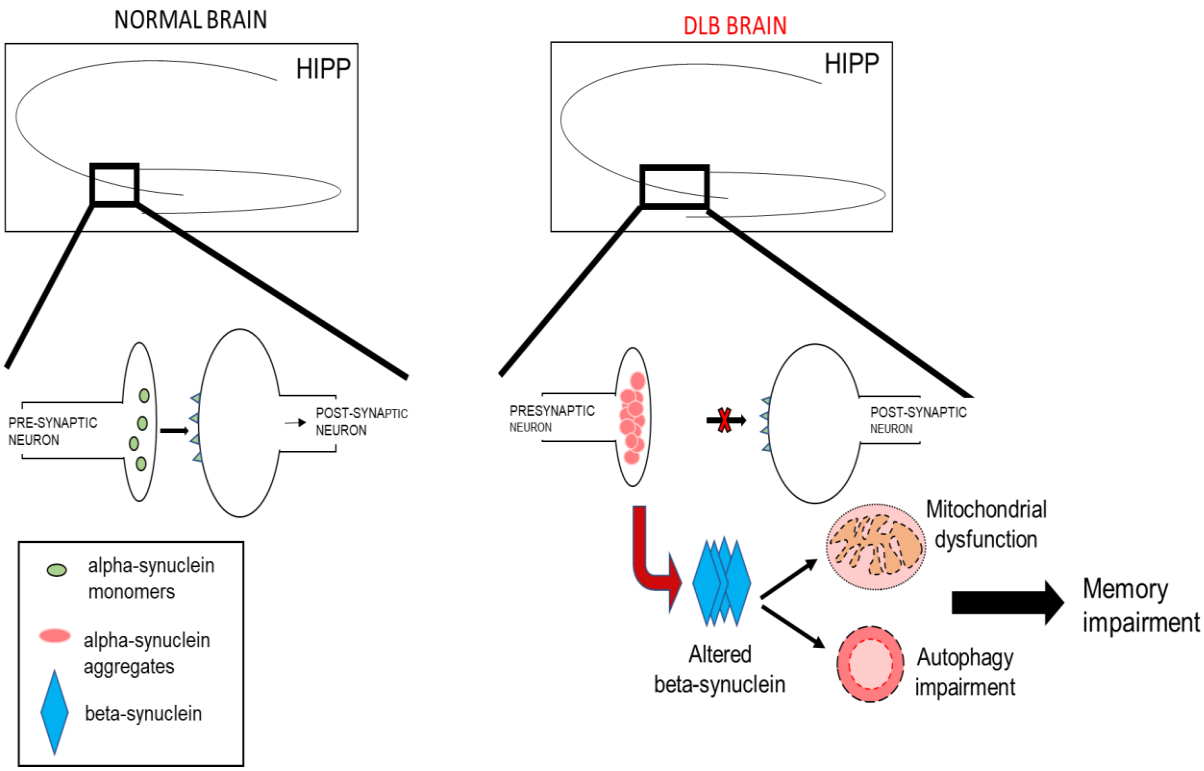

Figure 43. A possible hypothesis of the DLB-related neurochemical alterations in the hippocampus. In DLB, alpha-synuclein accumulates within the hippocampus, which affects beta-synuclein protein levels and cellular dysfunction, including mitochondrial function, synaptic function, and autophagy, leading to cognitive impairment. HIPP = hippocampus.

Normally, alpha-synuclein is found in the presynaptic nerve terminals and has a function in neurotransmission. In DLB brains, alpha-synuclein accumulates within the presynaptic neurons within the hippocampus, forming insoluble aggregates. Post-mortem brain tissue from DLB patients have shown that beta-synuclein protein levels are also affected [202], which is likely due to the presence of alpha-synuclein, which

was also seen in our mouse model, where a decrease in beta-synuclein was seen within the hippocampus. This hypothesis might also be true for other regions of the brain such as the cortex and olfactory bulb, which have been seen to be affected in DLB human brain [202], and so might provide another avenue of interest for future experiments. Using the data available from the experiments in this project, it might be possible to hypothesise that the reduction in beta-synuclein might be in response to the rapid accumulation of alpha-synuclein within neurons, as typically beta-synuclein has often been shown to have a more neuroprotective role. The overexpression of alpha-synuclein then leads to synaptic dysfunction, mitochondrial dynamics, and autophagy dysfunction, and as seen in my mouse model, the overexpression of human alpha-synuclein within the hippocampus leads to significant cognitive impairment, notably deficient recognition memory.

Bibliography

1. Vann Jones, S.A. and J.T. O'Brien, *The prevalence and incidence of dementia with Lewy bodies: a systematic review of population and clinical studies.* Psychol Med, 2014. **44**(4): p. 673-83.
2. Brunnström, H., et al., *Prevalence of dementia subtypes: a 30-year retrospective survey of neuropathological reports.* Arch Gerontol Geriatr, 2009. **49**(1): p. 146-9.
3. von Strauss, E., et al., *Aging and the occurrence of dementia: findings from a population-based cohort with a large sample of nonagenarians.* Arch Neurol, 1999. **56**(5): p. 587-92.
4. Corrada, M.M., et al., *Prevalence of dementia after age 90: results from the 90+ study.* Neurology, 2008. **71**(5): p. 337-43.
5. Ballard, C., et al., *The progression of cognitive impairment in dementia with Lewy bodies, vascular dementia and Alzheimer's disease.* Int J Geriatr Psychiatry, 2001. **16**(5): p. 499-503.
6. *Clinical and neuropathological criteria for frontotemporal dementia. The Lund and Manchester Groups.* J Neurol Neurosurg Psychiatry, 1994. **57**(4): p. 416-8.
7. Millar, D., et al., *Characterizing behavioral and cognitive dysexecutive changes in progressive supranuclear palsy.* Mov Disord, 2006. **21**(2): p. 199-207.
8. Montoya, A., et al., *Episodic memory impairment in Huntington's disease: a meta-analysis.* Neuropsychologia, 2006. **44**(10): p. 1984-94.
9. Duff, K., et al., *Cognitive deficits in Huntington's disease on the Repeatable Battery for the Assessment of Neuropsychological Status.* J Clin Exp Neuropsychol, 2010. **32**(3): p. 231-8.
10. Ballard, C., et al., *Attention and fluctuating attention in patients with dementia with Lewy bodies and Alzheimer disease.* Arch Neurol, 2001. **58**(6): p. 977-82.
11. Mondon, K., et al., *Visual recognition memory differentiates dementia with Lewy bodies and Parkinson's disease dementia.* J Neurol Neurosurg Psychiatry, 2007. **78**(7): p. 738-41.
12. Chan, P.C., et al., *REM Sleep Behavior Disorder (RBD) in Dementia with Lewy Bodies (DLB).* Behav Neurol, 2018. **2018**: p. 9421098.
13. McKeith, I.G., et al., *Diagnosis and management of dementia with Lewy bodies: Fourth consensus report of the DLB Consortium.* Neurology, 2017. **89**(1): p. 88-100.
14. Park, K.W., et al., *Dementia with Lewy Bodies versus Alzheimer's Disease and Parkinson's Disease Dementia: A Comparison of Cognitive Profiles.* J Clin Neurol, 2011. **7**(1): p. 19-24.
15. McKeith, I.G., et al., *More severe functional impairment in dementia with lewy bodies than Alzheimer disease is related to extrapyramidal motor dysfunction.* Am J Geriatr Psychiatry, 2006. **14**(7): p. 582-8.
16. Uchiyama, M., et al., *Pareidolias: complex visual illusions in dementia with Lewy bodies.* Brain, 2012. **135**(Pt 8): p. 2458-69.
17. McKeith, I.G., et al., *Diagnosis and management of dementia with Lewy bodies: third report of the DLB Consortium.* Neurology, 2005. **65**(12): p. 1863-72.
18. Aldridge, G.M., et al., *Parkinson's Disease Dementia and Dementia with Lewy Bodies Have Similar Neuropsychological Profiles.* Front Neurol, 2018. **9**: p. 123.

19. Jellinger, K.A. and A.D. Korczyn, *Are dementia with Lewy bodies and Parkinson's disease dementia the same disease?* BMC Med, 2018. **16**(1): p. 34.
20. Lippa, C.F., et al., *DLB and PDD boundary issues: diagnosis, treatment, molecular pathology, and biomarkers.* Neurology, 2007. **68**(11): p. 812-9.
21. McKeith, I., *Dementia with Lewy bodies.* Dialogues Clin Neurosci, 2004. **6**(3): p. 333-41.
22. Love, S., *Neuropathological investigation of dementia: a guide for neurologists.* J Neurol Neurosurg Psychiatry, 2005. **76 Suppl 5**: p. v8-14.
23. Niccoli, T. and L. Partridge, *Ageing as a risk factor for disease.* Curr Biol, 2012. **22**(17): p. R741-52.
24. Dick, F.D., et al., *Environmental risk factors for Parkinson's disease and parkinsonism: the Geoparkinson study.* Occup Environ Med, 2007. **64**(10): p. 666-72.
25. Bellou, V., et al., *Environmental risk factors and Parkinson's disease: An umbrella review of meta-analyses.* Parkinsonism Relat Disord, 2016. **23**: p. 1-9.
26. Boot, B.P., et al., *Risk factors for dementia with Lewy bodies: a case-control study.* Neurology, 2013. **81**(9): p. 833-40.
27. Noyce, A.J., et al., *Meta-analysis of early nonmotor features and risk factors for Parkinson disease.* Ann Neurol, 2012. **72**(6): p. 893-901.
28. Gallo, V., et al., *Exploring causality of the association between smoking and Parkinson's disease.* Int J Epidemiol, 2019. **48**(3): p. 912-925.
29. Hersi, M., et al., *Risk factors associated with the onset and progression of Alzheimer's disease: A systematic review of the evidence.* Neurotoxicology, 2017. **61**: p. 143-187.
30. Tsuang, D., et al., *APOE ε4 increases risk for dementia in pure synucleinopathies.* JAMA Neurol, 2013. **70**(2): p. 223-8.
31. Jellinger, K.A., *Neuropathological spectrum of synucleinopathies.* Mov Disord, 2003. **18 Suppl 6**: p. S2-12.
32. Braak, H., et al., *Staging of brain pathology related to sporadic Parkinson's disease.* Neurobiol Aging, 2003. **24**(2): p. 197-211.
33. Visanji, N.P., et al., *The prion hypothesis in Parkinson's disease: Braak to the future.* Acta Neuropathol Commun, 2013. **1**: p. 2.
34. Irizarry, M.C., et al., *Nigral and cortical Lewy bodies and dystrophic nigral neurites in Parkinson's disease and cortical Lewy body disease contain alpha-synuclein immunoreactivity.* J Neuropathol Exp Neurol, 1998. **57**(4): p. 334-7.
35. Byrne, E.J., et al., *Diffuse Lewy body disease: clinical features in 15 cases.* J Neurol Neurosurg Psychiatry, 1989. **52**(6): p. 709-17.
36. Marui, W., et al., *Progression and staging of Lewy pathology in brains from patients with dementia with Lewy bodies.* J Neurol Sci, 2002. **195**(2): p. 153-9.
37. Bozzali, M., et al., *Brain tissue damage in dementia with Lewy bodies: an in vivo diffusion tensor MRI study.* Brain, 2005. **128**(Pt 7): p. 1595-604.
38. Mak, E., et al., *Neuroimaging characteristics of dementia with Lewy bodies.* Alzheimers Res Ther, 2014. **6**(2): p. 18.
39. Taylor, J.P., et al., *Visual cortex in dementia with Lewy bodies: magnetic resonance imaging study.* Br J Psychiatry, 2012. **200**(6): p. 491-8.
40. Lobotesis, K., et al., *Occipital hypoperfusion on SPECT in dementia with Lewy bodies but not AD.* Neurology, 2001. **56**(5): p. 643-9.

41. Gómez-Tortosa, E., et al., *alpha-Synuclein immunoreactivity in dementia with Lewy bodies: morphological staging and comparison with ubiquitin immunostaining.* Acta Neuropathol, 2000. **99**(4): p. 352-7.
42. Spillantini, M.G., et al., *alpha-Synuclein in filamentous inclusions of Lewy bodies from Parkinson's disease and dementia with lewy bodies.* Proc Natl Acad Sci U S A, 1998. **95**(11): p. 6469-73.
43. Thomas, A.J., et al., *Autopsy validation of 123I-FP-CIT dopaminergic neuroimaging for the diagnosis of DLB.* Neurology, 2017. **88**(3): p. 276-283.
44. Fathy, Y.Y., et al., *Differential insular cortex subregional vulnerability to α-synuclein pathology in Parkinson's disease and dementia with Lewy bodies.* Neuropathol Appl Neurobiol, 2019. **45**(3): p. 262-277.
45. Elder, G.J., et al., *The influence of hippocampal atrophy on the cognitive phenotype of dementia with Lewy bodies.* Int J Geriatr Psychiatry, 2017. **32**(11): p. 1182-1189.
46. Papez, J.W., *A proposed mechanism of emotion. 1937.* J Neuropsychiatry Clin Neurosci, 1995. **7**(1): p. 103-12.
47. Lim, S.M., et al., *The 18F-FDG PET cingulate island sign and comparison to 123I-beta-CIT SPECT for diagnosis of dementia with Lewy bodies.* J Nucl Med, 2009. **50**(10): p. 1638-45.
48. Baba, M., et al., *Aggregation of alpha-synuclein in Lewy bodies of sporadic Parkinson's disease and dementia with Lewy bodies.* Am J Pathol, 1998. **152**(4): p. 879-84.
49. Witter, M.P., *The perforant path: projections from the entorhinal cortex to the dentate gyrus.* Prog Brain Res, 2007. **163**: p. 43-61.
50. Basu, J. and S.A. Siegelbaum, *The Corticohippocampal Circuit, Synaptic Plasticity, and Memory.* Cold Spring Harb Perspect Biol, 2015. **7**(11).
51. Santhakumar, V., et al., *Granule cell hyperexcitability in the early post-traumatic rat dentate gyrus: the 'irritable mossy cell' hypothesis.* J Physiol, 2000. **524 Pt 1**: p. 117-34.
52. Amaral, D.G., H.E. Scharfman, and P. Lavenex, *The dentate gyrus: fundamental neuroanatomical organization (dentate gyrus for dummies).* Prog Brain Res, 2007. **163**: p. 3-22.
53. Scharfman, H.E. and C.E. Myers, *Hilar mossy cells of the dentate gyrus: a historical perspective.* Front Neural Circuits, 2012. **6**: p. 106.
54. Andrews-Zwilling, Y., et al., *Hilar GABAergic interneuron activity controls spatial learning and memory retrieval.* PLoS One, 2012. **7**(7): p. e40555.
55. Dudek, S.M., G.M. Alexander, and S. Farris, *Rediscovering area CA2: unique properties and functions.* Nat Rev Neurosci, 2016. **17**(2): p. 89-102.
56. Larriva-Sahd, J.A., *Some predictions of Rafael Lorente de Nó 80 years later.* Front Neuroanat, 2014. **8**: p. 147.
57. Andersen, P., T.W. Blackstad, and T. Lömo, *Location and identification of excitatory synapses on hippocampal pyramidal cells.* Exp Brain Res, 1966. **1**(3): p. 236-48.
58. Arrigoni, E. and R.W. Greene, *Schaffer collateral and perforant path inputs activate different subtypes of NMDA receptors on the same CA1 pyramidal cell.* Br J Pharmacol, 2004. **142**(2): p. 317-22.
59. Szilágyi, T., et al., *Morphological identification of neuron types in the rat hippocampus.* Rom J Morphol Embryol, 2011. **52**(1): p. 15-20.
60. Naber, P.A., F.H. Lopes da Silva, and M.P. Witter, *Reciprocal connections between the entorhinal cortex and hippocampal fields CA1 and the subiculum*

are in register with the projections from CA1 to the subiculum. Hippocampus, 2001. **11**(2): p. 99-104.
61. Llorens-Martín, M., et al., *Selective alterations of neurons and circuits related to early memory loss in Alzheimer's disease.* Front Neuroanat, 2014. **8**: p. 38.
62. Langston, R.F., et al., *The role of hippocampal subregions in memory for stimulus associations.* Behav Brain Res, 2010. **215**(2): p. 275-91.
63. Farovik, A., L.M. Dupont, and H. Eichenbaum, *Distinct roles for dorsal CA3 and CA1 in memory for sequential nonspatial events.* Learn Mem, 2010. **17**(1): p. 12-17.
64. Whitwell, J.L., et al., *Focal atrophy in dementia with Lewy bodies on MRI: a distinct pattern from Alzheimer's disease.* Brain, 2007. **130**(Pt 3): p. 708-19.
65. Adamowicz, D.H., et al., *Hippocampal α-Synuclein in Dementia with Lewy Bodies Contributes to Memory Impairment and Is Consistent with Spread of Pathology.* J Neurosci, 2017. **37**(7): p. 1675-1684.
66. Kuruvilla, M.V. and J.A. Ainge, *Lateral Entorhinal Cortex Lesions Impair Local Spatial Frameworks.* Front Syst Neurosci, 2017. **11**: p. 30.
67. Boot, B.P., et al., *Treatment of dementia with lewy bodies.* Curr Treat Options Neurol, 2013. **15**(6): p. 738-64.
68. Spillantini, M.G., A. Divane, and M. Goedert, *Assignment of human alpha-synuclein (SNCA) and beta-synuclein (SNCB) genes to chromosomes 4q21 and 5q35.* Genomics, 1995. **27**(2): p. 379-81.
69. Ninkina, N.N., et al., *Organization, expression and polymorphism of the human persyn gene.* Hum Mol Genet, 1998. **7**(9): p. 1417-24.
70. Jakes, R., M.G. Spillantini, and M. Goedert, *Identification of two distinct synucleins from human brain.* FEBS Lett, 1994. **345**(1): p. 27-32.
71. Maroteaux, L., J.T. Campanelli, and R.H. Scheller, *Synuclein: a neuron-specific protein localized to the nucleus and presynaptic nerve terminal.* J Neurosci, 1988. **8**(8): p. 2804-15.
72. Han, H., P.H. Weinreb, and P.T. Lansbury, *The core Alzheimer's peptide NAC forms amyloid fibrils which seed and are seeded by beta-amyloid: is NAC a common trigger or target in neurodegenerative disease?* Chem Biol, 1995. **2**(3): p. 163-9.
73. Uéda, K., et al., *Molecular cloning of cDNA encoding an unrecognized component of amyloid in Alzheimer disease.* Proc Natl Acad Sci U S A, 1993. **90**(23): p. 11282-6.
74. Ji, H., et al., *Identification of a breast cancer-specific gene, BCSG1, by direct differential cDNA sequencing.* Cancer Res, 1997. **57**(4): p. 759-64.
75. Murphy, D.D., et al., *Synucleins are developmentally expressed, and alpha-synuclein regulates the size of the presynaptic vesicular pool in primary hippocampal neurons.* J Neurosci, 2000. **20**(9): p. 3214-20.
76. Bendor, J.T., T.P. Logan, and R.H. Edwards, *The function of α-synuclein.* Neuron, 2013. **79**(6): p. 1044-66.
77. Davidson, W.S., et al., *Stabilization of alpha-synuclein secondary structure upon binding to synthetic membranes.* J Biol Chem, 1998. **273**(16): p. 9443-9.
78. Eliezer, D., et al., *Conformational properties of alpha-synuclein in its free and lipid-associated states.* J Mol Biol, 2001. **307**(4): p. 1061-73.
79. Shibayama-Imazu, T., et al., *Cell and tissue distribution and developmental change of neuron specific 14 kDa protein (phosphoneuroprotein 14).* Brain Res, 1993. **622**(1-2): p. 17-25.

80. Li, X., et al., *Early stages of aggregation of engineered α-synuclein monomers and oligomers in solution.* Sci Rep, 2019. **9**(1): p. 1734.
81. Duffy, P.E. and M. Menefee, *Electron microscopic observations of neurosecretory granules, nerve and glial fibers, and blood vessels in the median eminence of the rabbit.* Am J Anat, 1965. **117**(2): p. 251-86.
82. Kuzuhara, S., et al., *Lewy bodies are ubiquitinated. A light and electron microscopic immunocytochemical study.* Acta Neuropathol, 1988. **75**(4): p. 345-53.
83. Schlossmacher, M.G., et al., *Parkin localizes to the Lewy bodies of Parkinson disease and dementia with Lewy bodies.* Am J Pathol, 2002. **160**(5): p. 1655-67.
84. Ishizawa, T., et al., *Colocalization of tau and alpha-synuclein epitopes in Lewy bodies.* J Neuropathol Exp Neurol, 2003. **62**(4): p. 389-97.
85. Bengoa-Vergniory, N., et al., *Alpha-synuclein oligomers: a new hope.* Acta Neuropathol, 2017. **134**(6): p. 819-838.
86. Walker, D.G., et al., *Changes in properties of serine 129 phosphorylated α-synuclein with progression of Lewy-type histopathology in human brains.* Exp Neurol, 2013. **240**: p. 190-204.
87. Anderson, J.P., et al., *Phosphorylation of Ser-129 is the dominant pathological modification of alpha-synuclein in familial and sporadic Lewy body disease.* J Biol Chem, 2006. **281**(40): p. 29739-52.
88. Karampetsou, M., et al., *Phosphorylated exogenous alpha-synuclein fibrils exacerbate pathology and induce neuronal dysfunction in mice.* Sci Rep, 2017. **7**(1): p. 16533.
89. Mbefo, M.K., et al., *Phosphorylation of synucleins by members of the Polo-like kinase family.* J Biol Chem, 2010. **285**(4): p. 2807-22.
90. Giasson, B.I., et al., *Oxidative damage linked to neurodegeneration by selective alpha-synuclein nitration in synucleinopathy lesions.* Science, 2000. **290**(5493): p. 985-9.
91. Liu, Y., et al., *A novel molecular mechanism for nitrated {alpha}-synuclein-induced cell death.* J Mol Cell Biol, 2011. **3**(4): p. 239-49.
92. Tofaris, G.K., et al., *Ubiquitination of alpha-synuclein in Lewy bodies is a pathological event not associated with impairment of proteasome function.* J Biol Chem, 2003. **278**(45): p. 44405-11.
93. Davies, S.E., et al., *Enhanced ubiquitin-dependent degradation by Nedd4 protects against α-synuclein accumulation and toxicity in animal models of Parkinson's disease.* Neurobiol Dis, 2014. **64**: p. 79-87.
94. Sugeno, N., et al., *Lys-63-linked ubiquitination by E3 ubiquitin ligase Nedd4-1 facilitates endosomal sequestration of internalized α-synuclein.* J Biol Chem, 2014. **289**(26): p. 18137-51.
95. Shin, Y., et al., *The co-chaperone carboxyl terminus of Hsp70-interacting protein (CHIP) mediates alpha-synuclein degradation decisions between proteasomal and lysosomal pathways.* J Biol Chem, 2005. **280**(25): p. 23727-34.
96. Lee, J.T., et al., *Ubiquitination of alpha-synuclein by Siah-1 promotes alpha-synuclein aggregation and apoptotic cell death.* Hum Mol Genet, 2008. **17**(6): p. 906-17.
97. Kasai, T., et al., *Cleavage of normal and pathological forms of alpha-synuclein by neurosin in vitro.* Neurosci Lett, 2008. **436**(1): p. 52-6.

98. Iwata, A., et al., *Alpha-synuclein degradation by serine protease neurosin: implication for pathogenesis of synucleinopathies.* Hum Mol Genet, 2003. **12**(20): p. 2625-35.
99. Choi, D.H., et al., *Role of matrix metalloproteinase 3-mediated alpha-synuclein cleavage in dopaminergic cell death.* J Biol Chem, 2011. **286**(16): p. 14168-77.
100. Mishizen-Eberz, A.J., et al., *Cleavage of alpha-synuclein by calpain: potential role in degradation of fibrillized and nitrated species of alpha-synuclein.* Biochemistry, 2005. **44**(21): p. 7818-29.
101. Liu, C.W., et al., *A precipitating role for truncated alpha-synuclein and the proteasome in alpha-synuclein aggregation: implications for pathogenesis of Parkinson disease.* J Biol Chem, 2005. **280**(24): p. 22670-8.
102. Rodriguez, J.A., et al., *Structure of the toxic core of α-synuclein from invisible crystals.* Nature, 2015. **525**(7570): p. 486-90.
103. Li, H.T., et al., *Structural transformation and aggregation of human alpha-synuclein in trifluoroethanol: non-amyloid component sequence is essential and beta-sheet formation is prerequisite to aggregation.* Biopolymers, 2002. **64**(4): p. 221-6.
104. Zarranz, J.J., et al., *The new mutation, E46K, of alpha-synuclein causes Parkinson and Lewy body dementia.* Ann Neurol, 2004. **55**(2): p. 164-73.
105. Taoufik, E., et al., *Synaptic dysfunction in neurodegenerative and neurodevelopmental diseases: an overview of induced pluripotent stem-cell-based disease models.* Open Biol, 2018. **8**(9).
106. Gelders, G., V. Baekelandt, and A. Van der Perren, *Linking Neuroinflammation and Neurodegeneration in Parkinson's Disease.* J Immunol Res, 2018. **2018**: p. 4784268.
107. Guo, F., et al., *Autophagy in neurodegenerative diseases: pathogenesis and therapy.* Brain Pathol, 2018. **28**(1): p. 3-13.
108. Johri, A. and M.F. Beal, *Mitochondrial dysfunction in neurodegenerative diseases.* J Pharmacol Exp Ther, 2012. **342**(3): p. 619-30.
109. Kramer, M.L. and W.J. Schulz-Schaeffer, *Presynaptic alpha-synuclein aggregates, not Lewy bodies, cause neurodegeneration in dementia with Lewy bodies.* J Neurosci, 2007. **27**(6): p. 1405-10.
110. Mazzulli, J.R., et al., *α-Synuclein-induced lysosomal dysfunction occurs through disruptions in protein trafficking in human midbrain synucleinopathy models.* Proc Natl Acad Sci U S A, 2016. **113**(7): p. 1931-6.
111. Hoffmann, A.C., et al., *Extracellular aggregated alpha synuclein primarily triggers lysosomal dysfunction in neural cells prevented by trehalose.* Sci Rep, 2019. **9**(1): p. 544.
112. Crews, L., et al., *Selective molecular alterations in the autophagy pathway in patients with Lewy body disease and in models of alpha-synucleinopathy.* PLoS One, 2010. **5**(2): p. e9313.
113. De Stefani, D., et al., *A forty-kilodalton protein of the inner membrane is the mitochondrial calcium uniporter.* Nature, 2011. **476**(7360): p. 336-40.
114. Jouaville, L.S., et al., *Regulation of mitochondrial ATP synthesis by calcium: evidence for a long-term metabolic priming.* Proc Natl Acad Sci U S A, 1999. **96**(24): p. 13807-12.
115. Maharjan, S., et al., *Mitochondrial impairment triggers cytosolic oxidative stress and cell death following proteasome inhibition.* Sci Rep, 2014. **4**: p. 5896.

116. Di Maio, R., et al., *α-Synuclein binds to TOM20 and inhibits mitochondrial protein import in Parkinson's disease.* Sci Transl Med, 2016. **8**(342): p. 342ra78.
117. Garcia-Esparcia, P., et al., *Dementia with Lewy Bodies: Molecular Pathology in the Frontal Cortex in Typical and Rapidly Progressive Forms.* Front Neurol, 2017. **8**: p. 89.
118. Gunter, T.E., et al., *The Ca2+ transport mechanisms of mitochondria and Ca2+ uptake from physiological-type Ca2+ transients.* Biochim Biophys Acta, 1998. **1366**(1-2): p. 5-15.
119. Ali, S.T., J.R. Coggins, and H.T. Jacobs, *The study of cell-death proteins in the outer mitochondrial membrane by chemical cross-linking.* Biochem J, 1997. **325 (Pt 2)**: p. 321-4.
120. Anderson, S., et al., *Sequence and organization of the human mitochondrial genome.* Nature, 1981. **290**(5806): p. 457-65.
121. Frey, T.G. and C.A. Mannella, *The internal structure of mitochondria.* Trends Biochem Sci, 2000. **25**(7): p. 319-24.
122. Wiedemann, N., A.E. Frazier, and N. Pfanner, *The protein import machinery of mitochondria.* J Biol Chem, 2004. **279**(15): p. 14473-6.
123. Pfanner, N. and M. Meijer, *The Tom and Tim machine.* Curr Biol, 1997. **7**(2): p. R100-3.
124. Guo, R., et al., *Architecture of Human Mitochondrial Respiratory Megacomplex I.* Cell, 2017. **170**(6): p. 1247-1257.e12.
125. Martínez-Reyes, I. and N.S. Chandel, *Mitochondrial TCA cycle metabolites control physiology and disease.* Nat Commun, 2020. **11**(1): p. 102.
126. Rutter, J., D.R. Winge, and J.D. Schiffman, *Succinate dehydrogenase - Assembly, regulation and role in human disease.* Mitochondrion, 2010. **10**(4): p. 393-401.
127. Sharma, L.K., J. Lu, and Y. Bai, *Mitochondrial respiratory complex I: structure, function and implication in human diseases.* Curr Med Chem, 2009. **16**(10): p. 1266-77.
128. Wittig, I., et al., *Supercomplexes and subcomplexes of mitochondrial oxidative phosphorylation.* Biochim Biophys Acta, 2006. **1757**(9-10): p. 1066-72.
129. Dimroth, P., G. Kaim, and U. Matthey, *Crucial role of the membrane potential for ATP synthesis by F(1)F(o) ATP synthases.* J Exp Biol, 2000. **203**(Pt 1): p. 51-9.
130. Beck, S.J., et al., *Deregulation of mitochondrial F1FO-ATP synthase via OSCP in Alzheimer's disease.* Nat Commun, 2016. **7**: p. 11483.
131. Zorova, L.D., et al., *Mitochondrial membrane potential.* Anal Biochem, 2018. **552**: p. 50-59.
132. Omura, T., *Mitochondria-targeting sequence, a multi-role sorting sequence recognized at all steps of protein import into mitochondria.* J Biochem, 1998. **123**(6): p. 1010-6.
133. Barsukova, A., et al., *Activation of the mitochondrial permeability transition pore modulates Ca2+ responses to physiological stimuli in adult neurons.* Eur J Neurosci, 2011. **33**(5): p. 831-42.
134. Hansson, M.J., et al., *Brain-derived respiring mitochondria exhibit homogeneous, complete and cyclosporin-sensitive permeability transition.* J Neurochem, 2004. **89**(3): p. 715-29.

135. Hunter, D.R. and R.A. Haworth, *The Ca2+-induced membrane transition in mitochondria. I. The protective mechanisms.* Arch Biochem Biophys, 1979. **195**(2): p. 453-9.
136. Briston, T., et al., *Mitochondrial permeability transition pore: sensitivity to opening and mechanistic dependence on substrate availability.* Sci Rep, 2017. **7**(1): p. 10492.
137. Kim, J.S., L. He, and J.J. Lemasters, *Mitochondrial permeability transition: a common pathway to necrosis and apoptosis.* Biochem Biophys Res Commun, 2003. **304**(3): p. 463-70.
138. Klingenberg, M., *The ADP and ATP transport in mitochondria and its carrier.* Biochim Biophys Acta, 2008. **1778**(10): p. 1978-2021.
139. Sharov, V.G., et al., *Cyclosporine A attenuates mitochondrial permeability transition and improves mitochondrial respiratory function in cardiomyocytes isolated from dogs with heart failure.* J Mol Cell Cardiol, 2007. **42**(1): p. 150-8.
140. Ferrer, I., et al., *Abnormal levels of prohibitin and ATP synthase in the substantia nigra and frontal cortex in Parkinson's disease.* Neurosci Lett, 2007. **415**(3): p. 205-9.
141. Parker, W.D., S.J. Boyson, and J.K. Parks, *Abnormalities of the electron transport chain in idiopathic Parkinson's disease.* Ann Neurol, 1989. **26**(6): p. 719-23.
142. Reeve, A.K., et al., *Mitochondrial dysfunction within the synapses of substantia nigra neurons in Parkinson's disease.* NPJ Parkinsons Dis, 2018. **4**: p. 9.
143. Martin, L.J., et al., *Parkinson's disease alpha-synuclein transgenic mice develop neuronal mitochondrial degeneration and cell death.* J Neurosci, 2006. **26**(1): p. 41-50.
144. Nakano, M., et al., *ATP Maintenance via Two Types of ATP Regulators Mitigates Pathological Phenotypes in Mouse Models of Parkinson's Disease.* EBioMedicine, 2017. **22**: p. 225-241.
145. Ludtmann, M.H.R., et al., *α-synuclein oligomers interact with ATP synthase and open the permeability transition pore in Parkinson's disease.* Nat Commun, 2018. **9**(1): p. 2293.
146. Reeve, A.K., et al., *Aggregated α-synuclein and complex I deficiency: exploration of their relationship in differentiated neurons.* Cell Death Dis, 2015. **6**: p. e1820.
147. Martinez, J.H., et al., *Drp-1 dependent mitochondrial fragmentation and protective autophagy in dopaminergic SH-SY5Y cells overexpressing alpha-synuclein.* Mol Cell Neurosci, 2018. **88**: p. 107-117.
148. Ishihara-Paul, L., et al., *PINK1 mutations and parkinsonism.* Neurology, 2008. **71**(12): p. 896-902.
149. Morais, V.A., et al., *Parkinson's disease mutations in PINK1 result in decreased Complex I activity and deficient synaptic function.* EMBO Mol Med, 2009. **1**(2): p. 99-111.
150. Lücking, C.B., et al., *Association between early-onset Parkinson's disease and mutations in the parkin gene.* N Engl J Med, 2000. **342**(21): p. 1560-7.
151. Matsuda, N., et al., *PINK1 stabilized by mitochondrial depolarization recruits Parkin to damaged mitochondria and activates latent Parkin for mitophagy.* J Cell Biol, 2010. **189**(2): p. 211-21.
152. Hyun, D.H., et al., *Effect of wild-type or mutant Parkin on oxidative damage, nitric oxide, antioxidant defenses, and the proteasome.* J Biol Chem, 2002. **277**(32): p. 28572-7.

153. Lee, J.Y., et al., *Disease-causing mutations in parkin impair mitochondrial ubiquitination, aggregation, and HDAC6-dependent mitophagy.* J Cell Biol, 2010. **189**(4): p. 671-9.
154. Lu, X.H., et al., *Bacterial artificial chromosome transgenic mice expressing a truncated mutant parkin exhibit age-dependent hypokinetic motor deficits, dopaminergic neuron degeneration, and accumulation of proteinase K-resistant alpha-synuclein.* J Neurosci, 2009. **29**(7): p. 1962-76.
155. Youle, R.J. and A.M. van der Bliek, *Mitochondrial fission, fusion, and stress.* Science, 2012. **337**(6098): p. 1062-5.
156. Otera, H. and K. Mihara, *Discovery of the membrane receptor for mitochondrial fission GTPase Drp1.* Small GTPases, 2011. **2**(3): p. 167-172.
157. Nunnari, J., et al., *Mitochondrial transmission during mating in Saccharomyces cerevisiae is determined by mitochondrial fusion and fission and the intramitochondrial segregation of mitochondrial DNA.* Mol Biol Cell, 1997. **8**(7): p. 1233-42.
158. Mizushima, N., et al., *Dissection of autophagosome formation using Apg5-deficient mouse embryonic stem cells.* J Cell Biol, 2001. **152**(4): p. 657-68.
159. Quinsay, M.N., et al., *Bnip3-mediated mitochondrial autophagy is independent of the mitochondrial permeability transition pore.* Autophagy, 2010. **6**(7): p. 855-62.
160. Wu, W., et al., *PINK1-Parkin-Mediated Mitophagy Protects Mitochondrial Integrity and Prevents Metabolic Stress-Induced Endothelial Injury.* PLoS One, 2015. **10**(7): p. e0132499.
161. Deas, E., H. Plun-Favreau, and N.W. Wood, *PINK1 function in health and disease.* EMBO Mol Med, 2009. **1**(3): p. 152-65.
162. Vives-Bauza, C., et al., *PINK1-dependent recruitment of Parkin to mitochondria in mitophagy.* Proc Natl Acad Sci U S A, 2010. **107**(1): p. 378-83.
163. Gogvadze, V., S. Orrenius, and B. Zhivotovsky, *Multiple pathways of cytochrome c release from mitochondria in apoptosis.* Biochim Biophys Acta, 2006. **1757**(5-6): p. 639-47.
164. Zoratti, M., et al., *Novel channels of the inner mitochondrial membrane.* Biochim Biophys Acta, 2009. **1787**(5): p. 351-63.
165. Boveris, A. and E. Cadenas, *Mitochondrial production of hydrogen peroxide regulation by nitric oxide and the role of ubisemiquinone.* IUBMB Life, 2000. **50**(4-5): p. 245-50.
166. Han, Y., et al., *Ca2+-Induced Mitochondrial ROS Regulate the Early Embryonic Cell Cycle.* Cell Rep, 2018. **22**(1): p. 218-231.
167. Chen, Q., et al., *Production of reactive oxygen species by mitochondria: central role of complex III.* J Biol Chem, 2003. **278**(38): p. 36027-31.
168. Edmondson, D.E., *Hydrogen peroxide produced by mitochondrial monoamine oxidase catalysis: biological implications.* Curr Pharm Des, 2014. **20**(2): p. 155-60.
169. Phaniendra, A., D.B. Jestadi, and L. Periyasamy, *Free radicals: properties, sources, targets, and their implication in various diseases.* Indian J Clin Biochem, 2015. **30**(1): p. 11-26.
170. Weisiger, R.A. and I. Fridovich, *Mitochondrial superoxide simutase. Site of synthesis and intramitochondrial localization.* J Biol Chem, 1973. **248**(13): p. 4793-6.

171. Okado-Matsumoto, A. and I. Fridovich, *Subcellular distribution of superoxide dismutases (SOD) in rat liver: Cu,Zn-SOD in mitochondria.* J Biol Chem, 2001. **276**(42): p. 38388-93.
172. Sheng, Y., et al., *Superoxide dismutases and superoxide reductases.* Chem Rev, 2014. **114**(7): p. 3854-918.
173. Das, K. and A. Roychoudhury, *Reactive oxygen species (ROS) and response of antioxidants as ROS-scavengers during environmental stress in plants.* Frontiers in Environmental Science, 2014. **2**: p. 53.
174. Radi, R., *Oxygen radicals, nitric oxide, and peroxynitrite: Redox pathways in molecular medicine.* Proc Natl Acad Sci U S A, 2018. **115**(23): p. 5839-5848.
175. Nisoli, E. and M.O. Carruba, *Nitric oxide and mitochondrial biogenesis.* J Cell Sci, 2006. **119**(Pt 14): p. 2855-62.
176. Lacza, Z., E. Pankotai, and D.W. Busija, *Mitochondrial nitric oxide synthase: current concepts and controversies.* Front Biosci (Landmark Ed), 2009. **14**: p. 4436-43.
177. Brown, G.C. and V. Borutaite, *Nitric oxide, cytochrome c and mitochondria.* Biochem Soc Symp, 1999. **66**: p. 17-25.
178. Nakajo, S., et al., *A new brain-specific 14-kDa protein is a phosphoprotein. Its complete amino acid sequence and evidence for phosphorylation.* Eur J Biochem, 1993. **217**(3): p. 1057-63.
179. Lavedan, C., *The synuclein family.* Genome Res, 1998. **8**(9): p. 871-80.
180. Surguchov, A., *Synucleins: are they two-edged swords?* J Neurosci Res, 2013. **91**(2): p. 161-6.
181. Biere, A.L., et al., *Parkinson's disease-associated alpha-synuclein is more fibrillogenic than beta- and gamma-synuclein and cannot cross-seed its homologs.* J Biol Chem, 2000. **275**(44): p. 34574-9.
182. Brown, J.W., et al., *β-Synuclein suppresses both the initiation and amplification steps of α-synuclein aggregation via competitive binding to surfaces.* Sci Rep, 2016. **6**: p. 36010.
183. Lavedan, C., et al., *Genomic organization and expression of the human beta-synuclein gene (SNCB).* Genomics, 1998. **54**(1): p. 173-5.
184. Quilty, M.C., et al., *Localization of alpha-, beta-, and gamma-synuclein during neuronal development and alterations associated with the neuronal response to axonal trauma.* Exp Neurol, 2003. **182**(1): p. 195-207.
185. Weingarten, J., et al., *The proteome of the presynaptic active zone from mouse brain.* Mol Cell Neurosci, 2014. **59**: p. 106-18.
186. Lee, D., S.R. Paik, and K.Y. Choi, *Beta-synuclein exhibits chaperone activity more efficiently than alpha-synuclein.* FEBS Lett, 2004. **576**(1-2): p. 256-60.
187. Snyder, H., et al., *beta-Synuclein reduces proteasomal inhibition by alpha-synuclein but not gamma-synuclein.* J Biol Chem, 2005. **280**(9): p. 7562-9.
188. Israeli, E. and R. Sharon, *Beta-synuclein occurs in vivo in lipid-associated oligomers and forms hetero-oligomers with alpha-synuclein.* J Neurochem, 2009. **108**(2): p. 465-74.
189. Vigneswara, V., et al., *Molecular ageing of alpha- and Beta-synucleins: protein damage and repair mechanisms.* PLoS One, 2013. **8**(4): p. e61442.
190. Hashimoto, M., et al., *beta-Synuclein inhibits alpha-synuclein aggregation: a possible role as an anti-parkinsonian factor.* Neuron, 2001. **32**(2): p. 213-23.
191. Windisch, M., et al., *Development of a new treatment for Alzheimer's disease and Parkinson's disease using anti-aggregatory beta-synuclein-derived peptides.* J Mol Neurosci, 2002. **19**(1-2): p. 63-9.

192. Masliah, E. and M. Hashimoto, *Development of new treatments for Parkinson's disease in transgenic animal models: a role for beta-synuclein.* Neurotoxicology, 2002. **23**(4-5): p. 461-8.
193. Fan, Y., et al., *Beta-synuclein modulates alpha-synuclein neurotoxicity by reducing alpha-synuclein protein expression.* Hum Mol Genet, 2006. **15**(20): p. 3002-11.
194. Janowska, M.K., K.P. Wu, and J. Baum, *Unveiling transient protein-protein interactions that modulate inhibition of alpha-synuclein aggregation by beta-synuclein, a pre-synaptic protein that co-localizes with alpha-synuclein.* Sci Rep, 2015. **5**: p. 15164.
195. Moriarty, G.M., et al., *A pH-dependent switch promotes β-synuclein fibril formation via glutamate residues.* J Biol Chem, 2017. **292**(39): p. 16368-16379.
196. Yamin, G., et al., *Forcing nonamyloidogenic beta-synuclein to fibrillate.* Biochemistry, 2005. **44**(25): p. 9096-107.
197. Zou, K., et al., *Amyloid beta-protein (Abeta)1-40 protects neurons from damage induced by Abeta1-42 in culture and in rat brain.* J Neurochem, 2003. **87**(3): p. 609-19.
198. Liu, C., et al., *Co-immunoprecipitation with Tau Isoform-specific Antibodies Reveals Distinct Protein Interactions and Highlights a Putative Role for 2N Tau in Disease.* J Biol Chem, 2016. **291**(15): p. 8173-88.
199. Ohtake, H., et al., *Beta-synuclein gene alterations in dementia with Lewy bodies.* Neurology, 2004. **63**(5): p. 805-11.
200. Galvin, J.E., et al., *Axon pathology in Parkinson's disease and Lewy body dementia hippocampus contains alpha-, beta-, and gamma-synuclein.* Proc Natl Acad Sci U S A, 1999. **96**(23): p. 13450-5.
201. Winslow, A.R., et al., *α-Synuclein impairs macroautophagy: implications for Parkinson's disease.* J Cell Biol, 2010. **190**(6): p. 1023-37.
202. Evans, T., et al., *Accumulation of beta-synuclein in cortical neurons is associated with autophagy attenuation in the brains of dementia with Lewy body patients.* Brain Res, 2018. **1681**: p. 1-13.
203. Wei, J., et al., *Enhanced lysosomal pathology caused by beta-synuclein mutants linked to dementia with Lewy bodies.* J Biol Chem, 2007. **282**(39): p. 28904-14.
204. Taschenberger, G., et al., *beta-synuclein aggregates and induces neurodegeneration in dopaminergic neurons.* Ann Neurol, 2013. **74**(1): p. 109-18.
205. Sekigawa, A., et al., *Distinct mechanisms of axonal globule formation in mice expressing human wild type alpha-synuclein or dementia with Lewy bodies-linked P123H beta-synuclein.* Mol Brain, 2012. **5**: p. 34.
206. Sekigawa, A., et al., *Role of alpha- and beta-Synucleins in the Axonal Pathology of Parkinson's Disease and Related Synucleinopathies.* Biomolecules, 2015. **5**(2): p. 1000-11.
207. Fujita, M., et al., *A β-synuclein mutation linked to dementia produces neurodegeneration when expressed in mouse brain.* Nat Commun, 2010. **1**: p. 110.
208. Li, J., P. Henning Jensen, and A. Dahlstrom, *Differential localization of alpha-, beta- and gamma-synucleins in the rat CNS.* Neuroscience, 2002. **113**(2): p. 463-78.
209. McCann, H., et al., *α-Synucleinopathy phenotypes.* Parkinsonism Relat Disord, 2014. **20 Suppl 1**: p. S62-7.

210. German, D.C., et al., *The neurotoxin MPTP causes degeneration of specific nucleus A8, A9 and A10 dopaminergic neurons in the mouse.* Neurodegeneration, 1996. **5**(4): p. 299-312.
211. Su, R.J., et al., *Time-course behavioral features are correlated with Parkinson's disease-associated pathology in a 6-hydroxydopamine hemiparkinsonian rat model.* Mol Med Rep, 2018. **17**(2): p. 3356-3363.
212. Polymeropoulos, M.H., et al., *Mutation in the alpha-synuclein gene identified in families with Parkinson's disease.* Science, 1997. **276**(5321): p. 2045-7.
213. Feng, G., et al., *Imaging neuronal subsets in transgenic mice expressing multiple spectral variants of GFP.* Neuron, 2000. **28**(1): p. 41-51.
214. Iacovitti, L., et al., *The hTH-GFP reporter rat model for the study of Parkinson's disease.* PLoS One, 2014. **9**(12): p. e113151.
215. Moser, M., et al., *Developmental expression of the prion protein gene in glial cells.* Neuron, 1995. **14**(3): p. 509-17.
216. Wang, X., et al., *Distribution of CaMKIIα expression in the brain in vivo, studied by CaMKIIα-GFP mice.* Brain Res, 2013. **1518**: p. 9-25.
217. Ross, O.A., et al., *Genomic investigation of alpha-synuclein multiplication and parkinsonism.* Ann Neurol, 2008. **63**(6): p. 743-50.
218. Rieker, C., et al., *Neuropathology in mice expressing mouse alpha-synuclein.* PLoS One, 2011. **6**(9): p. e24834.
219. Giraldo, G., et al., *Locomotor differences in mice expressing wild-type human α-synuclein.* Neurobiol Aging, 2018. **65**: p. 140-148.
220. Masliah, E., et al., *Dopaminergic loss and inclusion body formation in alpha-synuclein mice: implications for neurodegenerative disorders.* Science, 2000. **287**(5456): p. 1265-9.
221. Price, D.L., et al., *Alterations in mGluR5 expression and signaling in Lewy body disease and in transgenic models of alpha-synucleinopathy--implications for excitotoxicity.* PLoS One, 2010. **5**(11): p. e14020.
222. Miller, G.W., et al., *Immunochemical analysis of dopamine transporter protein in Parkinson's disease.* Ann Neurol, 1997. **41**(4): p. 530-9.
223. Pigott, K., et al., *Longitudinal study of normal cognition in Parkinson disease.* Neurology, 2015. **85**(15): p. 1276-82.
224. Tofaris, G.K., et al., *Pathological changes in dopaminergic nerve cells of the substantia nigra and olfactory bulb in mice transgenic for truncated human alpha-synuclein(1-120): implications for Lewy body disorders.* J Neurosci, 2006. **26**(15): p. 3942-50.
225. Wegrzynowicz, M., et al., *Depopulation of dense α-synuclein aggregates is associated with rescue of dopamine neuron dysfunction and death in a new Parkinson's disease model.* Acta Neuropathol, 2019.
226. Wakamatsu, M., et al., *Accumulation of phosphorylated alpha-synuclein in dopaminergic neurons of transgenic mice that express human alpha-synuclein.* J Neurosci Res, 2007. **85**(8): p. 1819-25.
227. Krüger, R., et al., *Familial parkinsonism with synuclein pathology: clinical and PET studies of A30P mutation carriers.* Neurology, 2001. **56**(10): p. 1355-62.
228. Appel-Cresswell, S., et al., *Alpha-synuclein p.H50Q, a novel pathogenic mutation for Parkinson's disease.* Mov Disord, 2013. **28**(6): p. 811-3.
229. van der Putten, H., et al., *Neuropathology in mice expressing human alpha-synuclein.* J Neurosci, 2000. **20**(16): p. 6021-9.
230. Sommer, B., et al., *Mouse models of alpha-synucleinopathy and Lewy pathology.* Exp Gerontol, 2000. **35**(9-10): p. 1389-403.

231. Gispert, S., et al., *Transgenic mice expressing mutant A53T human alpha-synuclein show neuronal dysfunction in the absence of aggregate formation.* Mol Cell Neurosci, 2003. **24**(2): p. 419-29.
232. Giasson, B.I., et al., *Neuronal alpha-synucleinopathy with severe movement disorder in mice expressing A53T human alpha-synuclein.* Neuron, 2002. **34**(4): p. 521-33.
233. Lee, M.K., et al., *Human alpha-synuclein-harboring familial Parkinson's disease-linked Ala-53 --> Thr mutation causes neurodegenerative disease with alpha-synuclein aggregation in transgenic mice.* Proc Natl Acad Sci U S A, 2002. **99**(13): p. 8968-73.
234. Matsuoka, Y., et al., *Lack of nigral pathology in transgenic mice expressing human alpha-synuclein driven by the tyrosine hydroxylase promoter.* Neurobiol Dis, 2001. **8**(3): p. 535-9.
235. Kahle, P.J., et al., *Subcellular localization of wild-type and Parkinson's disease-associated mutant alpha -synuclein in human and transgenic mouse brain.* J Neurosci, 2000. **20**(17): p. 6365-73.
236. Rockenstein, E., et al., *Differential neuropathological alterations in transgenic mice expressing alpha-synuclein from the platelet-derived growth factor and Thy-1 promoters.* J Neurosci Res, 2002. **68**(5): p. 568-78.
237. Freichel, C., et al., *Age-dependent cognitive decline and amygdala pathology in alpha-synuclein transgenic mice.* Neurobiol Aging, 2007. **28**(9): p. 1421-35.
238. Schell, H., et al., *Nuclear and neuritic distribution of serine-129 phosphorylated alpha-synuclein in transgenic mice.* Neuroscience, 2009. **160**(4): p. 796-804.
239. Gomez-Isla, T., et al., *Motor dysfunction and gliosis with preserved dopaminergic markers in human alpha-synuclein A30P transgenic mice.* Neurobiol Aging, 2003. **24**(2): p. 245-58.
240. Richfield, E.K., et al., *Behavioral and neurochemical effects of wild-type and mutated human alpha-synuclein in transgenic mice.* Exp Neurol, 2002. **175**(1): p. 35-48.
241. Emmer, K.L., et al., *E46K human alpha-synuclein transgenic mice develop Lewy-like and tau pathology associated with age-dependent, detrimental motor impairment.* J Biol Chem, 2011. **286**(40): p. 35104-18.
242. Masliah, E., et al., *beta-amyloid peptides enhance alpha-synuclein accumulation and neuronal deficits in a transgenic mouse model linking Alzheimer's disease and Parkinson's disease.* Proc Natl Acad Sci U S A, 2001. **98**(21): p. 12245-50.
243. Zhou, W., J.B. Milder, and C.R. Freed, *Transgenic mice overexpressing tyrosine-to-cysteine mutant human alpha-synuclein: a progressive neurodegenerative model of diffuse Lewy body disease.* J Biol Chem, 2008. **283**(15): p. 9863-70.
244. Michell, A.W., et al., *The effect of truncated human alpha-synuclein (1-120) on dopaminergic cells in a transgenic mouse model of Parkinson's disease.* Cell Transplant, 2007. **16**(5): p. 461-74.
245. Hall, K., et al., *Behavioural deficits in transgenic mice expressing human truncated (1-120 amino acid) alpha-synuclein.* Exp Neurol, 2015. **264**: p. 8-13.
246. Kahle, P.J., et al., *Hyperphosphorylation and insolubility of alpha-synuclein in transgenic mouse oligodendrocytes.* EMBO Rep, 2002. **3**(6): p. 583-8.
247. Fernagut, P.O. and M.F. Chesselet, *Alpha-synuclein and transgenic mouse models.* Neurobiol Dis, 2004. **17**(2): p. 123-30.

248. Magen, I. and M.F. Chesselet, *Mouse models of cognitive deficits due to alpha-synuclein pathology.* J Parkinsons Dis, 2011. **1**(3): p. 217-27.
249. Crabtree, D.M. and J. Zhang, *Genetically engineered mouse models of Parkinson's disease.* Brain Res Bull, 2012. **88**(1): p. 13-32.
250. Lim, Y., et al., *α-Syn suppression reverses synaptic and memory defects in a mouse model of dementia with Lewy bodies.* J Neurosci, 2011. **31**(27): p. 10076-87.
251. Yamaguchi, K., et al., *Abundant neuritic inclusions and microvacuolar changes in a case of diffuse Lewy body disease with the A53T mutation in the alpha-synuclein gene.* Acta Neuropathol, 2005. **110**(3): p. 298-305.
252. Aarsland, D., et al., *Mild cognitive impairment in Parkinson disease: a multicenter pooled analysis.* Neurology, 2010. **75**(12): p. 1062-9.
253. Cerejeira, J., L. Lagarto, and E.B. Mukaetova-Ladinska, *Behavioral and psychological symptoms of dementia.* Front Neurol, 2012. **3**: p. 73.
254. Duff, K., et al., *Psychiatric symptoms in Huntington's disease before diagnosis: the predict-HD study.* Biol Psychiatry, 2007. **62**(12): p. 1341-6.
255. Deacon, R.M., *Measuring motor coordination in mice.* J Vis Exp, 2013(75): p. e2609.
256. Lüesse, H.G., et al., *Evaluation of R6/2 HD transgenic mice for therapeutic studies in Huntington's disease: behavioral testing and impact of diabetes mellitus.* Behav Brain Res, 2001. **126**(1-2): p. 185-95.
257. Shiotsuki, H., et al., *A rotarod test for evaluation of motor skill learning.* J Neurosci Methods, 2010. **189**(2): p. 180-5.
258. Campos, F.L., et al., *Rodent models of Parkinson's disease: beyond the motor symptomatology.* Front Behav Neurosci, 2013. **7**: p. 175.
259. Zhu, X.R., et al., *Non-motor behavioural impairments in parkin-deficient mice.* Eur J Neurosci, 2007. **26**(7): p. 1902-11.
260. Graham, D.R. and A. Sidhu, *Mice expressing the A53T mutant form of human alpha-synuclein exhibit hyperactivity and reduced anxiety-like behavior.* J Neurosci Res, 2010. **88**(8): p. 1777-83.
261. Tatem, K.S., et al., *Behavioral and locomotor measurements using an open field activity monitoring system for skeletal muscle diseases.* J Vis Exp, 2014(91): p. 51785.
262. Kedia, S. and S. Chattarji, *Marble burying as a test of the delayed anxiogenic effects of acute immobilisation stress in mice.* J Neurosci Methods, 2014. **233**: p. 150-4.
263. Komada, M., K. Takao, and T. Miyakawa, *Elevated plus maze for mice.* J Vis Exp, 2008(22).
264. Walf, A.A. and C.A. Frye, *The use of the elevated plus maze as an assay of anxiety-related behavior in rodents.* Nat Protoc, 2007. **2**(2): p. 322-8.
265. Torres-Lista, V., S. López-Pousa, and L. Giménez-Llort, *Marble-burying is enhanced in 3xTg-AD mice, can be reversed by risperidone and it is modulable by handling.* Behav Processes, 2015. **116**: p. 69-74.
266. Bonito-Oliva, A., D. Masini, and G. Fisone, *A mouse model of non-motor symptoms in Parkinson's disease: focus on pharmacological interventions targeting affective dysfunctions.* Front Behav Neurosci, 2014. **8**: p. 290.
267. Pellow, S., et al., *Validation of open:closed arm entries in an elevated plus-maze as a measure of anxiety in the rat.* J Neurosci Methods, 1985. **14**(3): p. 149-67.

268. Dawson, G.R. and M.D. Tricklebank, *Use of the elevated plus maze in the search for novel anxiolytic agents.* Trends Pharmacol Sci, 1995. **16**(2): p. 33-6.
269. Deacon, R.M., *Digging and marble burying in mice: simple methods for in vivo identification of biological impacts.* Nat Protoc, 2006. **1**(1): p. 122-4.
270. Vorhees, C.V. and M.T. Williams, *Morris water maze: procedures for assessing spatial and related forms of learning and memory.* Nat Protoc, 2006. **1**(2): p. 848-58.
271. Morris, R., *Developments of a water-maze procedure for studying spatial learning in the rat.* J Neurosci Methods, 1984. **11**(1): p. 47-60.
272. Hölscher, C., *Stress impairs performance in spatial water maze learning tasks.* Behav Brain Res, 1999. **100**(1-2): p. 225-35.
273. Ryan, B.C., et al., *Olfactory cues are sufficient to elicit social approach behaviors but not social transmission of food preference in C57BL/6J mice.* Behav Brain Res, 2008. **193**(2): p. 235-42.
274. Doty, R.L., *Odor-guided behavior in mammals.* Experientia, 1986. **42**(3): p. 257-71.
275. Taglialatela, G., et al., *Intermediate- and long-term recognition memory deficits in Tg2576 mice are reversed with acute calcineurin inhibition.* Behav Brain Res, 2009. **200**(1): p. 95-9.
276. Lueptow, L.M., *Novel Object Recognition Test for the Investigation of Learning and Memory in Mice.* J Vis Exp, 2017(126).
277. Gouveia, K. and J.L. Hurst, *Optimising reliability of mouse performance in behavioural testing: the major role of non-aversive handling.* Sci Rep, 2017. **7**: p. 44999.
278. McLay, R.N., S.M. Freeman, and J.E. Zadina, *Chronic corticosterone impairs memory performance in the Barnes maze.* Physiol Behav, 1998. **63**(5): p. 933-7.
279. Contet, C., J.N. Rawlins, and R.M. Deacon, *A comparison of 129S2/SvHsd and C57BL/6JOlaHsd mice on a test battery assessing sensorimotor, affective and cognitive behaviours: implications for the study of genetically modified mice.* Behav Brain Res, 2001. **124**(1): p. 33-46.
280. Antunes, M. and G. Biala, *The novel object recognition memory: neurobiology, test procedure, and its modifications.* Cogn Process, 2012. **13**(2): p. 93-110.
281. Hammond, R.S., L.E. Tull, and R.W. Stackman, *On the delay-dependent involvement of the hippocampus in object recognition memory.* Neurobiol Learn Mem, 2004. **82**(1): p. 26-34.
282. Jackson, J., et al., *White matter tauopathy: Transient functional loss and novel myelin remodeling.* Glia, 2018. **66**(4): p. 813-827.
283. Andres, D., et al., *Morphological and functional differentiation in BE(2)-M17 human neuroblastoma cells by treatment with Trans-retinoic acid.* BMC Neurosci, 2013. **14**: p. 49.
284. Turrens, J.F., *Mitochondrial formation of reactive oxygen species.* J Physiol, 2003. **552**(Pt 2): p. 335-44.
285. Hall, A.M. and E.D. Roberson, *Mouse models of Alzheimer's disease.* Brain Res Bull, 2012. **88**(1): p. 3-12.
286. Zhang, J., X. Li, and J.D. Li, *The Roles of Post-translational Modifications on α-Synuclein in the Pathogenesis of Parkinson's Diseases.* Front Neurosci, 2019. **13**: p. 381.

287. Ulusoy, A., et al., *Co-expression of C-terminal truncated alpha-synuclein enhances full-length alpha-synuclein-induced pathology.* Eur J Neurosci, 2010. **32**(3): p. 409-22.
288. Cabin, D.E., et al., *Exacerbated synucleinopathy in mice expressing A53T SNCA on a Snca null background.* Neurobiol Aging, 2005. **26**(1): p. 25-35.
289. Bernis, M.E., et al., *Prion-like propagation of human brain-derived alpha-synuclein in transgenic mice expressing human wild-type alpha-synuclein.* Acta Neuropathol Commun, 2015. **3**: p. 75.
290. Leger, M., et al., *Object recognition test in mice.* Nat Protoc, 2013. **8**(12): p. 2531-7.
291. Prots, I., et al., *α-Synuclein oligomers induce early axonal dysfunction in human iPSC-based models of synucleinopathies.* Proc Natl Acad Sci U S A, 2018. **115**(30): p. 7813-7818.
292. Gaig, C., et al., *G2019S LRRK2 mutation causing Parkinson's disease without Lewy bodies.* J Neurol Neurosurg Psychiatry, 2007. **78**(6): p. 626-8.
293. Bandopadhyay, R., *Sequential Extraction of Soluble and Insoluble Alpha-Synuclein from Parkinsonian Brains.* J Vis Exp, 2016(107).
294. Neumann, M., et al., *Misfolded proteinase K-resistant hyperphosphorylated alpha-synuclein in aged transgenic mice with locomotor deterioration and in human alpha-synucleinopathies.* J Clin Invest, 2002. **110**(10): p. 1429-39.
295. Spinelli, K.J., et al., *Presynaptic alpha-synuclein aggregation in a mouse model of Parkinson's disease.* J Neurosci, 2014. **34**(6): p. 2037-50.
296. Reddy, P.H., et al., *Gene expression profiles of transcripts in amyloid precursor protein transgenic mice: up-regulation of mitochondrial metabolism and apoptotic genes is an early cellular change in Alzheimer's disease.* Hum Mol Genet, 2004. **13**(12): p. 1225-40.
297. Liesa, M., M. Palacín, and A. Zorzano, *Mitochondrial dynamics in mammalian health and disease.* Physiol Rev, 2009. **89**(3): p. 799-845.
298. Kamp, F., et al., *Inhibition of mitochondrial fusion by α-synuclein is rescued by PINK1, Parkin and DJ-1.* EMBO J, 2010. **29**(20): p. 3571-89.
299. Wang, H., et al., *Effects of overexpression of huntingtin proteins on mitochondrial integrity.* Hum Mol Genet, 2009. **18**(4): p. 737-52.
300. Wang, X., et al., *Amyloid-beta overproduction causes abnormal mitochondrial dynamics via differential modulation of mitochondrial fission/fusion proteins.* Proc Natl Acad Sci U S A, 2008. **105**(49): p. 19318-23.
301. Spano, M., et al., *The possible involvement of mitochondrial dysfunctions in Lewy body dementia: a systematic review.* Funct Neurol, 2015. **30**(3): p. 151-8.
302. Zhu, J.H., et al., *Localization of phosphorylated ERK/MAP kinases to mitochondria and autophagosomes in Lewy body diseases.* Brain Pathol, 2003. **13**(4): p. 473-81.
303. Chinta, S.J., et al., *Mitochondrial α-synuclein accumulation impairs complex I function in dopaminergic neurons and results in increased mitophagy in vivo.* Neurosci Lett, 2010. **486**(3): p. 235-9.
304. Banerjee, K., et al., *Alpha-synuclein induced membrane depolarization and loss of phosphorylation capacity of isolated rat brain mitochondria: implications in Parkinson's disease.* FEBS Lett, 2010. **584**(8): p. 1571-6.
305. Devi, L., et al., *Mitochondrial import and accumulation of alpha-synuclein impair complex I in human dopaminergic neuronal cultures and Parkinson disease brain.* J Biol Chem, 2008. **283**(14): p. 9089-100.

306. Hou, X., et al., *Age- and disease-dependent increase of the mitophagy marker phospho-ubiquitin in normal aging and Lewy body disease.* Autophagy, 2018. **14**(8): p. 1404-1418.
307. Nakamura, S. and T. Yoshimori, *New insights into autophagosome-lysosome fusion.* J Cell Sci, 2017. **130**(7): p. 1209-1216.
308. Grassi, D., et al., *Identification of a highly neurotoxic α-synuclein species inducing mitochondrial damage and mitophagy in Parkinson's disease.* Proc Natl Acad Sci U S A, 2018. **115**(11): p. E2634-E2643.
309. Xie, W. and K.K. Chung, *Alpha-synuclein impairs normal dynamics of mitochondria in cell and animal models of Parkinson's disease.* J Neurochem, 2012. **122**(2): p. 404-14.
310. Santos, D., et al., *The Impact of Mitochondrial Fusion and Fission Modulation in Sporadic Parkinson's Disease.* Mol Neurobiol, 2015. **52**(1): p. 573-86.
311. Beyer, K., et al., *Alpha- and beta-synuclein expression in Parkinson disease with and without dementia.* J Neurol Sci, 2011. **310**(1-2): p. 112-7.
312. Beyer, K., et al., *The decrease of β-synuclein in cortical brain areas defines a molecular subgroup of dementia with Lewy bodies.* Brain, 2010. **133**(Pt 12): p. 3724-33.
313. Benson, D.L., et al., *Differential gene expression for glutamic acid decarboxylase and type II calcium-calmodulin-dependent protein kinase in basal ganglia, thalamus, and hypothalamus of the monkey.* J Neurosci, 1991. **11**(6): p. 1540-64.